AN ANALOG/HYBRID COMPUTER SOLUTION OF ELECTROMAGNETIC SCATTERING PROBLEMS

by

Edgar Littleton Coffey, III

Dissertation submitted to the Graduate Faculty of the

Virginia Polytechnic Institute and State University

in partial fulfillment of the requirements for the degree of

DOCTOR OF PHILOSOPHY

in

Electrical Engineering

APPROVED:

W. L. Stutzman, Chairman

W. A. Blackwell

C. W. Bostian

J. A. Cochran

P. H. Wiley

June, 1976

Blacksburg, Virginia

ACKNOWLEDGEMENTS

The author wishes to express his thanks to the many people who assisted him in the research and writing of this dissertation. Without their support this program of effort might not have been completed

At the top of the list is Dr. Warren L. Stutzman, major professor, course advisor, and friend. His guidance through the past four years of graduate work has made that work immensely rewarding and satisfying. His help in planning the research for this dissertation was invaluable. He was always available and willing to discuss any of the author's problems. Most of the credit for the author's academic and professional development must go to Dr. Stutzman.

Grateful thanks are due the other members of my committee for fitting my questions and problems into their busy schedules and for reading and criticizing initial drafts of the dissertation. Drs. C. W. Bostian and P. H. Wiley were involved in full-time research much of the last year when help was most needed, but they were always available to the author. Dr. W. A. Blackwell as department head was constantly busy; yet, he too was always available to answer a question whenever I asked. Dr. J. A. Cochran made a major contribution to the author's mathematical development in his excellent graduate courses in partial differential equations, integral equations, and principles and techniques of applied mathematics. Without this background it would not have been possible to have carried out the research that I did. Even with his busy schedule as Faculty Senate Vice-President he was able to find time

to consult with me whenever needed.

Thanks are also due several people who did not serve on my committee. Dr. A. W. Bennett sparked the author's original interest in analog/hybrid computers, and he has been constantly available to the author whenever computer problems arose. and are to be thanked for maintaining the hybrid computer in fine shape and for repairing the slightest malfunction as soon as it was brought to their attention.

Finally, the biggest thanks of all goes to my wife who had to put up with a pretty cantankerous human being during the last month of my research. also found time to type both the rough draft and final copy of this dissertation in addition to her own Master's Thesis.

TABLE OF CONTENTS

LIST OF ILLUSTRATIONS

LIST OF TABLES

CHAPTER I

INTRODUCTION

The problem of electromagnetic scattering from obstacles has concerned many researchers over the years. From the point of view of classical physical theory, the scattering and diffraction of waves from obstacles has long been fully understood in the sense that the underlying differential equations and boundary conditions of the relevant variables are known. In principle, it is merely necessary to solve the equations subject to the boundary conditions appropriate to any particular source and object(s) in order to determine completely the scattered field. In practice this has proved quite formidable even under simple and idealized conditions. Analytic methods that attempted to generate closed-form solutions were obtained only for the simplest of objects. Approximate techniques that are used in the study of optical scattering are inadequate to deal with the more general electromagnetic problems that are encountered in radar, antenna design, and propagation, for example[1].

The advent of high-speed digital computers opened up algorithms that, while previously known, were impractical because of the large number of computations required. Matrix inversion techniques such as finite differences and finite elements, variational methods, and, of course, the method of moments, became practical with the development of computers such as the CDC 6600 which can multiply two 10-digit numbers in less than one microsecond. Work by Andreasen[2], Tanner[3],

Harrington[4], and others extended the scope of scattering problems that we may now solve.

At about the same time many investigators began using the integral equation theory that had been developed over the last half century. Again, more types of problems could be solved. As an illustration consider the problem of determining the current distribution along a wire antenna which is excited by a specified source. The problem can readily be formulated in terms of an inhomogeneous integral equation[5]. However, until electromagnetics engineers recognized that the integral equation could be solved numerically by using a digital computer, the formulation was academic. These numerical solutions permit calculation of input impedance and radiation pattern as well as current distribution for many types of wire objects.

It took until about 1974 or 1975 to fully explore the "method of moments - integral equations - digital computer" technique of solving scattering problems. From 1968 when Harrington published his text on moment methods[6] to the present, the prima donnas of electromagnetic engineering have been integral equations and moment methods. But the complexity of scatterers was severely limited by computational problems. All method of moments problems involved the solution of simultaneous equations, the number of which increases rapidly with the complexity of the scatterer. When used with integral equations, the matrices involved become dense and complex-valued. Even with large digital computers, it was not possible to handle matrix sizes much beyond 200 x 200 and be assured of meaningful results. This in turn limited

the size of the scatterer that could be solved on the computer by this method. And this restriction became more severe in higher dimensions. The method of moments had reached its limit. (Other methods, such as characteristic modes, have developed from the method of moments, but they suffer the same limitations as do all moment methods.)

In 1974, Mei introduced the "Unimoment Method" of solving antenna and scattering problems[7]. This technique extended the usefulness of the method of moments to multi-dimensional scatterers. By separating the scattering problem into one exterior problem and several interior problems, Mei was able to greatly reduce the number of computations necessary to solve a particular scattering problem, thus increasing the size and complexity of objects that could be considered in practice. At present the power of the Unimoment Method is limited by techniques in solving simultaneous equations described by sparse banded matrices.

All the numerical techniques mentioned above have been implemented on the high-speed digital computer. It is surprising that nowhere in the literature has there been reference to work done using the analog/hybrid computer. Wexler pointed this out in 1969 and stated that he felt that the hybrid computer was the only method left to solve large scale electromagnetics problems[8]. But no one has published any work using the hybrid machine since then.

This dissertation describes the development of an analog/hybrid computer technique that may be used with great efficiency in the solution of electromagnetics scattering problems. It is called

the "Unimoment - Monte Carlo Technique," and it combines the advantages of the Unimoment Method with the efficiency that occurs when the Monte Carlo method (method of random walks) is used on a modern hybrid computer. It will be shown that the hybrid computer is a viable alternative to the strictly digital computer when large-scale scattering problems are to be solved, and that the results obtained by this method are at least as accurate as results obtained from other popular methods.

In order to attack the development of a new computer method, much background into fundamental concepts is needed. Chapter II deals with the fundamental concepts of electromagnetics, digital computers and analog/hybrid computers. The sections on computer concepts have been included because it is necessary to understand the limitations of present day computing machinery in order to make intelligent decisions about the utilization of computing resources.

Chapter III reviews some of the current methods used in electromagnetic scattering studies. A summary of these methods is essential in order to avoid the mistakes and inefficiencies of the past and to have a standard of comparison for any new method.

The Unimoment - Monte Carlo Method is described in Chapters IV, V, and VI. Chapter IV contains a mathematical description of the method, its advantages, and its limitations. Chapter V describes the implementation of the method on the GE-4020/EAI-580 hybrid computer system in use at Virginia Polytechnic Institute and State University. Here some practical advantages and limitations are discussed.

Chapter VI describes how the method is used to solve various types of scattering problems, and a comparison of results with other methods and with measured data is given.

Finally, Chapter VII contains a summary of the method's effectiveness and efficiency and some suggestions for further work.

CHAPTER II

FUNDAMENTAL CONCEPTS

2.1 Introduction

In order to analyze different electromagnetic scattering problem solution methods properly, it is necessary to understand both fundamental electromagnetic concepts and the operation of the computational machinery involved to implement a particular solution method. Both will be presented in this chapter.

2.2 Electromagnetic Concepts

2.2.1 Maxwell's Equations and Boundary Conditions

Let $\overline{E}$ and $\overline{H}$ represent the vector fields in a linear, isotropic medium of permittivity $\varepsilon = \varepsilon(x,y,z)$ and permeability $\mu = \mu(x,y,z)$. Such fields will satisfy Maxwell's equations[9].

$$\begin{aligned} \nabla \times \overline{E} &= -\frac{\partial \overline{B}}{\partial t} - \overline{M} \\ \nabla \times \overline{H} &= \frac{\partial \overline{D}}{\partial t} + \overline{J} \\ \nabla \cdot \overline{B} &= m \\ \nabla \cdot \overline{D} &= q_v \end{aligned} \tag{2-1}$$

where $\overline{J}$ is the electric current density, $\overline{M}$ is the magnetic current density, q_v is the electric charge density, m is the magnetic charge density, and

$$\begin{aligned} \overline{B} &= \mu\overline{H} \\ \overline{D} &= \varepsilon\overline{E} \end{aligned} \tag{2-2}$$

If the sources creating the fields are single frequency sinusoids (time-harmonic), then equations (2-1) may be written in the frequency domain as

$$\begin{aligned} \nabla \times \overline{E} &= -j\omega\mu\overline{H} - \overline{M} \\ \nabla \times \overline{H} &= j\omega\varepsilon\overline{E} + \overline{J} \\ \nabla \cdot \overline{B} &= m \\ \nabla \cdot \overline{D} &= q_v \end{aligned} \tag{2-3}$$

where ω is the (radian) frequency of the sources and an $\exp(j\omega t)$ time dependence is assumed.

In order to completely describe the problem to be solved, both Maxwell's equations and appropriate boundary conditions on the fields are needed. If the scatterer and all sources are located within a finite distance from a fixed origin, $r = 0$, the fields $\overline{E}$ and $\overline{H}$ are required to satisfy the Silver - Müller radiation condition[10]

$$\lim_{r\to\infty}\{\overline{r} \times (\nabla \times \overline{E}) + jk\overline{E}\} = 0$$

$$\lim_{r\to\infty}\{\overline{r} \times (\nabla \times \overline{H}) + jk\overline{H}\} = 0$$

uniformly in $\hat{r}$. In the case of plane wave incidence, where the sources are at infinity, it is necessary to separate the incident fields from the scattered fields; the scattered fields are required to satisfy (2-4). For two-dimensional problems, equations (2-4) must be replaced by

$$\lim_{\rho\to\infty} \rho^{\frac{1}{2}}\left(\frac{\partial E_z}{\partial \rho} - jkE_z\right) = 0$$

$$\lim_{\rho\to\infty} \rho^{\frac{1}{2}}\left(\frac{\partial H_z}{\partial \rho} - jkH_z\right) = 0 \qquad (2\text{-}5)$$

uniformly in $\hat{\phi}$.

In addition to the boundary conditions at infinity of (2-4) and (2-5), the fields must satisfy other conditions at material boundaries (surfaces of obstacles where there is a discontinuity in ε and/or μ). At the interface of two media the tangential fields satisfy[11]

$$\hat{n} \times \{\overline{H}_a - \overline{H}_b\} = \overline{J}_s$$

$$\{\overline{E}_a - \overline{E}_b\} \times \hat{n} = \overline{M}_s \qquad (2\text{-}6)$$

where $\hat{n}$ is the unit normal directed from medium b to medium a. (See Figure 1.) Equations (2-6) apply whether there is a discontinuity or not. If ε and μ are finite in both regions a and b, and if the conductivity of both regions is finite, no induced surface current can result. Thus, tangential components of $\overline{E}$ and $\overline{H}$ are continuous across any material boundary, perfect conductors excepted[12]. In the case where region b is a perfect electric conductor, equations (2-6) reduce to[13]

$$\hat{n} \times \overline{H} = \overline{J}_s$$

$$\hat{n} \times \overline{E} = 0 \qquad (2\text{-}7)$$

There is some disagreement in the literature as to whether equations (2-6) and (2-7) should be called boundary conditions. Stratton[14] considers equations (2-6) as a vector form of the boundary

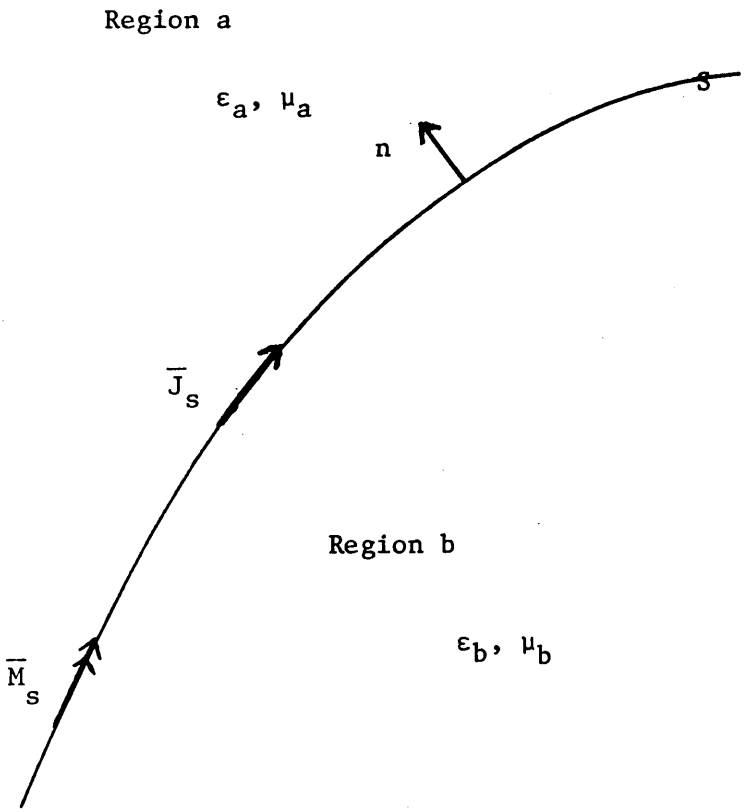

Figure 1. Surface currents at the interface of two media.

conditions associated with the Robbin boundary value problem[15]

$$\alpha\psi + \frac{\partial\psi}{\partial n} = 0 \qquad (2\text{-}8)$$

and equations (2-7) as the vector form of the boundary conditions associated with the Dirichlet (2-7b) or Neumann (2-7a) boundary value problems. Harrington[16] considers equations (2-6) to be manifestations of singularities in the fields that are caused by discontinuous permittivity and/or permeability. Regardless of the terminology, it is necessary to consider (2-6) or (2-7) as well as the radiation condition in any scattering problem because the differential form of Maxwell's equations (2-3) fails at the obstacle boundary due to discontinuities in ϵ and/or μ.

It is often convenient for mathematical purposes to consider the abrupt boundaries at obstacle surfaces to be the limiting cases of continuous, but rapid, change in the characteristics from medium a to medium b. By carefully making this approximation it may be possible to avoid some mathematical problems later on.

2.2.2 Definition of Scattering

Scattering is the particular formulation of an electromagnetics problem that allows one to describe the influence of an object on an impresses, or incident, field by the difference in the resultant and incident fields. This difference is defined as the scattered field.[17]

Referring to Figure 2, consider the problem of sources radiating in the presence of an obstacle. Define the incident or impressed

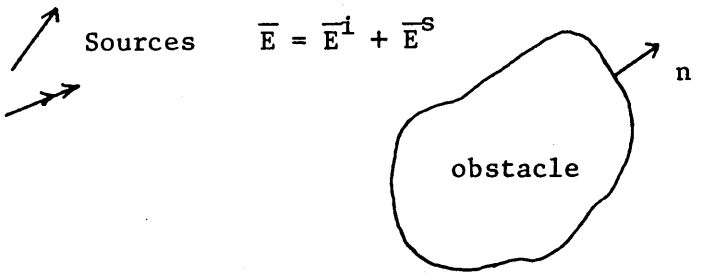

(a)

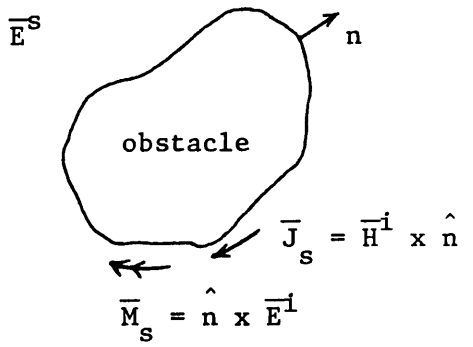

(b)

Figure 2. Illustration of the Induction Theorem. (a) original problem, (b) induction equivalent

field as the field supported by the sources with the obstacle not present, and denote these fields by $\overline{E^i}$ and $\overline{H^i}$. It is assumed that all sources are exterior to the obstacle in this formulation. If this is not so, then the problem may still be worked as a scattering problem by using the equivalence principle[18] to transfer the internal sources into currents along the surface of the obstacle. Then it is possible to use superposition and add the resultant fields together. By uniqueness[19] we know that the solution that is obtained will be the same as a solution obtained by other methods.

Define the scattered field as the difference between the field with the obstacle present ($\overline{E}$, $\overline{H}$) and the incident field.

$$\begin{aligned} \overline{E^s} &= \overline{E} - \overline{E^i} \\ \overline{H^s} &= \overline{H} - \overline{H^i} \end{aligned} \tag{2-9}$$

Since ($\overline{E}$, $\overline{H}$) and ($\overline{E^i}$, $\overline{H^i}$) have the same sources (external to the object), the scattered field is a source-free field external to the object.

An equivalent problem may now be posed. With the obstacle present assume that the total field ($\overline{E}$, $\overline{H}$) exists within it, and the scattered field ($\overline{E^s}$, $\overline{H^s}$) exists outside it. Both fields are source-free within their respective regions. In order for this to be, equations (2-6) demand that surface currents must exist on the surface of the obstacle, and these currents are defined by

$$\begin{aligned} \overline{J}_s &= \hat{n} \times \{\overline{H^s} - \overline{H}\} \\ \overline{M}_s &= \{\overline{E^s} - \overline{E}\} \times \hat{n} \end{aligned} \tag{2-10}$$

By substituting (2-9) into (2-10) we obtain[20]

$$\overline{J_s} = \overline{H^i} \times \hat{n}$$
$$\overline{M_s} = \hat{n} \times \overline{E^i} \qquad (2\text{-}11)$$

While this work has not decreased the complexity of the problem, it has at least shifted it. Even though the surface currents $\overline{J_s}$ and $\overline{M_s}$ are known (assuming $\overline{E^i}$ and $\overline{H^i}$ are known), it is not possible to calculate the magnetic and vector potentials directly and solve for $\overline{E^s}$ and $\overline{H^s}$ since the obstacle is still present. (This would not be true if we happened to know the Green's Function for this particular object.) The motivation behind the work in this section is to shift the difficulty to calculating the scattered fields rather than the total field. In addition simplifications occur if the object is of a particular shape[21].

2.2.3 Two-Dimensional Scattering

To take advantage of many simplifications and to avoid some unnecessary details, the equations for two-dimensional fields will be presented separately. A convenient way to think of these problems is to visualize solving three-dimensional problems with no variation in the "z" cartesian coordinate. Any coordinate may be chosen, but for consistency, the z-coordinate will be used throughout the remainder of this dissertation. A discussion of three-dimensional scattering will be delayed until the next section.

An arbitrary electromagnetic field can be expressed as the sum of a transverse magnetic (TM) part and a transverse electric (TE) part.

The TM field has only components of $\overline{H}$ transverse to z; the TE field has only components of $\overline{E}$ transverse to z. For two-dimensional fields in isotropic media, the TM field has only a z-component of $\overline{E}$, and the TE field has only a z-component of $\overline{H}$. This allows vector field problems to be reduced to equivalent scalar problems, simplifying the mathematics considerably.

It should be remembered that the curl and divergence operators now contain only derivatives with respect to x and y since nothing varies with z. Assuming no magnetic sources, the curl of the first Maxwell equation (2-3) is

$$\nabla \times \nabla \times \overline{E} = -j\omega(\nabla \times \mu\overline{H})$$
$$= -j\omega(\nabla\mu \times \overline{H} + \mu\nabla \times \overline{H}) \qquad (2\text{-}12)$$

For a homogeneous medium, $\nabla\mu = 0$. By substituting (2-3b) for $\nabla \times \overline{H}$ in (2-12) we obtain

$$\nabla \times \nabla \times \overline{E} = -j\omega\mu\{j\omega\epsilon\overline{E} + \overline{J}\} \qquad (2\text{-}13)$$

or

$$\nabla(\nabla \cdot \overline{E}) - \nabla^2\overline{E} = \omega^2\mu\epsilon\overline{E} - j\omega\mu\overline{J} \qquad (2\text{-}14)$$

Define $k = \omega\sqrt{\mu\epsilon} = 2\pi/\lambda$. In a homogeneous medium, $\nabla \cdot \overline{E} = q_v$, and we have

$$\nabla^2\overline{E} + k^2\overline{E} = j\omega\mu\overline{J} + \nabla q_v \qquad (2\text{-}15)$$

where ∇^2 operates on the rectangular components of $\overline{E}$. This is the (homogeneous) Helmholtz or wave equation.

By taking the curl of (2-3b) and following the same procedures as above we may obtain the Helmholtz equation for $\overline{H}$ (in a homogeneous medium).

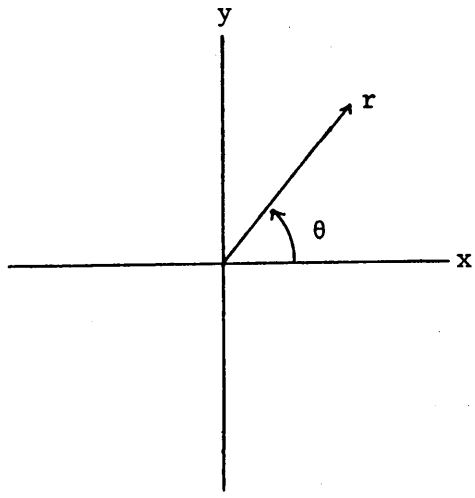

(a)

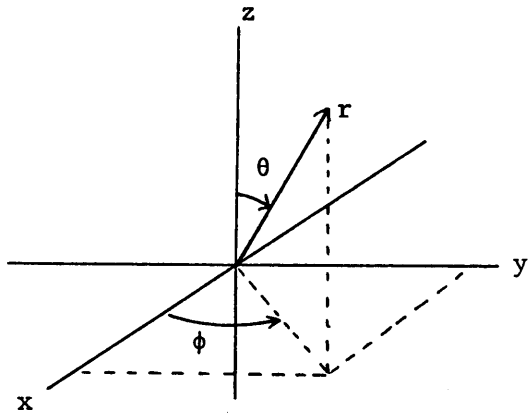

(b)

Figure 3. Coordinate system variables. (a) two dimensions, (b) three dimensions.

$$\nabla^2\overline{H} + k^2\overline{H} = -\nabla \times \overline{J} \tag{2-16}$$

For TM fields, $\overline{E} = E_z(x,y)\hat{z}$ and $\overline{J} = J_z(x,y)\hat{z}$ simplifying (2-15) to the scalar wave equation in E_z.

$$\nabla^2 E_z + k^2 E_z = j\omega\mu J_z \tag{2-17}$$

For TE fields, $\overline{H} = H_z(x,y)\hat{z}$ and (2-16) simplifies to

$$\nabla^2 H_z + k^2 H_z = 0 \tag{2-18}$$

since $\nabla \times (J_z\hat{z})$ will have no z-component.

If the medium is inhomogeneous, more care must be taken in deriving equations (2-17) and (2-18). Assume now that $\varepsilon = \varepsilon(x,y)$. (In two dimensions, ε is constant with respect to z.) Then $\nabla \cdot \overline{E}$ is not necessarily zero.

Equation (2-14) is true in general. For the inhomogeneous case we wish to find an expression for $\nabla \cdot \overline{E}$. For a source free region $q_v = 0$ and

$$\nabla \cdot \overline{D} = 0 = \nabla \cdot (\varepsilon\overline{E}) = \nabla\varepsilon \cdot \overline{E} + \varepsilon\nabla \cdot \overline{E}$$

$$\nabla \cdot \overline{E} = -(\nabla\varepsilon \cdot \overline{E})/\varepsilon \tag{2-19}$$

But $\nabla\varepsilon(x,y)$ will have only components transverse to $\overline{E}$ in two dimensions. Therefore, for TM fields $\nabla \cdot \overline{E} = 0$, and (2-17) may be written as

$$\nabla^2 E_z + k^2(x,y)E_z = j\omega\mu J_z \tag{2-20}$$

where $k^2 = k^2(x,y) = \omega^2\mu\varepsilon(x,y)$.

For TE fields, a different approach must be used. In taking the curl of (2-3b) the term $\nabla \times (\varepsilon\overline{E})$ appears. This may be expanded as

$$\nabla \times \varepsilon\overline{E} = \varepsilon(\nabla \times \overline{E}) + \nabla\varepsilon \times \overline{E} \tag{2-21}$$

The $\nabla \times \overline{E}$ term may be replaced by $-j\omega\mu\overline{H}$ as before, but the other term, $\nabla\varepsilon \times \overline{E}$, must be dealt with. The steps in the derivation are as follow:

$$\nabla \times \nabla \times \overline{H} = j\omega\epsilon(\nabla \times \overline{E}) + j\omega\epsilon_o \nabla\epsilon_r \times \overline{E}$$

$$\nabla(\nabla \cdot H) - \nabla^2\overline{H} = j\omega\epsilon(-j\omega\mu\overline{H}) + \nabla\epsilon_r/\epsilon_r \times j\omega\epsilon\overline{E}$$

$$-(\nabla^2 H_z)\hat{z} = k_o^2\epsilon_r H_z\hat{a} + \nabla\epsilon_r/\epsilon_r \times (\nabla \times H_z\hat{z} - J_z\hat{z})$$

$$\nabla^2 H_z\hat{z} + \nabla\epsilon_r/\epsilon_r \times (\nabla H_z \times \hat{z}) + k_o^2\epsilon_r H_z\hat{z} = 0$$

$$\nabla^2 H_z - \nabla\epsilon_r/\epsilon_r \cdot \nabla H_z + k_o^2\epsilon_r H_z = 0$$

$$\nabla^2 H_z - \frac{\epsilon_r \nabla\epsilon_r \cdot \nabla H_z}{\epsilon_r^2} + k_o^2\epsilon_r H_z = 0$$

$$\nabla^2 H_z + \epsilon_r \nabla\left(\frac{1}{\epsilon_r}\right) \cdot \nabla H_z + k_o^2\epsilon_r H_z = 0$$

$$\frac{1}{\epsilon_r}\nabla^2 H_z + \nabla\left(\frac{1}{\epsilon_r}\right) \cdot \nabla H_z + k_o^2\epsilon_r H_z = 0$$

$$\nabla \cdot \left(\frac{1}{\epsilon_r}\nabla H_z\right) + k_o^2 H_z = 0 \qquad (2\text{-}22)$$

If the inhomogeneity occurs in μ rather than ϵ, similar equations may be derived.

The more general case of both $\epsilon = \epsilon(x,y)$ and $\mu = \mu(x,y)$ may be expressed as

$$\frac{1}{\epsilon_r}\nabla \cdot \left(\frac{1}{\mu_r}\nabla E_z\right) + k_o^2 E_z = \frac{j\omega\mu_o J_z}{\epsilon_r} \qquad (2\text{-}23)$$

for TM fields, and

$$\frac{1}{\mu_r}\nabla \cdot \left(\frac{1}{\epsilon_r}\nabla H_z\right) + k_o^2 H_z = 0 \qquad (2\text{-}24)$$

for TE fields.

Finally, if the medium possesses fintie conductivity, σ, a conduction current $\overline{E}$- field, $\overline{J} = \sigma\overline{E}$, must be added to (2-3b).

$$\begin{aligned}\bar{H} &= j\omega\epsilon\bar{E} + \sigma\bar{E} + \bar{J} \\ &= j\omega(\epsilon - j\sigma/\omega)\bar{E} + \bar{J} \\ &= j\omega\epsilon_o(\epsilon_r' - j\epsilon_r'')\bar{E} + \bar{J}\end{aligned} \tag{2-25}$$

where $\bar{J}$ now represents source currents, not conduction currents, and a complex relative permittivity has been defined as

$$\epsilon_r = \epsilon_r' - j\epsilon_r'' \tag{2-26}$$

with $\epsilon_r' = \epsilon_r$ and $\epsilon_r'' = \sigma/\omega$ [22]. By making this definition, equations (2-23) and (2-24) still are valid with complex permittivity representing finite conductivity.

To finish describing the problem to be solved, appropriate boundary conditions must be stated in addition to the differential equation. These were discussed in section (2.2). However more than one formulation is possible for a particular problem.

As an example consider TM scattering from a perfectly conducting cylinder. One set of boundary conditions might be that $\bar{E}^s = -\bar{E}^i$ on the cylinder surface ($\bar{E} = \bar{E}^s + \bar{E}^i$ there) and $\bar{E}^s$ satisfies the radiation condition at infinity. An alternative formulation might require that $\bar{E}^s = 0$ on the surface of the cylinder, satisfy the radiation condition at infinity, but also introduce a delta-function current on the surface of the cylinder that would appear in equation (2-23). This second formulation is a result of applying the induction theorem to the first formulation. While it might be more difficult to solve the second formulation analytically due to the delta-function current, the second formulation should not be ignored since some numerical methods are more efficient using it rather than the first formulation.

2.2.4 Three-Dimensional Scattering

The differential equations for three-dimensional scattering are quite a bit more difficult to solve for inhomogeneous media. However the Helmholtz equation for a homogeneous medium is derived from Maxwell's equations in the same manner that has been done for two-dimensional problems. We will have

$$\begin{aligned} \nabla^2\overline{E} + k^2\overline{E} &= j\omega\mu\overline{J} \\ \nabla^2\overline{H} + k^2\overline{H} &= -\nabla \times \overline{J} \end{aligned} \tag{2-27}$$

But because of the three-dimensional nature of the problem, we do not have a clear choice on which coordinate to base TM and TE fields. Two possibilities are TM and TE to z and TM and TE to r[23]. One of these may be chosen, or it may be more convenient not to separate the field[24]. Any symmetry in geometry may dictate the proper choice. Objects with spherical symmetries require TM and TE to r separations if it is desired to solve uncoupled scalar partial differential equations as in the two-dimensional case[25]. The biconical antenna with azimuthal symmetry requires the solution of[26]

$$\begin{aligned} &\frac{\partial^2\psi}{\partial r^2} - \frac{\partial}{\partial r}(\ln\varepsilon)\frac{\partial\psi}{\partial r} + \frac{1}{r^2}\left[\frac{-\partial}{\partial\theta}(\ln\varepsilon) - \cot(\theta)\right]\frac{\partial\psi}{\partial\theta} \\ &\qquad + \frac{1}{r^2}\frac{\partial^2\psi}{\partial\theta^2} + k^2\psi = 0 \end{aligned} \tag{2-28}$$

where $\psi = r \sin\theta H_\phi$ subject to appropriate boundary conditions. For inhomogeneous bodies of revolution with ε and μ independent of the ϕ-coordinate, it is necessary to solve a pair of coupled scalar partial differential equations[27].

$$\sin\theta D_R(\varepsilon_r f_m R^2 D_R\psi_1) + D_\theta(\varepsilon_r f_m \sin\theta D_\theta\psi_1) + \varepsilon_r/\sin\theta$$
$$+ m(D_\theta f_m D_R\psi_2 - D_R f_m D_\theta\psi_2) = 0$$

$$\sin\theta D_R(\mu_r f_m R^2 D_R\psi_2) + D_\theta(\mu_r f_m \sin\theta D_\theta\psi_2) + \mu_r/\sin\theta$$
$$+ m(D_R f_m D_\theta\psi_1 - D_\theta f_m D_R\psi_1) = 0 \qquad (2\text{-}29)$$

where the fields have exp (jmϕ) axial variation and

$$R = k_o r$$
$$f_m(R,\theta) = (\varepsilon_r\mu_r R^2\sin^2\theta - m^2)^{-1} \qquad (2\text{-}30)$$

and E and H are derivable from ψ_1 and ψ_2.

But for a general three-dimensional scatterer, the best that can be done with differential equations is to write down the vector Helmholtz equations

$$\nabla \times \nabla \times \overline{E} - k^2\overline{E} = -j\omega\mu\overline{J}$$

and $\qquad (2\text{-}31)$

$$\nabla \times \nabla \times \overline{H} - k^2\overline{H} = \nabla \times \overline{J}$$

with boundary conditions suitable for the particular problem to be solved. We now must solve three simultaneous, three-dimensional, partial differential equations, a dubious undertaking at best.

2.2.5 Integral Equation Formulation of the Scattering Problem

The last section showed that while two-dimensional scattering problems may be reduced to equivalent scalar problems, the only three-dimensional problems that reduce to scalar problems are those that possess certain symmetries. The more general three-dimensional

problems must be solved by the simultaneous solution of three partial differential equations.

An alternative mathematical model of a scattering problem may be obtained by the use of integral equations rather than differential equations. There are two integral equation formulations of the scattering problem in use: the Electric Field Integral Equation(EFIE), which is better suited to thin wire objects, and the Magnetic Field Integral Equation (MFIE) which is better suited to more bulky objects[28]. While the analytic solution of an integral equation formulation may be no easier than solving the equivalent differential equation formulation, the more approximate (and practical) numerical solutions may be easier to handle. In fact, most of the more recent numerical methods for solving scattering problems rely on the integral equation formulation rather than the differential equation formulation. First two-dimensional integral equation formulations will be presented, then three-dimensional formulations.

In section (2.2.3) the scalar Helmholtz equation (2-17) was derived to describe TM fields in a homogeneous medium. Integral equation solutions may then be obtained by first finding the field from a two-dimensional point source, and integrating over all sources. The field at $\bar{\rho} = x\hat{x} + y\hat{y}$ due to a point current I at $\bar{\rho}' = x'\hat{x} + y'\hat{y}$ is[29]

$$E_z = \frac{-k\eta}{4} I H_o^{(2)}(k|\bar{\rho} - \bar{\rho}'|) \qquad (2\text{-}32)$$

where $\eta = \sqrt{\mu/\varepsilon} \simeq 120\pi$ is the intrinsic impedance of free space and $H_o^{(2)}$

is the Hankel function of the second kind, zero, order. A general solution is obtained by superposition.

$$E_z(\bar{\rho}) = \frac{-k\eta}{4} \iint J_z(\bar{\rho}')H_o^{(2)}(k|\bar{\rho} - \bar{\rho}'|)\, dS' \tag{2-33}$$

where the integration is over the cylinder currents J_z. See Figure 4. In this formulation both E_z and J_z are unknown. If the scatterer is of infinite conductivity, then (2-33) may be specialized to

$$E_z^i(\bar{\rho}) = \frac{k\eta}{4} \int_C J_z(\bar{\rho}')H_o^{(2)}(k|\bar{\rho} \quad \bar{\rho}'|)\, dl' \qquad \rho \text{ on } C \tag{2-34}$$

and since $E_z^i = -E_z^s$ on the boundary of the scatterer. Thus equation (2-34) is an integral equation describing the unknown surface currents J_z in terms of the known incident E-field, E_z^i. In the case of dielectric cylinders equation (2-34) may be modified to

$$E_z^i = \frac{J_z}{j\omega(\epsilon-\epsilon_o)} - \frac{k\eta}{4} \iint_S J_z(\bar{\rho}')H_o^{(2)}(k|\bar{\rho} - \bar{\rho}'|)\, dS' \tag{2-35}$$

where now the integration must be performed over the entire region S, and J_z is the polarization current rather than the conduction current.

In the case of TE fields, the integral equations are written in terms of H_z. The scattered field is related to its sources by[30]

$$H_z^s = \hat{z} \cdot \nabla \times \frac{1}{4j} \int_C J\, H_o^{(2)}(k|\bar{\rho} - \bar{\rho}'|)\, d\bar{l}' \tag{2-36}$$

where $d\bar{l}'$ designates the direction of J. For conducting cylinders we may write[31]

$$J = -(H_z^i + \hat{z} \cdot \nabla \times \int_{C^+} J\, H_o^{(2)}(k|\bar{\rho} - \bar{\rho}'|)d\bar{l}') \tag{2-37}$$

or

$$-H_z^i = J + \hat{z} \cdot \nabla \times \int_{C^+} J\, H_o^{(2)}(k|\bar{\rho} - \bar{\rho}'|)\, d\bar{l}' \tag{2-38}$$

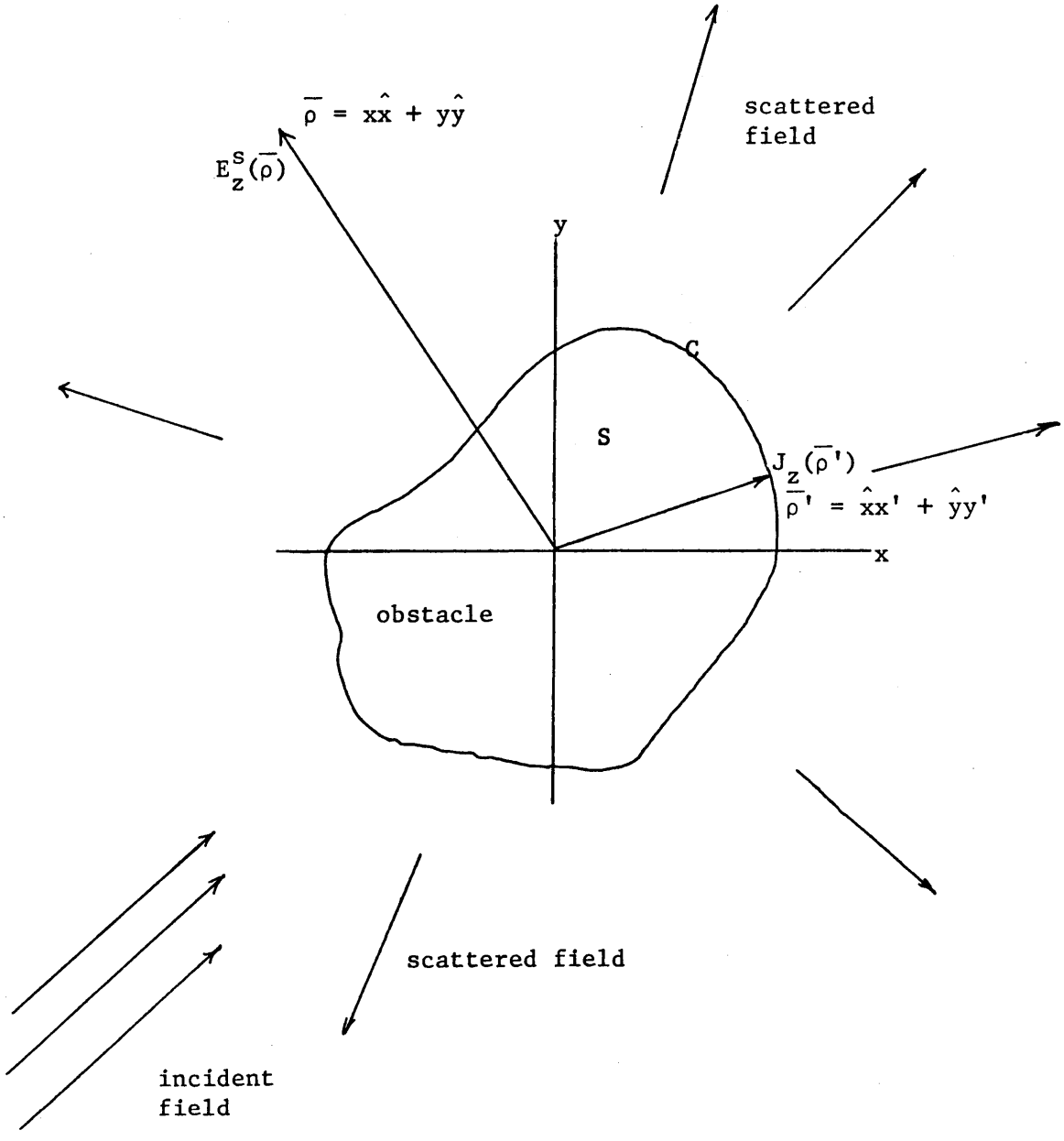

Figure 4. The two-dimensional scattering problem.

where C^+ indicates that the integration is performed just external to S. In the case of dielectric TE scattering we have[32]

$$j\omega\mu \iint_S J(\bar{\rho}')H_o^{(2)}(k|\bar{\rho} - \bar{\rho}'|)dS' + \nabla\left(\frac{1}{\varepsilon} \iint_S \left(\frac{-1}{\omega} \nabla \cdot \bar{J}\right) H_o^{(2)}(k|\bar{\rho} - \bar{\rho}'|)dS'\right) + \frac{kn}{4} \iint_S \bar{J}(\bar{\rho}')H_o^{(2)}(k|\bar{\rho} - \bar{\rho}'|)dS' = 0 \qquad (2\text{-}38)$$

In the case of three-dimensional scattering one obtains the following equations when the scatterer is a perfect electric conductor[33].

$$\hat{n} \times \bar{E}^i(\bar{r}) = \frac{\hat{n}}{4\pi j\omega\varepsilon} \times \int_S (-\omega^2\mu\varepsilon\bar{J}_s\phi + \nabla'_s \cdot \bar{J}_s\phi')dS' \qquad \text{(EFIE)} \qquad (2\text{-}39)$$

$$\bar{J}_s(\bar{r}) = 2\hat{n} \times \bar{H}^i(\bar{r}) + \frac{\hat{n}}{2\pi} \times \int_S \bar{J}_s \times \nabla'\phi dS' \qquad \text{(MFIE)}$$

where

$$\phi = \frac{e^{-jk|\bar{r}-\bar{r}'|}}{|\bar{r}-\bar{r}'|} \qquad (2\text{-}40)$$

and $\bar{r}$ is on the surface S. Either of these equations can be used to solve for the equivalent surface current. The Electric Field Integral equation is ideally suited for thin cylinders and wire antennas. The Magnetic Field Integral Equation is best suited for large, smooth conductors since geometrical factors often make the integral of secondary importance[34].

If the scatterers are dielectric bodies, equations (2-39) become[35]

$$\hat{n} \times \bar{E}^i(\bar{r}) = \hat{n}/4\pi \times \int_S \{j\omega\mu\bar{J}_s(\phi_1+\phi_2) + \bar{K}_s \times \nabla'(\phi_1+\phi_2)$$

$$+ \frac{1}{j\omega\epsilon} \nabla'_s \cdot \bar{J}_s \nabla'(\phi_1 + \frac{\epsilon_1}{\epsilon_2}\phi_2)\} dS' \qquad \text{(EFIE)}$$

$$\hat{n} \times \bar{H}^i(\bar{r}) = \hat{n}/4\pi \times \int_S \{j\omega\epsilon\bar{K}_s(\phi_1+ \frac{\epsilon_2}{\epsilon_1}\phi_2) - \bar{J}_s \times \nabla'(\phi_1+\phi_2)$$

$$+ \frac{1}{j\omega\mu} \nabla'_s \cdot \bar{K} \nabla'(\phi_1+\phi_2)\} dS' \qquad \text{(MFIE)} \qquad (2\text{-}41)$$

where

$$\bar{J}_s = \hat{n} \times \bar{H}$$

$$\bar{K}_s = -\hat{n} \times \bar{E}$$

$$\phi_i = \frac{e^{-jk_i|\bar{r}-\bar{r}'|}}{|\bar{r}-\bar{r}'|} \qquad (2\text{-}42)$$

$$k_i = \omega\sqrt{\mu\epsilon_i}$$

$$\hat{n}_2 = -\hat{n}_1$$

Each of the equations (2-41) represent four equations in four unknowns. While it appears that the symbolic representation of the problem is more complicated than the partial differential equation it represents, it is sometimes easier to formulate a numerical solution technique to the integral equation form.

2.3 Digital Computer Concepts

Any "new" method for solving electromagnetic scattering problems should take into account the technology available in computing, especially the limitations of present-day high-speed digital computers, when formulating the mathematics of such a method. The most elegant

theoretical technique will be of little practical use unless one has the computing ability to produce results efficiently for specific cases of interest.

2.3.1 Digital Computer Resource Limitations

The three main resource limitations of today's digital computer are finite word length, finite core storage area, and, for all practical purposes (and pocketbooks), finite execution time. The finite word length limitation manifests itself in roundoff and truncation errors, thus limiting the accuracy of an otherwise sound algorithm. As an example, the inverse of a 300 x 300 matrix may be obtained in a reasonable amount of time by using Gauss elimination methods. However, the results of such an undertaking will probably be rendered worthless by the roundoff and truncation errors that occur during arithmetic operations. Furthermore, available computer storage will limit the size of the problem that can be solved. A typical large-scale computer system such as the IBM 370/158 in use at Virginia Polytechnic Institute and State University limits the user to about 512K bytes, the amount required to store a 700 x 700 matrix without resorting to prohibitively slow offline storage. Finally, execution time will limit the user in the scope of porblem to be solved especially if the problem posed is not well-suited to serial computation.

2.3.2 Digital Computer Characteristics

Despite the above disadvantages, the digital computer has assumed

a lion's share of the computer market. A list of general characteristics of digital computers is given next[36].

1. Handling of dependent variables, and indeed all data within the computer, in quantized or discretized form.

2. Serial operation, involving the time-sharing of all operational and memory units, only one or a limited number of operations being carried out at one time.

3. Accuracy relatively independent of the quality of system components and determined primarily by the number of bits contained in memory registers and by the specific numerical technique selected for a specific problem.

4. Solution times relatively long and determined by the complexity (i.e., the number of arithmetic operations required for the solution) of a problem.

5. Ability to "trade off" solution time and accuracy, i.e., to reduce errors inherent in the computer solution by increasing the length of time required to obtain the solution on the computer.

6. Ability to perform a limited number of arithmetic operations including particularly addition and multiplication; more complex operations such as integration and differentiation must be performed by approximate (numerical) techniques.

7. Facility for memorizing numerical and nonnumerical data indefinitely.

8. Facility to perform logical operations and decisions utilizing numerical as well as nonnumerical data.

9. Facility for floating-point operation, thereby eliminating scale-factor problems.

10. Programming techniques, often bearing little direct relationship to the engineering problem under study, but facilitated by compilers and special interpretive routines.

11. Facility for automatically altering and controlling the topology of the data flow within the machine on the basis of calculations.

2.4 Analog Computer Characteristics

The chief distinction between analog and digital computers is the way in which the dependent variables are handled within the computer. In analog machines, the dependent variables appear in continuous form and may be recorded with as many significant figures as the quality of the circuit components permit (usually about 0.1% of full scale). In digital computers, all variables appear in discrete form, and the accuracy of the data which are manipulated depends on the word length of the computer as discussed in section 2.3.1.

As a direct result of the difference in handling the data within the machine, the basic organization of analog and digital computers developed along different lines. Consequently, there is a different set of characteristics associated with analog computer systems:[37]

1. Dependent variables within the machine treated in continuous form.
2. Accuracy limited by the quality of the computer components, and rarely better than 0.01% of full-scale for electronic equipment.
3. Parallel operation, with all computational elements operating simultaneously.
4. High-speed or "real-time" operation, with computing speeds limited primarily by the bandwidth characteristics of the computing elements, and not by the complexity of the problem.
5. Ability to perform efficiently such operations as multiplication, addition, integration, and nonlinear function generations; on the other hand, very limited ability to make logical decisions, store numerical data, provide extended time delays, and handle nonnumerical information.

6. Programming techniques which consist largely of substituting analog computing elements for corresponding elements in a physical system under simulation, i.e., providing computer elements having transfer characteristics analogous to those of the original system under study.

7. Facility for including analog hardware from a system under study in the computer simulation.

8. Provisions to permit the engineer to experiment by adjusting coefficient settings on the computer, thereby gaining direct insight into system operation.

The limitations of an analog computer system differ from those of the digital computer and generally fall into three categories -- (1) hardware limitations in the number of computing elements, (2) control functions such as mode control, and (3) simulation of digital elements.

2.5 Hybrid Computer Characteristics

Hybrid computer techniques represent an effort to combine in one computer system some of the characteristics normally associated with analog computer systems and some of the characteristics associated with digital computer systems in order to obtain the best of both worlds. In a more narrow sense, hybridization involves the actual interconnecting of analog and digital portions within the system through a suitable interface. The following are the chief motivations for interconnecting analog and digital computers:[38]

1. To combine the speed of an analog computer with the accuracy of the digital computer.

2. To permit the use of system hardware in a digital simulation.

3. To increase the flexibility of an analog simulation by using digital memory and control.

4. To increase the speed of a digital computation by utilizing analog subroutines.

5. To permit the processing of incoming data which are partially discrete and partially continuous.

By far, the most widespread application for hybrid computer systems has been in the simulation of physical systems. A mathematical model of the system to be studied is first formulated, and the equations constituting this model are programmed on a hybrid computer. Since both analog and digital computing elements are present, most of the time a great reduction in computer time can be realized in assigning variables to a particular portion of the machine depending upon how they occur in nature. Hybrid computer systems may be used in the solution of general electromagnetics problems in that the continuous nature of the analog portion of the system may eliminate the large matrices usually needed if the problem is to be studied on a purely digital machine. However, to date little work has been done in this area.

CHAPTER III

PRESENTATION OF SCATTERING SOLUTION TECHNIQUES

3.1 Introduction

This chapter will present some of the better known techniques for solving electromagnetic scattering problems. The various techniques are divided into six categories:

1. Analytical Methods
2. Moment Methods
3. Subsectional Methods
4. Probabilistic Methods
5. Analog/Hybrid Methods
6. Integral Equation Methods

The divisions are completely arbitrary, and one method may fit into several categories. For example, the method of moments is listed under Moment Methods because of its mathematical formulation. However, when used in practice, the method of moments frequently solves integral equations using subsectional basis functions.

Only a survey of scattering methods is presented. This chapter does not claim to have listed all methods or even all categories of methods, but it is hoped that a broad enough cross section of methods has been included so that a basis of comparison for any "new" method might be obtained.

The format that will be used with each method is to first present a description of the method. Then in some cases, a practical example

of a scattering problem will be worked using the method. If an example is not worked, references are given where one might look in the literature for examples that have been worked in detail. Finally, comments on the effectiveness of the method, its advantages and disadvantages will be made. In order to avoid unnecessary complications with the mathematics, only two-dimensional scattering problems will be given as examples. It is frequently stated at this point in most papers that only a minor extension of the method is needed to enable one to use it in higher dimensions. This may be mathematically correct, but practically unfeasible due to computational limitations[39]. Such limitations will be discussed with each method.

3.2 Numerical Solution Methods

The mathematical formulations which will be presented are of little use unless they can be reduced to forms which can provide information about the physical problem being studied. The procedure of solving an electromagnetics problem may be divided into three basic steps[40]. First it is necessary to present in mathematical form the relationship between the physical quantities involved. In electromagnetics this is done through Maxwell's equation (2-2) with assumptions appropriate to the problem being solved (e.g., allowing for a spatial dielectric variation in inhomogeneous media). Other assumptions are made tacitly, such as assuming a linear, time-invarient madium at rest so that relativistic effects may be neglected.

A second step in the solution involves specifying the spatial

behavior of various field and source quantities required by the scattering obstacles. This procedure may utilize various simplifying approximations, such as assuming a metallic scatterer has perfect conductivity, even though these assumptions may not be physically exact.

The final step in solving the problem is that of reducing the mathematical "recipe" to a numerical result. Regardless of the theoretical formulation, it ultimately becomes necessary to resort to numerical computation for all but the most trivial problems. The relative effectiveness of the procedures outlined below depends on how well they are adaptable to numerical computation. Consequently, emphasis will be given to those techniques which are best suited to numerical algorithms.

3.3 Analytical Methods

Analytic solutions are available for scattering from only a few simple shaped objects. Exact solutions are possible only for the separable geometries or the so-called Wiener-Hopf geometries, of which there are only a few. There are a number of techniques, such as the low- and high-frequency expansions and ray-optical methods, that extend the scope of the analytical solutions. However, even with these additional tools, the range of application of analytical methods remains considerably limited. On the other hand, the analytical methods, when applicable, offer efficiency of computation, superior accuracy, physical insight to the problem, and so on[41]. Frequently it is possible to combine analytical and numerical techniques, especially

for problems that are "close" to the Weiner-Hopf geometries. Instead of getting to the final numerical computations, usually matrix inversion, as soon as possible, one is sometimes able to derive an auxiliary matrix equation by performing a certain amount of analytical preprocessing. For instance, the size of the matrix needed for a given accuracy may be smaller, the routines may have built-in convergence checks, or the asymptotic behavior of the fields may be guaranteed in the neighborhood of obstacle surfaces, edges, and corners[42]. It is difficult to reproduce this behavior using a strictly numerical approach. Some examples of this "hybrid" method are given in Mittra[43].

Although several analytic attacks on a given problem may be feasibly pursued, there may be a significant variation in the computational effort required to obtain results of comparable accuracy.

3.3.1 Separation of Variables

The method of separation of variables, or the so-called product method, is a useful analytical technique in electromagnetic scattering when the geometry of the scatterer coincides with a coordinate system in which the Helmholtz equation is separable. (It has been shown by Eisenhart[44] that the Helmholtz equation is separable in eleven three-dimensional coordinate systems.) This constrains the geometry of the scatterer severely, but when the geometries of the scatterer and a separable coordinate system do coincide, it is possible to obtain a series solution to the Helmholtz equation in terms of known functions.

As an example consider separating the two-dimensional Helmholtz equation in the polar coordinate system of Figure 3a. (This example is chosen because the results will be used later in Chapter IV.) In a homogeneous medium the Helmholtz equation becomes

$$\nabla^2\psi + k^2\psi = 0 \tag{3-1}$$

or

$$\frac{1}{\rho}\frac{\partial}{\partial\rho}\left(\rho\frac{\partial\psi}{\partial\rho}\right) + \frac{1}{\rho^2}\frac{\partial^2\psi}{\partial\phi^2} + k^2\psi = 0 \tag{3-2}$$

where $\psi = H_z$ for TE fields and $\psi = E_z$ for TM fields. Assuming a separable solution of the form

$$\psi = R(\rho)\Phi(\phi) \tag{3-3}$$

we obtain the following equation by substituting (3-3) into (3-2) and dividing by ψ.

$$\frac{1}{\rho R}\frac{d}{d\rho}\left(\rho\frac{dR}{d\rho}\right) + \frac{1}{\rho^2\Phi}\frac{d^2\Phi}{\phi^2} + k^2 = 0 \tag{3-4}$$

Multiplying by ρ^2 gives

$$\frac{\rho}{R}\frac{d}{d\rho}\left(\rho\frac{dR}{d\rho}\right) + \frac{1}{\Phi}\frac{d^2\Phi}{d\phi^2} + k^2\rho^2 = 0 \tag{3-5}$$

The second term in (3-5) is independent of ρ, and the other terms are independent of ϕ. Therefore we may write

$$\frac{1}{\Phi}\frac{d^2\Phi}{d\phi^2} = -n^2 \tag{3-6}$$

and

$$\rho\frac{d}{d\rho}\left(\rho\frac{dR}{d\rho}\right) + (k^2\rho^2 - n^2)R = 0 \tag{3-7}$$

The two solutions of (3-6) are the sinusoids $\sin(n\phi)$ and $\cos(n\phi)$; the

two solutions of (3-7) are Bessel functions. For exterior problems the appropriate Bessel functions are the Hankel functions $H_n^{(1)}(k\rho)$ and $H_n^{(2)}(k\rho)$. To satisfy the radiation condition (2-5), only $H_n^{(2)}(k\rho)$ is acceptable for outgoing waves with $\exp(j\omega t)$ time dependence. Therefore the most general solution to this problem would be

$$\psi(\rho,\phi) = \sum_{n=0}^{\infty} (A_n \cos(n\phi) + B_n \sin(n\phi)) H_n^{(2)}(k\rho) \qquad (3\text{-}8)$$

where A_n and B_n may be determined by a Fourier series expansion of ψ on the circular boundary of the scatterer.

Numerically, the solution (3-8) is never exact since an infinite summation is involved. However, the number of terms needed for any desired accuracy may be found quite simply by observing the behavior of $\{A_n\}$ and $\{B_n\}$.

The extension of this method to a suitable three-dimensional coordinate system involves separating ψ into three single-variable functions and obtaining a series such as (3-8) containing summation over two indices. For three-dimensional scattering from a sphere, the usual choices of expansion functions are the associated Legendre polynomials and the modified spherical Bessel functions.

3.3.2 Conformal Mapping

As shown in the last section, the exact solution of two-dimensional scattering problems is known for only a few simple shapes. For more general shapes, various approximation methods have been developed that require a certain degree of smoothness of the boundary, usually the

continuity of the curvature.

Certain types of singularities of the boundary can be handled by carefully mapping the region which is exterior to the scatterer into another region with a geometrically simpler boundary[45]. Such a conformal transformation preserves the right angle between the direction of propagation of the wave and the wavefront. The scattered field satisfies a transformed wave equation and boundary conditions; the radiation condition remains invariant. This transformed boundary value problem can be formulated in terms of a Fredholm integral equation of the second kind[46]. Hong and Goodrich[47] have solved this equation for scattering by an almost circular cylinder with a smooth surface and by a circular cylinder with discontinuities in the surface. Applications of conformal mapping to some other problems may be found in the literature.[48-52]

Conformal mapping may not be used in three-dimensional studies because it is based on complex variable theory which is a two-dimensional technique.

3.3.3 Other Analytical Methods

Many other analytical methods abound. Geometrical optics, physical optics, Keller's theory, the Luneburg-Kline expansion, etc. have all played an important role in high frequency scattering. It is not the purpose of this dissertation to comment on all methods, but to concentrate on those methods leading to numerical solutions of scattering problems at frequencies where either low frequency (quasi-

static) or high frequency approximations fail. A good summary of other analytical methods may be found in the literature.[53,54]

3.4 Moment Methods

3.4.1 The Method of Moments

It has been said that the unifying concept in the treatment of radiation and scattering problems is the method of moments[55]. This general approach is essentially a reduction of an integral equation to a system of linear algebraic equations which describe a "nearby" problem. Credit for this technique is usually given to Harrington[56] by electromagneticists, but the method of moments is really an extrapolation made by Harrington of the more mathematically sound Rayleigh-Ritz-Galerkin variational method[57]. This is not to say that the method of moments technique of Harrington is not useful. Quite to the contrary, the method of moments has been heralded as one of the most important breadthroughs in electromagnetics numerical techniques. And indeed the volume of papers published (circa. 1968 - 1975) bears witness to this statement. However, the method of moments technique requires that the kernels of the integral equations involved by Hermitian in order for the theory of Raleigh-Ritz methods to hold. Since the kernels of almost all scattering problems are complex-symmetric[58], data obtained by Harrington's moment methods must be scrutinized to see if it actually describes the phenomenum being investigated. Mittra[59] provides some suggestions on how accuracy checks might be made.

The method of moments will be described here since it is more popular for electromagnetics problems than some of the other variational methods. A description of other variational methods may be found in the literature.[60,61] The discussion that follows is a general procedure for solving linear equations as given by Harrington.

Consider the inhomogeneous equation

$$L(f) = g \tag{3-9}$$

where L is a linear operator, g is a known function, and f is to be determined. In electromagnetics, L is frequently the partial differential equations (2-23) and (2-24) or an integral equation such as equations (2-35) and (2-36). Let f be expanded in a series of functions f_n in the domain of L, as

$$f = \sum_n \alpha_n f_n \tag{3-10}$$

where $\{\alpha_n\}$ are constants to be determined. The $\{f_n\}$ are called expansion functions. For approximate solutions, (3-10) is usually a finite summation. Substituting (3-10) into (3-9) and using the linearity of L, we have

$$\sum_n \alpha_n L(f_n) = g \tag{3-11}$$

Now define a set of weighting functions $\{w_m\}$ in the range of L, and take the inner product of (3-11) with each w_m. The result is

$$\sum_n \alpha_n \langle w_m, Lf_n \rangle = \langle w_m, g \rangle \qquad m = 1,2,3,\ldots \tag{3-12}$$

This may be written in matrix form as

$$(l_{mn})(\alpha_n) = (g_m) \tag{3-13}$$

where

$$(l_{mn}) = \begin{bmatrix} \langle w_1, Lf_1 \rangle & \langle w_1, Lf_2 \rangle & \cdots \\ \langle w_2, Lf_1 \rangle & \langle w_2, Lf_2 \rangle & \cdots \\ & \vdots & \end{bmatrix} \tag{3-14}$$

$$(\alpha_n) = \begin{bmatrix} \alpha_1 \\ \alpha_2 \\ \vdots \end{bmatrix} \qquad (g_m) = \begin{bmatrix} \langle w_1, g \rangle \\ \langle w_2, g \rangle \\ \vdots \end{bmatrix} \tag{3-15}$$

If the matrix (l) is nonsingular its inverse $(l)^{-1}$ exists, the $\{\alpha_n\}$ are given by

$$(\alpha_n) = (l_{mn})^{-1} (g_m) \tag{3-16}$$

and the problem is solved. This solution may be exact or approximate, depending upon the choice of the $\{f_n\}$ and $\{w_m\}$.

One of the main tasks of any moment methods problem is the selection of the $\{f_n\}$ and $\{w_m\}$. Some of the factors which affect this choice are given by Harrington.[62]

1. The accuracy of solution desired
2. The ease of evaluation of the matrix elements
3. The size of the matrix that can be inverted
4. The realization of a well conditioned matrix

Unfortunately, computer limitations frequently require the selection of $\{f_n\}$ and $\{w_m\}$ on the basis of (2) and (3) above with little regard to (1) or (4). It is at this point that the method of moments usually

breaks down, especially when it is used in the solution of large-scale scattering problems. Nonetheless, the method of moments has provided solutions of acceptable quality to many problems that were hard or impossible to cope with using other methods.

Examples of scattering problems abound in the literature. The example of TM scattering from conducting cylinders will be given here since this formulation will be used later.

Consider the perfectly conducting cylinder in Figure 5. Using boundary conditions (2-7) with the integral equation (2-33) we may obtain

$$E_z^i(\bar{\rho}) = -E_z^s(\bar{\rho}) = \tfrac{1}{4}k\eta \int_C J_z(\bar{\rho}') \, H_o^{(2)}(k|\bar{\rho}-\bar{\rho}'|)dl' \qquad (3\text{-}17)$$

with $\bar{\rho}$ on C, where E_z^s is known on the cylinder surface and J_z is the unknown current to be determined. The simplest numerical solution may be obtained by using pulse functions for the basis $\{f_n\}$ and delta functions for the $\{w_m\}$. Referring to Figure 5, the scatterer contour is divided into N segments ΔC_n. That is,

$$f_n(\bar{\rho}) = \begin{cases} 1 & \text{on } \Delta C_n \\ 0 & \text{elsewhere} \end{cases} \qquad (3\text{-}18)$$

Letting $J_z = \sum_{n=1}^{N} \alpha_n f_n$ will give a crude but useful approximation to the actual surface current present. Substituting into (3-17) gives the matrix equation

$$(l_{mn})(\alpha_n) = (g_m) \qquad (3\text{-}19)$$

with

$$g_m = E_z^i(x_m, y_m) \qquad (3\text{-}20)$$

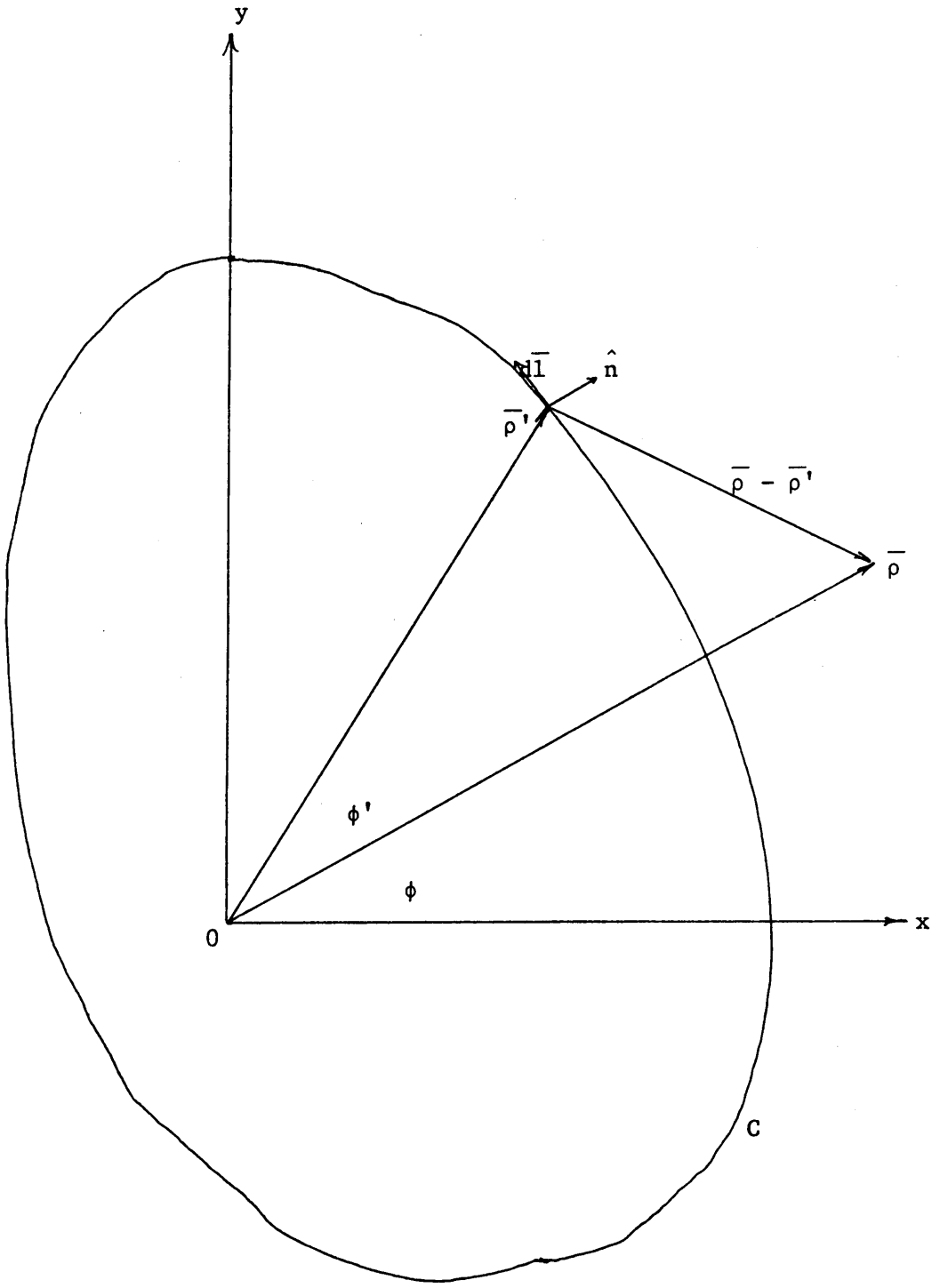

Figure 5. Cross section of a cylinder and coordinate system.

and

$$l_{mn} = \tfrac{1}{4}k\eta\int_{\Delta C_n} H_o^{(2)}\left(k\sqrt{(x-x_m)^2+(y-y_m)^2}\right)dl' \qquad (3\text{-}21)$$

There is no simple analytic expression for (3-21). While it is possible to numerically integrate (3-21) over each C_n, computer time considerations usually prohibit doing so. A crude approximation to (3-21) may be obtained by treating an element $J_z\ C_n$ as a filament of current when $m \neq n$, giving

$$l_{mn} = \tfrac{1}{4}k\eta\Delta C_n H_o^{(2)}\left(k\sqrt{(x_n-x_m)^2+(y_n-y_m)^2}\right) \qquad (3\text{-}22)$$

When $m = n$, the Hankel function has an integrable singularity, and the integral (3-21) must be evaluated more carefully. For this, ΔC_n is approximated by a straight line and the small argument formula is used for $H_o^{(2)}$.

$$H_o^{(2)} \simeq 1 - \frac{j2}{\pi}\ln\left(\frac{\gamma z}{2}\right) \qquad (3\text{-}23)$$

where $\gamma = 0.5772...$ is Euler's constant. An evaluation of (3-21) using (3-23) gives

$$l_{nn} = \tfrac{1}{4}k\eta\Delta C_n\left(1 - \frac{j2}{\pi}\ln\left(\frac{\gamma k\Delta C_n}{4e}\right)\right) \qquad (3\text{-}24)$$

where $e = 2.71828...$ It should be pointed out that because of the above approximations the solution of the algebraic problem will not converge to the exact solution as N is increased.

To illustrate the accuracy that can be obtained by such a crude numerical approximation, the results of plane-wave scattering from an ellipse (Figure 6) are presented. The g_m elements become

$$g_m = E_z^i(x_m,y_m) = \exp(jk\{x_m\cos\phi_i+y_m\sin\phi_i\}) \qquad (3\text{-}25)$$

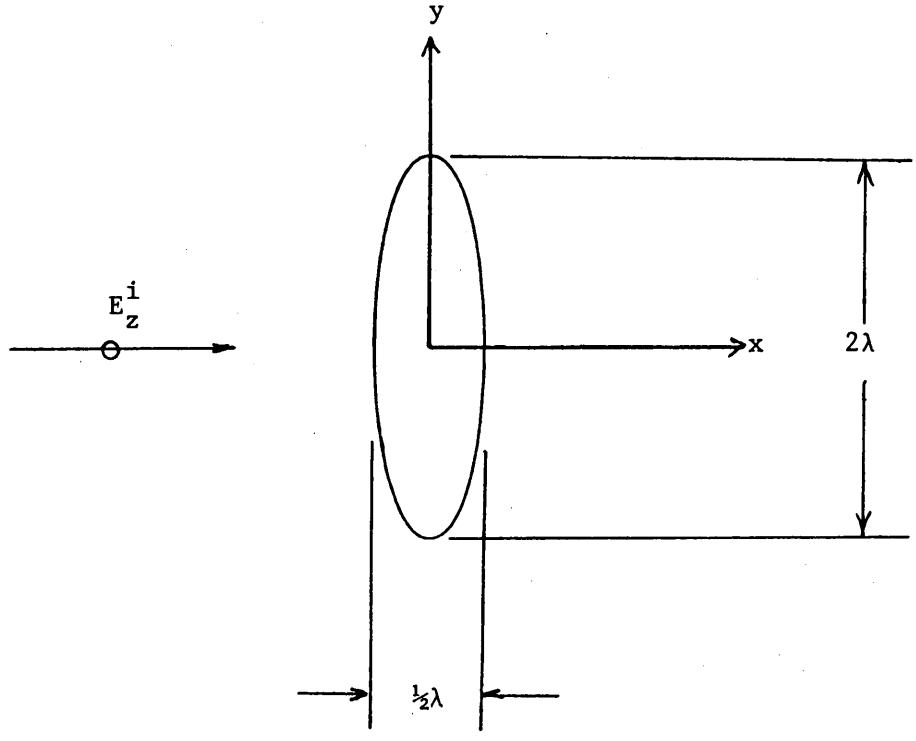

Figure 6. Cross section of an elliptical cylinder.

where ϕ_i is the angle of incidence of the TM field. The scattering cross section,

$$\sigma(\rho) = 2\pi\rho \left| \frac{E^s(\rho)}{E^i} \right|^2 \qquad (3\text{-}26)$$

and surface current J_z, as computed by Andreasen and the above formulas, are illustrated in Figure 7. As predicted above, the calculated current J_z differs somewhat because of the approximations made. However the scattering cross section of the method of moments solution is almost identical with the scattering cross section computed by Andreasen. This is because σ is insensitive to small variations in J_z.

It has been shown that one may obtain meaningful results using moment methods even with such crude approximations as pulse-function bases and delta-function (point matching) weighting. It was stated that it was necessary to use these approximations in order to conserve computer resources. Unfortunately even this is not enough in higher dimensional problems. The example just given was a one-dimensional problem, i.e., integration along the contour of the cylinder. Two- and three-dimensional problems require the solution of much larger matrices. Consider the example of TM scattering from a dielectric cylinder. Now the operator of (3-9) is a two-dimensional integral over the entire area of the scatterer[63]. Thus, this is a two-dimensional problem. The increase in matrix size needed to solve this problem may be estimated as follows. Suppose it is determined that N match points per wavelength are needed for a solution to yield acceptable results. Then while a one-dimensional problem would require the solution of an N x N matrix

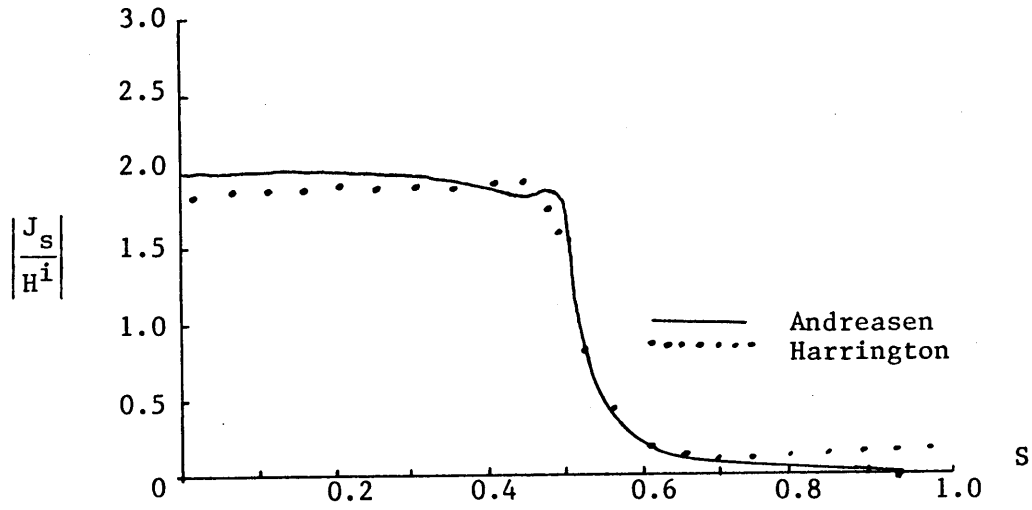

Figure 7a. Current density on a conducting elliptic cylinder excited by a plane wave, TM case.

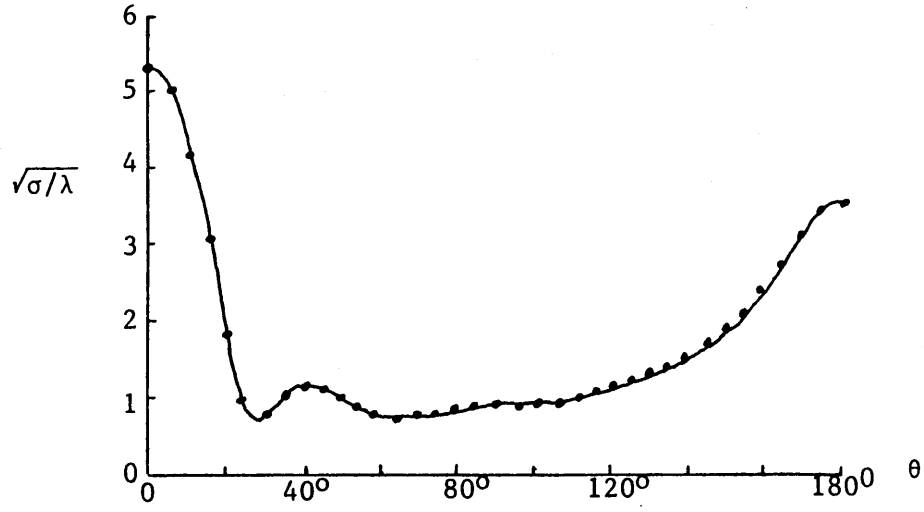

Figure 7b. Scattered field pattern for a conducting cylinder excited by a plane wave, TM case.

problem, an equivalent two-dimensional problem would require the inversion of an $N^2 \times N^2$ matrix. A simple two-dimensional scattering problem such as a perfectly conducting cylinder that would require a 50 x 50 matrix might require a 2500 x 2500 matrix if the scatterer were a dielectric instead. For three-dimensional scattering, $N^3 \times N^3$ or 125000 x 125000 matrices would have to be dealt with. Obviously, we do not have the computers to handle 1000 x 1000 matrices, much less the larger matrices required in higher dimensions. Thus, while the method of moments might provide acceptable solutions in one dimension, it would fail miserably when the size or complexity of the scatterer was increased.

There have been two spin-offs of the method of moments which have addressed this difficulty, and both of these will be considered next.

3.4.2 Characteristic Modes

In considering the advantages and disadvantages of various basis functions that might be used in a method of moments problem, one might ask whether or not there exists a "best" choice of functions. Until a definition of "best" is made the question must go unanswered, but there indeed does exist one set of functions that are at least "very good." They are called "characteristic modes."

These functions have several useful mathematical properties. First, they characterize the scatterer shape independent of any specific excitation. Secondly, they are orthogonal, thus the power scattered by each mode may be considered independently of any other mode. The

orthogonality of these modes also makes it practical to consider large scatterers since the matrices involved will be diagonal. It is then a trivial matter to invert the diagonal matrix, regardless of its size.

The concept of characteristic modes is not new, for they have long been used in the analysis of radiation and scattering by conducting bodies whose surfaces coincide with one of the coordinate systems in which the Helmholtz equation is separable. (See section 3.3.1) Garbacz[64] proposed that such modes exist for perfectly conducting objects of arbitrary shape. He later succeeded in finding the characteristic modes for several simple cases[65]. However, the calculation of the individual modes remained quite tedious until Harrington and Mautz[66] approached the characteristic mode problem from the moment method viewpoint. The result was that general formulas were derived which permitted the calculation of characteristic modes of arbitrary bodies in a relatively straightforward manner. In 1973, Marin tackled the characteristic mode problem from an integral equation theory point of view[67]. Using Fredholm determinant theory he solved the resultant magnetic field integral equation and showed that[68]

A. There exist two types of singularities (modes):
   1. Singularities of the source (incident field)
   2. Singularities of the object

B. There exist an infinite number of modes. However, they occur at discrete frequencies.

C. For perfect conductors, only simple modes (poles) exist.

D. Dielectric scatterers possess characteristic modes,

also, in the complex frequency domain.

Many scattering problems have been solved using characteristic modes that were previously beyond the reach of the method of moments or other numerical methods. Harrington and Mautz have solved for the scattered fields from bodies of revolution such as the cone-sphere, wire objects such as a wire arrow and a dipole, and planar objects such as the disk[69].

The number of modes obtained is limited only by the speed and storage capabilities of the computer, not by inherent computational difficulties. It should be noted that for irregularly shaped objects the majority of the computing time is spent, not on calculating the characteristic modes, but in determining the boundaries of the object.

Characteristic modes have been most widely used in wire antenna studies. Thiele[70] and others have calculated characteristic modes for various wire objects and found that good agreement is obtained with other solution techniques, in particular, the method of moments using Galerkin's method. Marin's paper[71] points out that general three-dimensional objects will be difficult to handle, even with all the theory that has so far been developed. However, if time is spent on the analytical work necessary, a representation of transient scattered fields may be obtained.

In summary, characteristic mode theory has been developed to a point where many problems beyond the reach of the method of moments may now be solved. The matrices involved in the calculation of the scattered fields are large, but diagonal. Thus they are trivial to

invert. Despite this breakthrough, many scattering problems cannot be solved by this method because computer resources limit the complexity and/or size of the scatterer. This is not a limitation on matrix inversion, but on the actual calculation of the individual characteristic modes. Straightforward as it may be, this calculation still takes a great deal of time and effort. However, once the modes have been calculated, the scattering due to any source field may be found.

3.4.3 The Unimoment Method

One of the most promising solution techniques to be introduced in the past several years is the unimoment method[72]. Developed in late 1974 by Dr. K. K. Mei, it is an extension of the method of moments. The significant advantage of the unimoment method over the method of moments is that, when applied to scattering problems, it decouples the exterior scattering problem from the interior boundary value problem(s). This is done by solving an interior problem many times so that N linearly independent solutions are generated. The continuity conditions are then enforced by a linear combination of the N independent solutions. This may be accomplished by matrix inversion. The size of the matrices involved are quite small compared to standard method of moments techniques; thus a substantial reduction of computer time may be obtained. Since use of this method will be made in future chapters, the development of the method will be discussed in detail.

Consider the problem of scattering by the arbitrary (two-dimension-

al) object shown in Figure 8. If the scatterer is a perfect conductor, the mathematical problem is to solve the scalar Helmholtz equation subject to the illuminating field ϕ^{inc} such that

$$\phi = \phi^{inc} + \phi^{scat} = 0 \tag{3-27}$$

on the boundary of the object and that ϕ satisfies the radiation condition as $r \to \infty$. If the object is a dielectric scatterer, the scalar Helmholtz equation is solved such that ϕ and $\partial\phi/\partial n$ are appropriately related on the boundary C and that the radiation condition holds at infinity.

In order to implement the unimoment method it is necessary to construct an imaginary surface C' exterior to C where, if ϕ and $\partial\phi/\partial n$ were known on C', a convenient representation for ϕ exterior to C' could be developed. In two dimensions the simplest such surface is a circle which completely encloses the scatterer. (See Figure 9.) The total field exterior to C', ϕ^o, may be represented by[73]

$$\phi^o(r,\theta) = \sum_{n=0}^{\infty} (A_n^e \cos(n\theta) + A_n^o \sin(n\theta)) H_n^{(2)}(kr) \tag{3-28}$$

assuming $\exp(j\omega t)$ time dependence and a homogeneous medium exterior to C'. A_n^e and A_n^o are related to the Fourier coefficients of the function ϕ on C' by the factor $H_n^{(2)}(ka)$, where a is the radius of C'. This assumes that ϕ is sufficiently smooth on C' that the Fourier series converges, and the rest of this section will be limited by this constraint.

If three-dimensional problems are to be considered, the surface C' may be chosen to be a sphere in which case the field exterior to C'

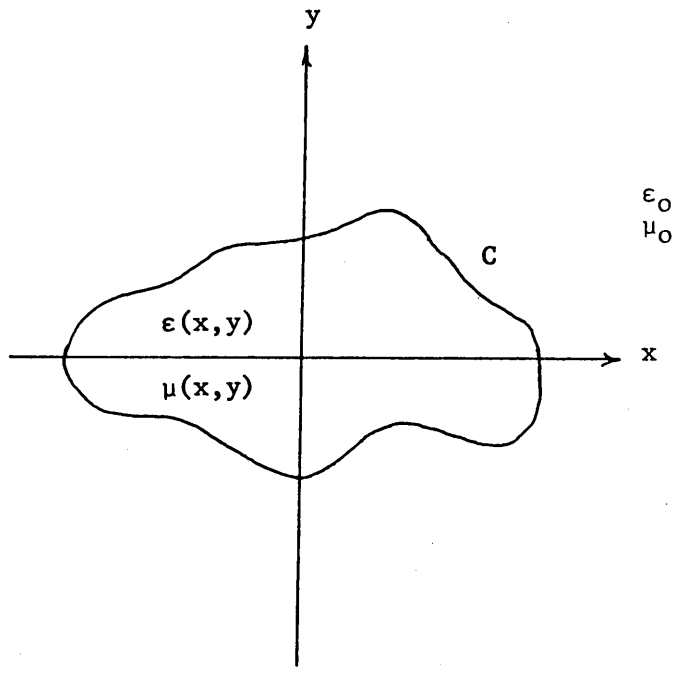

Figure 8. Finite two-dimensional scatterer in free space.

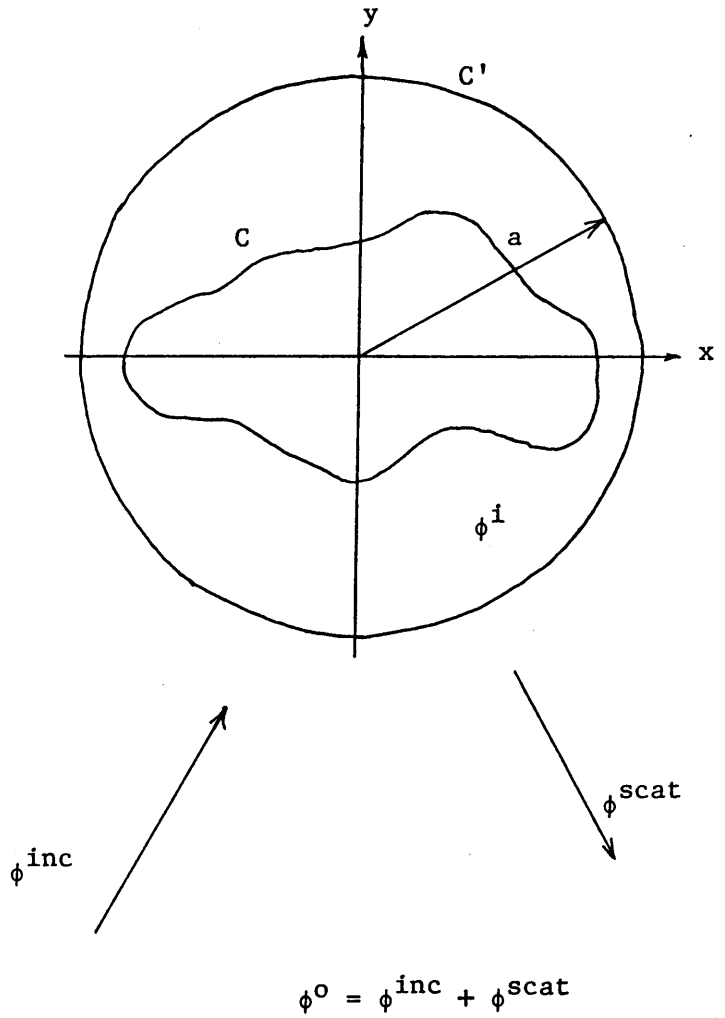

$$\phi^o = \phi^{inc} + \phi^{scat}$$

Figure 9. Scatterer C surrounded by a circle of radius a.

may be written as a double summation of associated Legendre polynomials and modified spherical Hankel functions[74].

The method continues by postulating a set of trial functions $\{\psi_i\}_{i=1}^{2N}$ which solve the Helmholtz equation interior to C' for different boundary conditions $\{\psi_i(C')\}$. After each solution ψ_i is obtained, the normal derivative $\partial\psi_i/\partial n$ may be calculated. An approximation to the complete solution $\phi(a,\theta)$ (on C') may be found by representing the complete interior solution ϕ^i by

$$\phi^i = \sum_{i=1}^{2N} a_i\psi_i \quad \text{and} \quad \partial\phi^i/\partial n = \sum_{i=1}^{2N} a_i\partial\psi_i/\partial n \tag{3-29}$$

Since the function pairs $\{\psi_i\}$ and $\{\partial\psi_i/\partial n\}$ are obtained from the solutions of the wave equation inside C', enforcing the continuity of $\{\psi_i\}$ and $\{\partial\psi_i/\partial n\}$ across C' will be sufficient to determine the expansion coefficients.

Assuming that the $\{\psi_i\}$ have been found it is only necessary to calculate $\{a_i\}_1^{2N}$, $\{A_n^e\}_0^N$, and $\{A_n^o\}_1^N$ for the "best" representation of the exterior solution ϕ^o. This may be done by either collocation (point matching) or the method of weighted functions, either of which results in having to solve 4N+1 linear equations. For fairly regular objects, N is small and on the order of min(2ka, ka+15)[75].

The successful application of the unimoment method depends on how fast the trial function pairs $\{\psi_i\}$ and $\{\partial\psi_i/\partial n\}$ can be generated. Mei considered several possible solution techniques for the function pairs, all of which required the solution of the Helmholtz equation in the region interior to C' even though only the derivatives along C' were

needed. His work included using finite-element methods, finite difference methods, shooting methods, and Ricatti transformations.[76,77] The results that Mei gives in his publications use finite differences with Ricatti transformations. Finite difference methods will be discussed in a later section. While he did not consider objects other than those that fit into a separable coordinate system or those that were in some sense "close" to a separable coordinate system, Mei obtained results that agreed with previously measured and calculated data, and he obtained these results with very little computing time.

In summary, the power of the unimoment method is great in that a typical exterior scattering problem is reduced to solving several much simpler interior boundary value problems. It is then possible to replace integral equations with finite difference or finite element equations. The disadvantage of the unimoment method is the lack of solution techniques available for computing the trial function pairs $\{\psi_i\}$, $\{\partial\psi_i/\partial n\}$. For objects that are more irregular than those that Mei discusses, a further limitation is imposed in that it is difficult to locate the finite-difference modes. This is not a limitation of the unimoment method, but a limitation in the finite-difference -- finite-element solution techniques. Mei suggests that the power of the unimoment method will be further enhanced when better solution techniques of solving sparse matrices are found. Even this will not eliminate the node point location difficulty, however.

3.5 Subsectional Methods

3.5.1 Finite Difference Methods

Because of the discrete nature of the digital computer, any computer solution of differential equations requires discretization of all the variables. One of the more obvious and well-known techniques employing this is the method of finite differences. Briefly, a linear differential equation, or system of equations, is transformed into a discrete operator equation by replacing all derivatives with a discrete approximation. For example, $u'(x)$ in $u'(x) + au(x) = 0$ might be replaced by

$$\frac{u(x+\frac{1}{2}h) - u(x-\frac{1}{2}h)}{h} \tag{3-30}$$

where the interval in which the solution is desired is divided into h equal pieces. Of course, as $h \to 0$, this approximation becomes exact. Higher order derivatives are replaced by similar discrete approximations.

Consider the problem of solving

$$\begin{aligned} &u''(x) + au'(x) + bu(x) = 0 \\ &u(0) = 0 \qquad u(1) = A \end{aligned} \tag{3-31}$$

where a and b are known and may be functions of x. To solve this equation on a digital computer it is necessary to divide the interval $[0,1]$ into N equal segments of length $h = 1/N$. Then define $x_i = ih$. If $u''(x)$ and $u'(x)$ are replaced by the finite difference approximations

$$u''(x) = \frac{u(x_{i+1}) + u(x_{i-1}) - 2u(x_i)}{h^2}$$

$$u'(x) = \frac{u(x_{i+1}) - u(x_{i-1})}{h} \qquad (3\text{-}32)$$

we will obtain a set of simultaneous equations

$$\frac{u(x_{i+1}) + u(x_{i-1}) - 2u(x_i)}{h^2} + a(x_i)\frac{u(x_{i+1}) - u(x_{i-1})}{2h}$$

$$+ b(x_i)u(x_i) = 0 \qquad (i = 1,2,3,\ldots) \qquad (3\text{-}33)$$

which may be solved by standard matrix methods. As h is decreased, the finite difference solution approaches the true solution u(x), and the size of the matrix increases.

This technique may be extended to higher dimensions. The two-dimensional Helmholtz equation may be written in finite difference form for each node point i as

$$\phi_{i+N} + \phi_{i+1} + (k^2h^2-4)\phi_i + \phi_{i-1} + \phi_{i-N} = 0 \qquad (3\text{-}34)$$

where the points i are shown in Figure 10, and the step size h is the distance between any two adjacent points along either the x or the y axis. Again, the problem is reduced to the problem of solving MN linear equations.

Finite difference methods have been used primarily in the solution of interior problems[79] because of the difficulties encountered in considering the infinite region of an exterior problem and enforcing the radiation condition at infinity. Recent work by Mei et al.[80], Silvester and Hsieh[81], and McDonald and Wexler[82] has essentially pointed the way to incorporate the radiation condition into finite

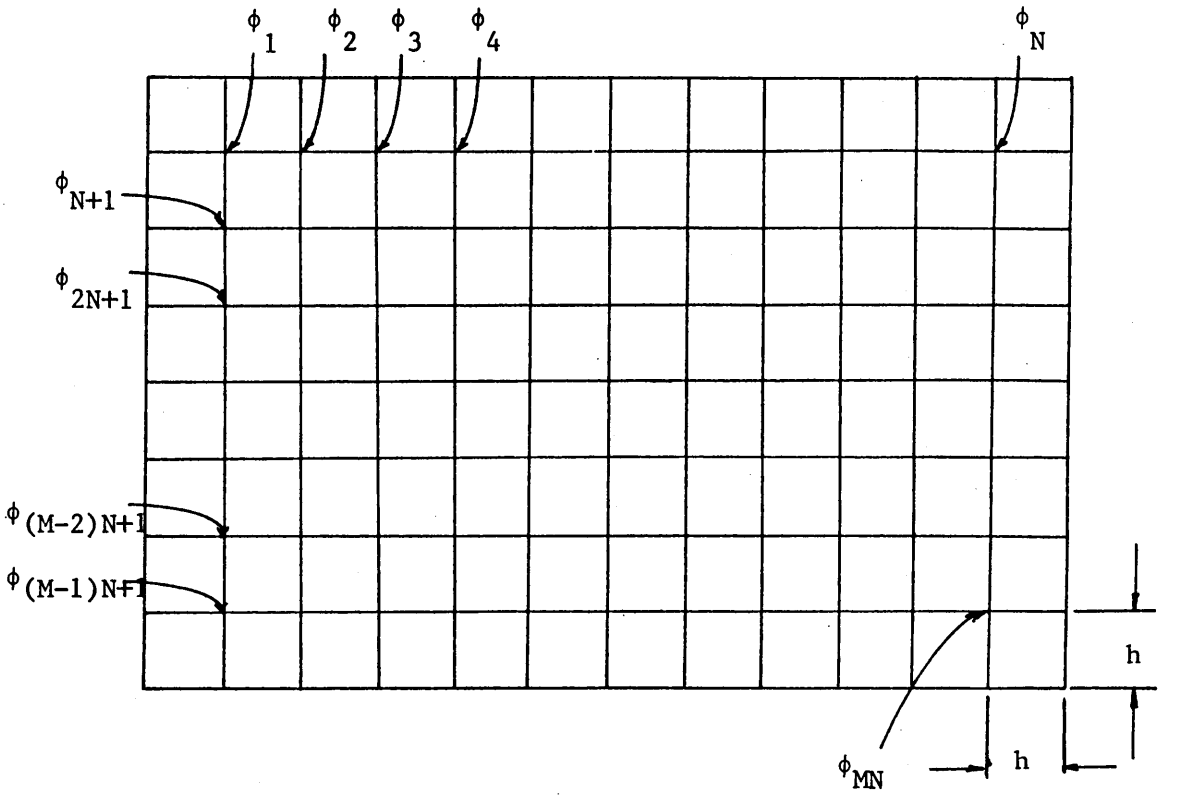

Figure 10. Finite difference grid for a rectangular region, M=7, N=11.

difference methods, but the required computation does not make the finite difference method competitive with other methods.

Another computational difficulty arises when the domain of the problem is of irregular shape. Then it is necessary (1) to modify equations (3-34) near the boundary of the region and (2) to devise a method of locating mesh points near the boundary. The second difficulty may be overcome by entering each mesh point location as data, but this soon becomes impractical for large-scale scatterers. Then the only method left is computer calculation of each mesh point. When this becomes necessary, frequently more computer time is spent in calculating point locations than in solving the problem itself.

A further practical limitation is the tremendous amount of computer storage and execution time needed for higher-dimensional problems. For example, if in Figure 10, M = 50 and N = 25, then 1250 simultaneous equations must be solved -- one for each node point. To store the matrix would require 1562500 memory locations. This is beyond the limits of most computing systems, so slower offline storage must be used. In addition, direct inversion of these large matrices is impractical, and iterative methods are slow and always diverge when the source frequency is higher than a critical value, usually the lowest resonant frequency of the finite difference region[83]

When a small interior problem must be solved, such as the ones in the previous section, finite difference methods become quite practical. Mei obtained good results for scattering from several two-dimensional objects using finite differences with Ricatti transformations and the

unimoment method[84]. It should be remembered, however, that the problems that Mei tackled were small compared with a wavelength.

It is disappointing to note that in spite of the great amount of work done, in practice the solution of many problems exhausts the capabilities of modern digital machines. Forsythe and Wasow have estimated one week for a problem having 10,000 nodes, a not unrealistic number. A three-dimensional problem solved in fine detail could easily take 1000 years!

3.5.2 The Finite Element Method

The finite element method can be described as a variational technique using piecewise polynomials to approximate the solution to a differential equation. Suppose that the problem to be solved is in variational form -- it may be required to find the function u that minimizes a given expression of potential energy. This minimizing property leads to a differential equation for u (the Euler equation), but normally an exact solution is impossible to obtain, and some approximation is necessary. The traditional Rayleigh-Ritz-Galerkin approach is to choose a finite number of trial functions $\psi_1,\ldots,\psi_N$, and among their linear combinations $\sum q_j\psi_j$ to find the one which is minimizing. The unknown coefficients q_j are determined by a system of N discrete algebraic equations. The minimizing process automatically seeks out the combination which is closest to the exact solution. Therefore, the goal is to choose the trial functions ψ_j which are convenient enough for the potential energy to be computed and minimized, and at the same time

general enough to approximate closely the unknown solution u. It is the first condition that is the motivation for finite elements.

The underlying idea is similar to finite differences. It starts with a subdivision of the region of physical interest into smaller pieces. Then within each piece the trial functions are given an extremely simple form. Normally they are polynomials. If the subregions are carefully chosen, then the boundary conditions between adjacent regions are much easier to enforce than boundary conditions along a more complicated boundary. Usually in two-dimensions the subregions are rectangles or triangles. The accuracy of the approximation may be increased, if necessary, not by including more complicated trial functions, but by making further subdivisions. (This is the same technique that is used with the method of moments and subsectional basis functions.)

When using the finite element method with the Helmholtz equation, the functional to be minimized is[85]

$$I = \int_S (|\nabla\phi|^2 - 2k^2\phi)\, dS \tag{3-35}$$

If the area of the rectangular grid of Figure 10 is chosen as the subareas, then $\phi(x,y)$ is assumed to have a piecewise bilinear form

$$\phi(x,y) = a_o + a_1 x + a_2 y + a_3 xy \tag{3-36}$$

in each subregion[86]. This form assures that $\phi(x,y)$ is continuous within the entire region of interest[87]. The values of the four coefficients are determined by the values of ϕ at the corners of the rectangle. More complicated polynomials may be used if continuity of derivatives is important. However, it has been shown that for second order operators this does not greatly improve convergence[88]. It should be mentioned

that to guarantee convergence of the finite element method, the differential operator must be self-adjoint. This is immaterial in electromagnetics since the Helmholtz equation is self-adjoint in linear media.

When equation (3-35) is minimized, the original differential equation problem is transformed into a matrix problem with the coefficients of each piecewise function as unknowns. This may now be solved by standard techniques. It should be noted that when the method of moments is used with a self-adjoint operator and with weight functions equal to basis functions, the matrix equations are identical to finite element equations.

The advantage of the finite element method over other subsectional methods, such as finite differences, is the speed of its convergence. The mathematical details of such a comparison are beyond the scope of this study, but may be found in Reference 78. The disadvantages of the finite element method are the same as those of the finite difference method. For large-scale multi-dimensional problems, the matrices involved become unmanageable. For irregularly shaped boundaries, the subregions adjacent to the boundary must be given special consideration, and it is easy to spend more computer time locating the subareas than working the problem.

Harrington has successfully used the finite element idea in solving for waveguide modes in rectangular and circular guides[89]. As mentioned previously several other investigators have successfully applied the finite element method to exterior scattering problems[90,91,92] but the

computer execution time involved makes this method prohibitive for use in a general scattering method.

3.6 Probabilistic Methods -- The Monte Carlo Method

An alternative approach to the solution of partial differential equations is based on the theory of probability. This method does not solve the differential equation at every point, but rather determines the solution at one particular point. In principle, the Monte Carlo method involves the selection of some point of interest within a bounded region and the commencing of a series of so-called random walks from this point. Each such walk consists of a sequence of small steps, such that each step begins at the end of the proceeding step, but the direction of each step is random. Eventually, each random walk will reach some point on the boundary. The value of the function at this point is recorded, and a new walk is begun, starting from the same point of interest. Provided that (1) enough random walks are taken and (2) each step in the walk is sufficiently small, it can be shown that the weighted average of the boundary values converges to the function value at the point of interest[93]. The Monte Carlo method has been most widely used in the solution of Laplace's equation and Poisson's equation with Dirichlet boundary conditions, but the method is also applicable to other types of problems. Little[94] has shown that the solution of the Helmholtz equation is no more difficult than the solution of Laplace's equation. The only additional computation required is the calculation of $\exp(\alpha t)$ where t is the time required for a random walk and α is a

parameter related to the problem being solved and the statistics of the random noise source used in taking the random walks.

The chief difficulty with the Monte Carlo method as described above is the length of time required for the many random walks that must be performed at each point for which a solution is desired. Typically 500 to 1000 random walks are required to attain solution accuracies of better than 1%[95], and solution accuracy varies inversely as the square root of the number of random walks[96]. These considerations have limited the application of Monte Carlo methods to only a few field problems. However, a study performed at the University of Michigan[97] showed that a fast analog computer together with a modest digital computer could obtain Monte Carlo solutions at rates competitive with standard finite difference methods. Handler[98] has employed the high speed ASTRAC II hybrid computer and obtained over 1000 random walks in less than one second.

The chief advantage of the Monte Carlo method is that when it is properly programmed on a modern hybrid computer, the average time it takes to complete a random walk decreases when the dimension of the problem increases[99]. This makes the Monte Carlo method unique among the methods studied thus far. It is the only method that does not require a tremendous increase in computer time in higher dimensions.

It should be noted, though, that the Monte Carlo method is an interior boundary value problem method, and as such it is not suited to exterior scattering problems. While exterior problems have been solved for the diffusion equation[100], the computation time required

is tremendous. Another disadvantage is that both analog and digital computers are required for efficient solution.

Finally, the real advantage of the Monte Carlo method is that the Helmholtz equation need not be solved everywhere, just at points of interest. For example, if the input impedance of an antenna is needed, only the feed point need be considered.

3.7 Analog/Hybrid Computer Methods

3.7.1 Analog Computer Methods

Since the analog computer is a parallel device, one-dimensional differential equations may be solved exactly (within the computer's electronic tolerances). The simulation of two or three- dimensional partial differential equations is somewhat more difficult. Laplace's and Poisson's equations have been solved in two dimensions by using resistance paper analog models[101] and in three dimensions by using an electrolytic tank model[102]. These are static models, and they are not suited to solving the Helmholtz equation directly. Any analog model would probably involve an electronic's approximation of the field problem itself. For example, a study of TEM fields present in a two-wire transmission line might be modelled as an LC ladder equivalent network.

Some improvement over finite difference and finite element methods may be had for two-dimensional problems by approximating one spatial derivative of the Helmholtz equation by finite differences and then solving the resultant set of simultaneous ordinary differential equations

on the analog computer. For example, the Helmholtz equation could be approximated as

$$\frac{\phi_{i+1}(y) + \phi_{i-1}(y) - 2\phi_i(y)}{h^2} + \frac{d^2\phi_i}{dy^2} + k^2\phi_i(y) = 0 \qquad (3\text{-}37)$$

$$i = 1,2,\ldots,N-1$$

where $\phi_i(y) = \phi(x_i,y)$ and "i" is the i^{th} discretization of the x spatial coordinate. The resulting N-1 coupled second order differential equations with variables $\phi_1,\phi_2,\ldots,\phi_{N-1}$ may be simulated on an analog computer[103], even when k is a function of x and y. The accuracy of the solution depends on the electronic hardware implemented on the analog computer. Each equation (3-37) requires two analog integrators; thus the number of equations (discretizations) is severely limited.

Another possible analog solution method would be to solve the Helmholtz equation in the time domain by discretizing space and letting time be the (natural) continuous variable. Again, the number of discretizations is limited by the number of integrators available on the analog computer. Because of this limitation, the technique is used only in transient problems with one spatial dimension, for example, transmission line problems or propagation through stratified media[104]. However, the need for transient solutions of scattering problems may aid in the development of hardware for a large-scale analog computer.

3.7.2 Hybrid Computer Methods

The chief shortcoming of the analog techniques described in the previous section is the direct proportion between the number of finite

difference grid points and the analog hardware required for the simulation. In the case of the homogeneous Helmholtz equation, at least two integrators are required for each point; if the problem is inhomogeneous, at least one function generator must also be supplied at each point. Since the minimization of error usually demands a large number of grid points, obtaining accurate solutions is difficult even for one-dimensional problems.

It has been suggested that hybrid computing techniques be employed to time-share a limited amount of analog equipment[105]. The region of interest is broken up into as many subregions as are required for a specified accuracy, and the analog elements needed to simulate the behavior of a single subregion are multiplexed among all the different subregions. It is then necessary to employ iterative techniques to "match" all the time-shared sections. The iteration procedure and multiplexing are controlled by the digital computer.

Figure 11 shows a simple system that is useful for solving a linear wave equation. A digital computer together with the necessary interface equipment is used to simulate the adjacent sections of the domain by applying to the analog network the transient fields which would be generated by the integrators associated with the nearby sections if a purely analog system were used instead. The digital computer records the fields generated by the analog system, which are in turn used as "boundary" fields for other subsections. Initially the "boundary" values for the interior sections are arbitrarily assumed, perhaps on the basis of a crude approximation obtained by another method. After the first

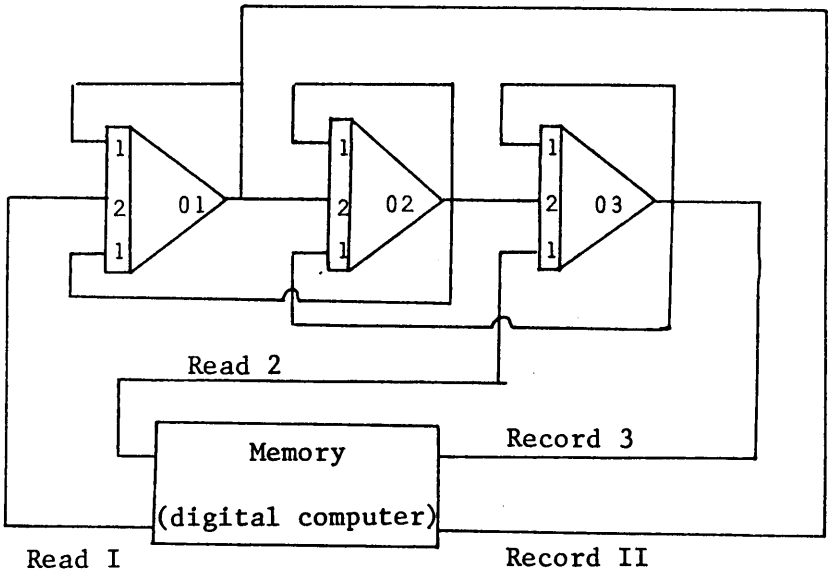

Figure 11. Simplified block diagram of a hybrid computer program used to solve partial differential equations.

iterative pass, the digital computer will have stored the solution values generated by the analog system in each subsection. These in turn serve as the boundary values for the next iterations. These iterative cycles are repeated until convergence to the correct solution has been reached.

Hsu and Howe[106] have published a feasibility study on the solution of the wave equation by hybrid computation. The procedure mentioned above is more fully explained in their paper.

Vichnevetsky[107,108], Anderson[109], and Nelson[110] have made more recent studies on the utilization of hybrid computers in the sutdy of partial differential equations. A fairly complete bibliography is contained in the literature.[107] The hybrid solution of partial differential equations is still in its infancy and little has been reported on actual computing times. However, even some preliminary reports indicate speeds an order of magnitude greater than digital computing for such problems[111].

This section is intended to show that the digital computer has no monopoly on computing technology. The analog machine integrates naturally, all elements operate in parallel, and the parameters relax to the correct solution. Matrix inversion takes less than two microseconds, regardless of the size of the matrix. With the ability of the digital machine to perform logical operations and store information, it stands to reason that working as a pair, substantial reductions in computing time will be gained.

3.7.3 Summary of Analog/Hybrid Techniques

Analog/Hybrid computers permit the use of computational techniques that are ill-suited to the digital computer alone. These tasks include the much needed functions of integration, matrix inversion, and function generation. It has been predicted that substantial savings in computer time would be gained if a digital computer could turn over some of these ill-suited tasks to an analog computer[112] but still remain in control of the algorithm as a whole. While no work has been done with hybrid computers in the study of electromagnetic scattering, much work has been begun in the study of partial differential equations. If the scattering problem can be cast into the correct form and if certain other difficulties can be overcome, much of the previous work in differential equations should carry over into the study of scattering.

3.8 Integral Equation Methods

An alternative to posing a problem in terms of partial differential equations is to cast it into the form of an integral equation. The two integral equations most often used in electromagnetic scattering were discussed in Section 2.2.5. This approach is only practical where the Green's function is known in advance, such as in some antenna problems, or in problems where image theory, etc. may be used to remove the obstacle. Even when the Green's function is known, the integral equation formulation may not be the most efficient. This is due to the fact that with arbitrarily shaped scatterers the numerical solution of the Green's function, for each source point, is as difficult as the

solution of the original problem itself.

This section is included, however, because integral equation formulations of electromagnetic scattering problems are seen frequently in the literature. With the notable exception of Andreasen[113,114] and others, most investigators have solved the integral equations, not by techniques in integral equation theory, but by techniques such as finite differences[115], finite elements[116], and method of moments[117]. These methods have been discussed in other sections.

Standard integral equation techniques may be used with some success also. When studying scattering from wire objects the vector integral equation of section 2.2.5 reduces to a scalar integral equation. The electric field integral equation of a straight wire antenna with conductor radius "a" oriented along the z-axis becomes[118]

$$E_z^s(z) = \frac{1}{4\pi j\omega\varepsilon} \int_{\text{antenna}} I(z')[\exp(-jkr)]r^{-5}\cdot[(1+jkr)(2r^2-3a^2) + k^2a^2r^2]\, dz' \qquad (3\text{-}38)$$

when z is on the antenna itself and $r = |z-z'|$. This is a Fredholm integral equation of the first kind. By approximating the kernel of (3-38) by a finite summation of functions of z multiplied by functions of z' such as

$$K(z,z') = \sum_{\nu=1}^{n} A_\nu(z)\overline{B}_\nu(z') \qquad (3\text{-}39)$$

the integral equation (3-38) may be solved as an equivalent matrix problem if $E_z^s(z)$ may be written as a linear combination of the $\{A_\nu\}$[119]. This is the degenerate kernel approximation.

The solution to equation (3-38) is obviously not unique, since any solution of the homogeneous integral equation (equation (3-38) with $E_z^s(z) = 0$) may be added to a solution of (3-38) and still satisfy (3-38)[120]. Physically, however, the solution must be unique, and from considerations that are not contained in the integral equation mathematical model, one may eliminate the extraneous solution.

Equation (3-38) may be solved by more elegant mathematical techniques if one is willing to perform the necessary preliminary analytical work. As early as 1922, Carleman showed how to solve equations of the type[121]

$$f(x) = \int_{-a}^{a} k(x-y)\phi(y)dy \qquad (3\text{-}40)$$

if the kernel happened to be either a logarithm or a power. Latta[122] later improved Carleman's technique so that (3-40) could be solved if the kernel satisfied a linear differential equation with constant coefficients. Cochran[123] gives a brief description of the fundamentals of Latta's method and includes an example where $k(x,y) = \ln(|x-y|)$.

When the scatterer is a bulky multidimensional object, the magnetic field integral equation formulation is usually the formulation that is best suited. This is because the geometrical factors make the contribution from the integral of (2-39b) of only second-order importance[124]. The magnetic field integral equation (2-39b) is a two-dimensional complex-valued vector Fredholm integral equation of the second kind. Because of its vector nature, degenerate kernel analysis is quite difficult. However, because (2-39b) is of the second kind, a Neumann

series expansion[125] or successive substitution may be made. The first guess at the current on the object is taken as the physical optics approximation

$$\bar{J}_s = \begin{cases} 2\hat{n} \times \bar{H}^{inc} & \text{illuminated region} \\ 0 & \text{shadow region} \end{cases} \tag{3-41}$$

This value of current is then substituted into (2-39b) to obtain a better approximation for $\bar{J}_s$. This new approximation is now substituted into (2-39b), and the process continues until the solution is obtained within a desired accuracy. The solution converges fairly rapidly for large objects such as reflector antennas[126]. The disadvantage of such a technique is the time needed to perform the vector operations and integrations required by (2-39b). Even for a simple scatterer, such as a sphere, the time necessary for each iteration is tremendous. On an IBM 370/158 system, nearly 20 minutes is required for each iteration if a sufficiently large number of points is used to obtain a reasonable solution. (In terms of computing dollars, this comes to about $50.00 per iteration.)

To circumvent this difficulty various degrees of physical optics-type approximation may be used in an attempt to obtain the current more accurately without requiring a large number of computer iterations. A typical approximation is to use a "pseudo" physical optics method which employs the standard physical optics current for the illuminated portion of the scatterer, but uses the integral equation to find the current in the shadow region. That is[127]

$$\bar{J}_s = \begin{cases} 2\hat{n} \times \bar{H}^{inc} & \text{illuminated region} \\ 2\hat{n} \times \bar{H}^{inc} + \frac{1}{2\pi} \hat{n} \left[\int_{\substack{\text{shadow} \\ \text{region}}} \bar{J}_s \times \nabla' \psi dS' + \int_{\substack{\text{illum.} \\ \text{region}}} (2\hat{n}' \times \bar{H}^{inc}) \right. & \\ \left. + \nabla' \psi dS' \right] & \text{shadow region} \end{cases} \quad (3\text{-}42)$$

where the integral equation for the shadow region currents uses the already-determined physical optics currents on the illuminated region to reduce the number of unknowns.

Poggio and Miller[128] have used both the electric field integral equation and magnetic field integral equation formulations to study scattering from many different types of objects. Bistatic cross sections, input impedance, and scattered field patterns are given for the sphere, monopole antenna, prolate spheroid, the cone sphere, a stub cylinder, a slotted wire grid, and several different wire antennas.

In summary, integral equation techniques generally require more mathematical "preprocessing" than most electromagnetics engineers would care to undertake. Except for some objects of special shape, the integral equation formulation is usually reduced to a finite difference or finite element technique rather than solved by classical integral equation theory. On the other hand, integral equation theory sometimes gives insight into a scattering problem that is not given by other more numerical techniques. For example, Marin was able to state several new properties of characteristic modes by consideration of Fredholm determinant theory[129]. In addition, integral equation techniques are sometimes modified as in the case of equation (3-42) so that a solution

of acceptable accuracy may be obtained within a reasonable amount of computer execution time.

3.9 Summary

Several different types of analytical and numerical techniques that are commonly used in antenna and scattering problems have been presented. Each technique had certain advantages but all techniques shared common disadvantages the most restrictive of which was the requirement of large matrix inversion. These methods for the most part are not limited by the mathematics on which they are founded but by the computational machinery used to solve them. This limitation is most apparent in the methods that "reduce" the original problem to a matrix problem and then rely on the digital computer to solve the matrix problem. The most popular numerical techniques -- finite differences, finite elements, and the method of moments -- all fall into this class.

From this observation it can be said that any "new" method for solving scattering problems should take into account the technology available in computing, especially the limitations of present-day high-speed digital computers, when formulating the mathematics for such a method. The most elegant theoretical technique will be of little use to the practicing engineer unless he has the technology to obtain practical results that are meaningful to his particular problem.

CHAPTER IV

THE UNIMOMENT - MONTE CARLO METHOD

In Chapter III several methods for solving electromagnetic scattering problems were presented. From the analysis of these techniques several weaknesses can be found. Some of these limitations are common to all the methods; some methods have only one or two of these restrictions. However, all the techniques presented so far do have limitations on the size of the problem that can be solved or the type of problem that can be solved.

It is the purpose of this chapter to tabulate the more severe limitations of the methods introduced in Chapter III. From these weaknesses the characteristics of an "ideal" scattering technique will be presented. Then a new scattering technique, the Unimoment-Monte Carlo Method, will be advanced. It will then be shown that this new method overcomes most of the limitations of the other methods. Finally the advantages and disadvantages of the Unimoment - Monte Carlo technique will be tabulated so that a comparison can be made with the other methods.

4.1 The Limitations of Present Scattering Methods

Scattering techniques used today are inadequate to solve many problems that are frequently encountered. These problems range from antenna design to interference studies (undesirable scattering).

Analytical methods require special geometries (as in the case of separation of variables) or a massive amount of mathematical work that must be reformulated every time a new scatterer is studied (as in the case of conformal mapping). Such work is beneficial in that it usually leads to a better understanding of the particular physical problem being studied without resorting to artificial solution methods such as discretization and matrix inversion in the solution of a continuous problem. However, to perform a complete analysis on every particular problem that requires a solution is not practical considering the time required.

Integral equations have a few more desirable properties. Unlike differential equations, the boundary conditions, including the radiation condition, are built into the integral equation mathematical model. Integral equations lead to a more general technique since solution by successive substitution or degenerate kernels can be programmed on a computer. The only modification that is necessary when the scatterer is changed is the subroutine that determines the region over which integration is performed. However, integral equations have their limitations also. The complex-valued vectors present in equations (2-39) require special routines to handle the vector multiplications. Scatterers other than perfect conductors are difficult to handle because the Green's function is more cumbersome.

The Monte Carlo method presents interesting possibilities. Its greatest advantages are that the fields at only the particular

points of interest need be calculated and that solution times do not increase with an increase of the dimension of the problem. Its disadvantages are that it is a solution technique for interior problems and that it requires external hardware (an analog computer and a multi-dimensional random noise generator) in order for it to be competitive with other methods.

Analog/hybrid computer methods hold promise because the speed of the analog computer may be combined with the accuracy of a digital computer. The parallel nature of the analog computer also allows one variable to be represented continuously; thus matrix sizes can be reduced, especially if hybrid computer subregion multiplexing is used. The disadvantages of analog/hybrid computing are twofold. First, the problems that may be solved efficiently must be bounded in space. Secondly, a modern hybrid computer is not available to most potential users, or at least not as available as a large-scale digital computer.

The aforementioned scattering techniques are not used by the majority of investigators. Instead the so-called "matrix methods" -- finite differences, finite elements, method of moments, characteristic modes, and unimoment method -- are the most popular. While proper use of these methods will result in the reduction of a scattering problem to an equivalent matrix problem, two difficulties occur when one attempts to make this transformation with a "real-world" problem.

First, the mechanics of the reduction process may be more involved than the solution of the problem itself. This may occur if the object

is large and each matrix element must be numerically integrated. Even after taking advantage of any symmetries in the scatterer, a great number of matrix elements still must be calculated. Difficulties also occur when the boundary of the scatterer is irregular or unusual. The problems this difficulty presents vary among the matrix methods. In finite differences or finite elements, the difficulty appears as the previously mentioned node-point location problem. In the method of moments, characteristic modes method and unimoment method, the problem is one of specifying the limits of integration to calculate the matrix elements.

The second limitation associated with matrix techniques is not a numerical difficulty but a computational difficulty. Digital computers cannot handle matrices beyond a certain size without resorting to slow off-line storage. Even if enough core storage were available, the amount of computation time needed to solve a large scale matrix problem would be prohibitive. Iterative techniques and sparse matrix algorithms have increased the efficiency of matrix methods somewhat, but the barrier still remains. Finally, even if computer time were not an important factor, the results of the matrix inversion may be of dubious accuracy due to the roundoff and truncation errors present in every digital arithmetic operation. An alternative to digital computer matrix inversion would be analog computer matrix solution techniques. Time is not a factor since the unknowns "relax" to the correct solution in less then two microseconds regardless of the size of the matrix. The limitation of analog methods is a

hardware restriction in that at least one operational amplifier is needed for each equation. A typical medium-scale analog computer might have only eighty operational amplifiers. The largest system commercially available, the Comcor Ci-5000/5 system, has only four hundred operational amplifiers. The number of simultaneous equations that may be solved by each system are less than eighty and four hundred respectively.

The unimoment method detours around the matrix size problem by solving several smaller scale interior problems. Thus, the matrix elements are easier to calculate than those of a classical moment method technique. This separation of interior and exterior domains creates other problems; namely, the calculation of the trial function pairs leads to sparse, but huge, matrices. Also, a new matrix problem must be solved for each mode.

To summarize briefly, the limitations of present scattering techniques may be divided into two categories -- numerical limitations and computer limitations. Numerical limitations are the least restrictive because one may frequently choose a different numerical technique to avoid a particular difficulty. One example of this would be choosing integral equation techniques over partial differential equation techniques to solve an exterior scattering problem since the radiation condition, which sometimes is difficult to enforce with differential equations, is built into the equivalent integral equation.

Computer limitations, on the other hand, are more severe and not as easy to circumvent. This is because these difficulties are an

indication that a numerical method is being pushed past its limit of advisable use, e.g., using the method of moments to solve large-scale three dimensional problems.

4.2 Characteristics of an Ideal Method

The limitations of currently used scattering techniques were presented in the previous section. From this material valuable insight may be gained into what an ideal method should be able to do. Any new technique developed from these considerations should certainly have the capability of solving scattering problems that cannot presently be solved or, at the very least, be more efficient in solving types of problems that can already be solved. This may seem like a trivial statement, but much work has been done in many fields of engineering that merely reformulates the work of others.

Only numerical solution techniques will be considered, because an ideal method should have the capability of studying different scatterers without a complete reformulation of the mathematics of such a technique. The only analytical methods discussed that are capable of being incorporated into a general computer program are either too inaccurate (physical optics) or too mathematically involved (conformal mapping). The physical optics method is quite simple, but the solutions it gives quickly become inaccurate at lower frequencies. Conformal mapping is a powerful technique, but a new mapping function must be found for every scatterer.

Computationally, an ideal method should be able to handle problems of increased complexity without a much greater increase in computer time. Most of the methods discussed in Chapter III, especially the matrix methods, do not meet this requirement. It has been shown by Waterman[130] that for scatterers which are bodies of revolution, computer time for matrix solutions increases roughly proportional to $(ka)^4$, where a is the radius of the smallest sphere that completely contains the scatterer and $k = 2\pi/\lambda_o$. That is, a scatterer whose size is doubled will require sixteen times more computer time than did the original scatterer. If the scatterer does not possess rotational symmetry, then computer time increases as $(ka)^6$. The only numerical method discussed in Chapter III that does not significantly increase in complexity with scatterer size is the Monte Carlo method, because the fields at a point of interest may be found without having to solve for the fields everywhere.

The drawbacks in using the Monte Carlo method are that an analog computer is required and that only interior problems may be solved. The second difficulty may be avoided if the unimoment method is used to separate the scattering problem into an exterior problem and several interior problems. Then the Monte Carlo method may be used to solve each of the interior problems, and the exterior problem may be solved from the interior problem solutions. The need for an analog computer, or preferably a hybrid computer, is a hardware problem. If one is available for use then the problem does not exist. If one is not available, then the cost of procuring

one will make this approach prohibitively expensive.

The final consideration to be made in defining criteria for an ideal method is the technique that will be used in detecting boundaries and locating mesh points within the region of interest. All matrix methods require that this be done. The digital computer detects boundaries by comparing the spatial coordinates with a given boundary function. Since the digital computer must perform all operations serially, the time used to calculate the boundary function, compare the calculated boundary function with a given set of coordinates, and make a logical decision based upon the comparison is time taken away from the numerical technique being used to solve the problem. Also, it may be necessary to calculate the boundary function at several points and compare each of these calculations with the coordinates of interest. This becomes quite time consuming with objects that are approximated by piecewise-linear line segments. Then each mesh point must be compared with each piece of the boundary.

The mesh point coordinates are fairly easy to calculate by incrementing a distance "h" from some point of origin. The difficulty arises in that each mesh point must also be tested against the boundary function in order to confirm that it is indeed within the region of interest. After this is done, the computer must calculate an adjacency matrix so that it will know how to compute the matrix actually used in solving the scattering problem. Again, time involved in these preliminary operations is time taken away from solving the actual problem.

The inefficiencies of the digital computer in dealing with boundary detection may be overcome if an analog computer is available. The continuous, parallel nature of the analog computer is well used in this type of problem, and as a result no time is taken away from the main scattering problem; it can be solved simultaneously. In addition, analog computing elements make the necessary function generation along the boundary quite simple.

From the above discussion one may summarize the most important criteria for any new electromagnetic scattering problem solution technique:

1. It must be capable of solving "new" problems, or old problems more efficiently.
2. It must be a general technique. Different scatterers should not require a number of program changes.
3. Problems of increased size, complexity or dimension should not greatly increase computer time requirements.
4. The boundaries of the obstacle(s) and mesh points of the region of interest should be computable in an efficient manner.

No single technique thus far presented can satisfy all four requirements. Most of the methods fail either (3) or (4). However, a method is proposed in this dissertation which does satisfy all four requirements. When the unimoment method is solved by Monte Carlo techniques and implemented on a hybrid computer, not only are all four requirements met, but the total cost of computing machinery being used is substantially less than the cost of the typical large-scale digital computer needed to implement other numerical techniques. This new method is

called the "Unimoment - Monte Carlo Method."

4.3 Details of the Unimoment - Monte Carlo Method

The unimoment method was discussed in Section 3.4.3 as a spinoff of the method of moments. There it was stated that the power of the method was limited by the difficulty in calculating the trial function pairs. This difficulty may be overcome if the Monte Carlo method is used with an analog computer. The mathematics of this development in two dimensions will be presented next, followed by a summary of the advantages and disadvantages of the Unimoment - Monte Carlo method when compared to the methods discussed in Chapter III.

4.3.1 Mathematics of the Unimoment - Monte Carlo Method in Two Dimensions

Referring to Figure 12, let all space be divided into two regions:

$$\begin{aligned} &\text{Region I:} \quad r < a \\ &\text{Region II.} \quad r > a \end{aligned} \tag{4-1}$$

with $\varepsilon = \varepsilon_o$, $\mu = \mu_o$, $\sigma = 0$. As long as the scatterer is finite this partition can be made with a circle of finite radius "a". For infinite objects, such as the parallel plate waveguide, the definition (4-1) may be modified so that a straight line (circle of infinite radius) divides the two regions. Infinite scatterers will not be considered because a separate set of mathematical details must be presented. However, the unimoment method has been used successfully in solving for

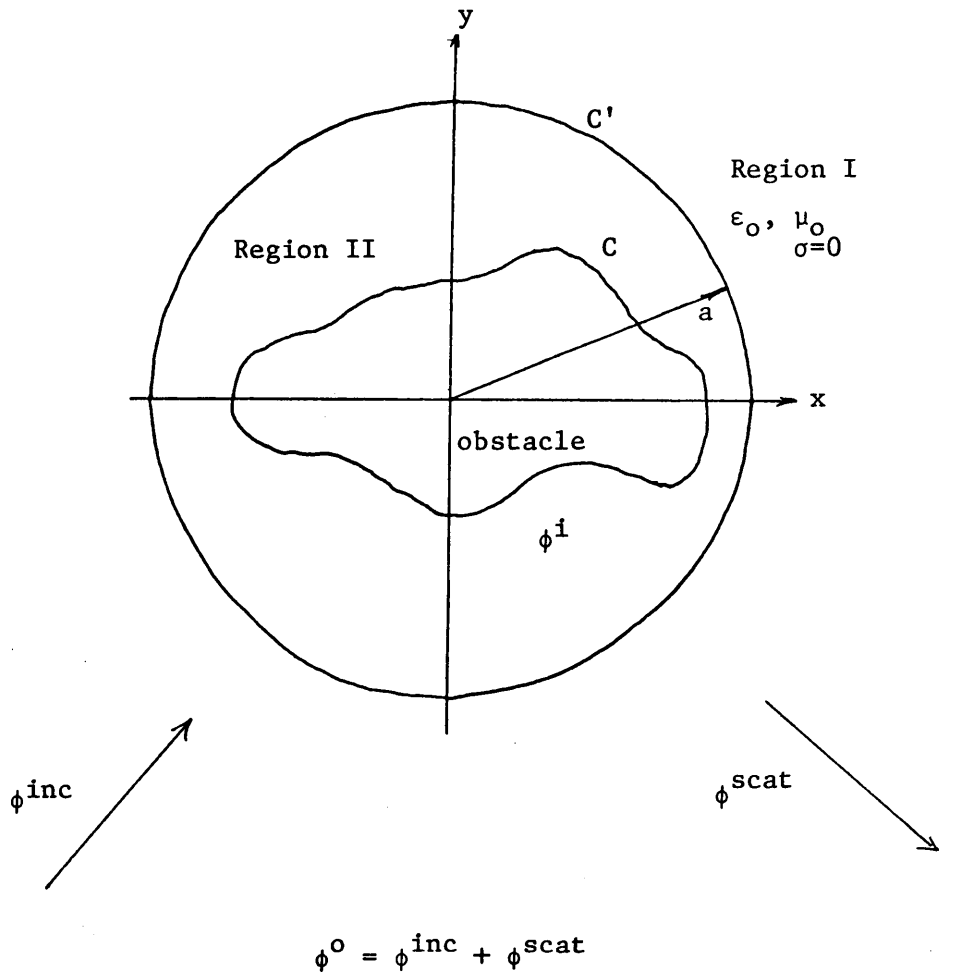

Figure 12. Unimoment - Monte Carlo formulation of the scattering problem.

the scattered fields from infinite objects. The Unimoment - Monte Carlo method may be used similarly.

The boundary of Regions I and II is denoted by C'. Define ϕ^i to be the solution of the appropriate Helmholtz equation (2-17), (2-18), (2-23), or (2-24) in Region I (inside). The equation used will depend upon the constituitive parameters of the scatterer and the type of scattering to be studied (TM or TE). Similarly, define ϕ^o to be the solution of the homogeneous Helmholtz equation in Region II (outside). The variable ϕ represents E_z for TM scattering and H_z for TE scattering. Both ϕ^o and ϕ^i must satisfy boundary conditions appropriate to each region. ϕ^o must satisfy the radiation condition (2-5) at infinity. ϕ^i must satisfy any boundary conditions required by the scatterer. Since C' lies entirely in free space, an additional condition of continuity is required on this boundary.

$$\phi^o(a,\theta) = \phi^i(a,\theta)$$
$$\frac{\partial \phi^o}{\partial r}(a,\theta) = \frac{\partial \phi^i}{\partial r}(a,\theta) \qquad (4\text{-}2)$$

Let ϕ^o further be divided into an incident field ϕ^{inc} and a scattered field ϕ^{scat}. ϕ^{inc} is the field (E_z or H_z) that would be present without the scatterer, and ϕ^{scat} may be written as

$$\phi^{scat}(r,\theta) = \sum_{n=0}^{N} (A_n^e \cos(n\theta) + A_n^o \sin(n\theta)) H_n^{(2)}(kr) \qquad (4\text{-}3)$$
$$\text{for } r < a$$

so that ϕ^{scat} satisfies the radiation condition for $\exp(j\omega t)$ time dependence and the (A_n^e) and (A_n^o) may be chosen so that equation (4-2)

holds at C'.

Let the interior field ϕ^i be represented by

$$\phi^i = \sum_{n=0}^{N} a_n^e \psi_n^e + a_n^o \psi_n^o \tag{4-4}$$

where $\{\psi_n^e\}$ and $\{\psi_n^o\}$ are even and odd trial functions respectively. Information regarding the form of these functions and their normal derivatives will be determined later by hybrid Monte Carlo methods. Assuming the ψ functions are known, the continuity of ϕ in equation (4-2) can be imposed to give

$$\phi^{inc}(a,\theta) + \sum_{n=0}^{N} (A_n^e \cos(n\theta) + A_n^o \sin(n\theta)) H_n^{(2)}(ka)$$

$$= \sum_{n=0}^{N} (a_n^e \cdot \psi_n^e(a,\theta) + a_n^o \cdot \psi_n^o(a,\theta)) \tag{4-5a}$$

and

$$\frac{\partial \phi^{inc}(a,\theta)}{\partial r} + \sum_{n=0}^{N} (A_n^e \cos(n\theta) + A_n^o \sin(n\theta)) \frac{d}{dr}(H_n^{(2)}(kr))\Big|_{r=a}$$

$$= \sum_{n=0}^{N} (a_n^e \frac{\partial \psi_n^e(a,\theta)}{\partial r} + a_n^o \frac{\partial \psi_n^o(a,\theta)}{\partial r}) \tag{4-5b}$$

If ϕ^{inc} and its derivatives are expressed as a series of sinusoids,

$$\phi^{inc}(a,\theta) = \sum_{n=0}^{N} (\alpha_n^e \cos(n\theta) + \alpha_n^o \sin(n\theta))$$

$$\frac{\partial \phi^{inc}}{\partial r}(a,\theta) = \sum_{n=0}^{N} (\beta_n^e \cos(n\theta) + \beta_n^o \sin(n\theta)) \tag{4-6}$$

and each of the ψ functions is expressed as a series of sinusoids,

$$\psi_j^e(a,\theta) = \sum_{n=0}^{N} a_{jn}^e \cos(n\theta)$$

$$j = 0,1,2,\ldots,N \qquad (4\text{-}7)$$

$$\psi_j^o(a,\theta) = \sum_{n=0}^{N} b_{jn}^o \sin(n\theta)$$

$$\frac{\partial \psi_j^e(a,\theta)}{\partial r} = \sum_{n=0}^{N} (c_{jn}^e \cos(n\theta) + c_{jn}^o \sin(n\theta))$$

$$j = 0,1,2,\ldots,N \qquad (4\text{-}8)$$

$$\frac{\partial \psi_j^o(a,\theta)}{\partial r} = \sum_{n=0}^{N} (d_{jn}^e \cos(n\theta) + d_{jn}^o \sin(n\theta))$$

then by substituting (4-6), (4-7), and (4-8) into (4-5) we obtain

$$\sum_{n=0}^{N} (\alpha_n^e \cos(n\theta) + \alpha_n^o \sin(n\theta)) + \sum_{n=0}^{N} (A_n^e \cos(n\theta) + A_n^o \sin(n\theta)) H_n^{(2)}(ka)$$

$$= \sum_{n=0}^{N} (a_n^e \{ \sum_{j=0}^{N} (a_{nj}^e \cos(j\theta) + a_{nj}^o \sin(j\theta)) \}$$

$$+ a_n^0 \{ \sum_{n=0}^{N} (b_{nj}^e \cos(j\theta) + b_{nj}^o \sin(j\theta)) \}) \qquad (4\text{-}9)$$

and

$$\sum_{n=0}^{N} (\beta_n^e \cos(n\theta) + \beta_n^o \sin(n\theta))$$

$$+ \sum_{n=0}^{N} (A_n^e \cos(n\theta) + A_n^o \sin(n\theta)) \frac{d}{dr} H_n^{(2)}(kr) \Big|_{r=a}$$

$$= \sum_{n=0}^{N} (a_n^e \{ \sum_{n=0}^{N} (c_{nj}^e \cos(j\theta) + c_{nj}^o \sin(j\theta)) \}$$

$$+ a_n^o \{ \sum_{j=0}^{N} (d_{nj}^e \cos(j\theta) + d_{nj}^o \sin(j\theta)) \}) \qquad (4\text{-}10)$$

Because of the linear independence of {cos(nθ)} and {sin(nθ)}, equation (4-9) and (4-10) may be written as the set of equations:

$$\alpha_n^e + A_n^e H_n^{(2)}(ka) = \sum_{n=0}^{N} a_{mn}^e a_m^e \qquad n = 0,1,2,\ldots,N$$

$$\alpha_n^o + A_n^o H_n^{(2)}(ka) = \sum_{m=0}^{N} b_{mn}^o a_m^o \qquad n = 0,1,2,\ldots,N \tag{4-11a}$$

$$\beta_n^e + A_n^e \frac{d}{dr} H_n^{(2)}(kr)\Big|_{r=a} = \sum_{m=0}^{N} (c_{mn}^e a_m^e + d_{mn}^e a_m^o) \qquad n = 0,1,\ldots,N$$

$$\beta_n^o + A_n^o \frac{d}{dr} H_n^{(2)}(kr)\Big|_{r=a} = \sum_{m=0}^{N} (c_{mn}^o a_m^e + d_{mn}^o a_m) \qquad n = 1,2,\ldots,N \tag{4-11b}$$

The $\{A_n^{e,o}\}$, and $\{a_n^{e,o}\}$ may now be found in terms of the known $\{\alpha_n^{e,o}\}$ and $\{\beta_n^{e,o}\}$.

To simplify the mathematics somewhat let $a_{jn}^e = \delta_{jn}$ and $b_{jn}^o = \delta_{jn}$, where δ_{ij} is the Kronecker delta function

$$\delta_{ij} = \begin{cases} 1 & i = j \\ 0 & i \neq j \end{cases} \tag{4-12}$$

Then equations (4-11) reduce to

$$\alpha_n^e + A_n^e H_n^{(2)}(ka) = a_n^e \qquad n = 0,1,2,\ldots,N$$

$$\alpha_n^o + A_n^o H_n^{(2)}(ka) = a_n^o \qquad n = 1,2,3,\ldots,N \tag{4-13}$$

The resulting 4N + 2 equations may be solved by standard matrix techniques. For fairly regular objects 4N + 2 equations rarely reaches the upper limit of digital computer matrix inversion. The number of equations may be reduced to 2N + 1 if the incident field and scatterer surface are symmetric with respect to either the

x-axis or the y-axis. When x-axis symmetry is present, all the sine coefficients are zero. When y-axis symmetry is present, all cosine coefficients (except n = 0) are zero.

4.3.2 Calculation of the Trial Function Pairs

After the unimoment method is used to decouple the exterior problem from the interior problem, the trial functions and their derivatives may be calculated by solving interior boundary value problems with boundary conditions specified on C' by $\psi_j(a,\theta)$ and appropriate boundary or continuity conditions on the surface of the scatterer C. For TM scattering from a perfect conductor

$$\psi_j(C) = 0. \tag{4-14}$$

For TE scattering from a perfect conductor

$$\frac{\partial \psi_j}{\partial n}(C) = 0. \tag{4-15}$$

For scattering from a perfect dielectric it is not necessary to specify continuity conditions for either TM or TE scattering if the change in dielectric constant is taken into account when formulating the partial differential equations (2-23) and (2-24). It should be noted that in equation (2-23) the only change is a change in wave number k. However, in equation (2-24) a discontinuity in ε_r will produce a singularity. This difficulty can be avoided if one is willing to approximate the discontinuity in ε_r by a continuous but rapid change in ε_r. (See Section 2.2.1)

Since the $\{\psi_j\}$ are given on the boundary C', all one must do to solve (4-11) is to calculate $\{\partial\psi_j/\partial n\}$ at C'. An estimate of the normal derivative may be obtained by solving the differential equations at points on a circle C" of radius a - h where h is small. Refer to Figure 13. We may then approximate $\partial\psi_j/\partial n$ by

$$\frac{\partial\psi_j}{\partial n} = \frac{\psi_j(C') - \psi_j(C'')}{h} \tag{4-16}$$

As $h \to 0$ the approximation becomes exact.

The Monte Carlo method allows the calculation of $\psi_j(C'')$ without also having to calculate ψ_j everywhere interior to C'. The circle C" in Figure 13 is divided into discrete points, the number of which is determined by the size and shape of the scatterer. An estimate of the number of modes, N, needed for an accurate solution may be obtained from Section 3.4.4. Then the highest order trial function will have a sinusoidal variation in $N\theta$ along the boundary C'. If a sinusoid is sampled at a rate of 50 samples per cycle, the sampling error will be less than 0.1%[132] which is the same error encountered when using electronic analog computing elements. Thus to maintain this error bound, C" should be divided into at least 50N points. For ten modes (N = 10), we will need 500 points. Thus the Monte Carlo method will have to calculate the field at 500 different points for each mode.

A presentation of the mathematics for the Monte Carlo method is given in Reference 94. A more concise but less rigorous explanation may be found in Reference 100. The result that will be used in the

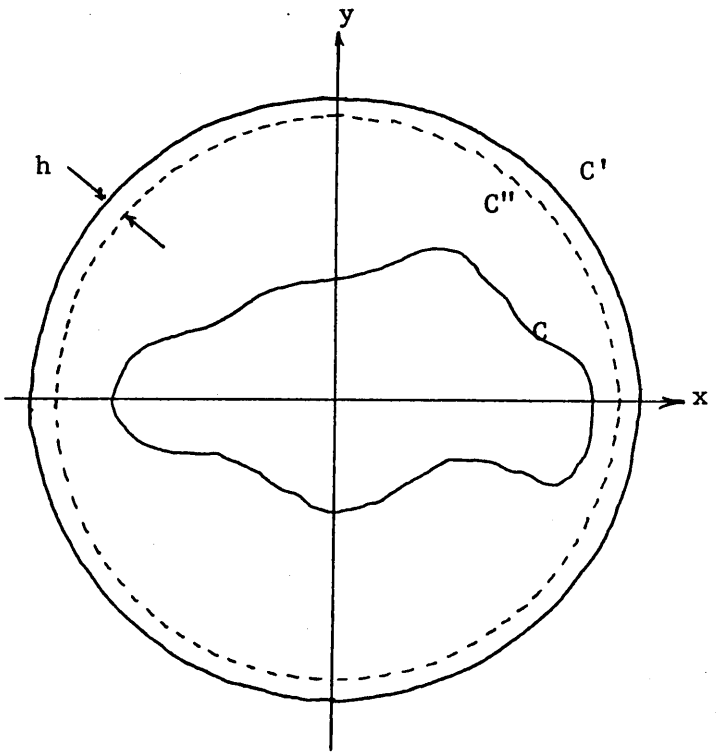

Figure 13. Boundaries C' and C'' enclosing the scatterer C.

solution of the Helmholtz equation is the fact that the solution ψ_j at a point (x,y) may be approximated by[133]

$$\psi_j(x,y) = \frac{1}{M} \sum_{i=1}^{M} \gamma_i \, \psi_j(x_i,y_i) \tag{4-17}$$

where (x_i,y_i) is where the i^{th} random walk intersects the boundary, and $\{\gamma_i\}$ are the weighting coefficients defined by

$$\gamma_i = \exp\left(\int_0^{\tau_i} Dk^2(x,y)dt \right) \tag{4-18}$$

Here k(x,y) is the wave number of the Helmholtz equation, D is the power spectral density of the noise source used to take the random walks, and τ_i is the time it takes the random walk to reach the boundary. Equation (4-18) may be implemented using standard analog computer components. Equation (4-17) will be programmed on the digital computer.

The result of calculating $\partial\psi_j/\partial n$ by the methods above is that $\partial\psi_j/\partial n$ will be tabulated at discrete points $0 \leq \theta \leq 2\pi$. To obtain the coefficients $\{c_{ij}^{e,o}\}$ and $\{d_{ij}^{e,o}\}$ it will be necessary to calculate a Fourier series representation numerically from the discrete data. A suitable algorithm is the one given by Goertzel[134]. The Fourier analysis will be performed by the digital computer.

Finally, the equations (4-11) may be solved using standard matrix techniques, such as Gauss-Jordan elimination. Since the number of equations will be small, they may be quickly solved on any digital computer.

4.3.3 Boundary Detection

Since the random walks are simulated on the analog computer, boundary detection will also be done on the analog computer. When a random walk begins, a mode control flip-flop is placed into the "run" state. This flip-flop is reset (placed in the "stop" state) when a random walk reaches a boundary. At this time the boundary values are read into the digital computer along with the elapsed time integral (4-18). Thus it is necessary to provide appropriate electronics to reset the mode control flip-flop. This may be programmed into the analog computer using standard analog computing elements.

The boundaries of problems with two or more spatial variables can be detected using function generators and voltage comparators. In the case where the boundary C may be divided into two single-valued functions

$$\begin{aligned} y &= C_1(x) \qquad y > 0 \\ y &= C_2(x) \qquad y < 0 \end{aligned} \tag{4-19}$$

as shown in Figure 14, it is clear that a random walk reaches the boundary of the scatterer whenever the instantaneous coordinates of the random walk (x,y) satisfy either

$$y = C_1(x)$$

or (4-20)

$$y = C_2(x)$$

If C may not be divided according to Figure 14, it is frequently possible to make a coordinate transformation so that two single-valued

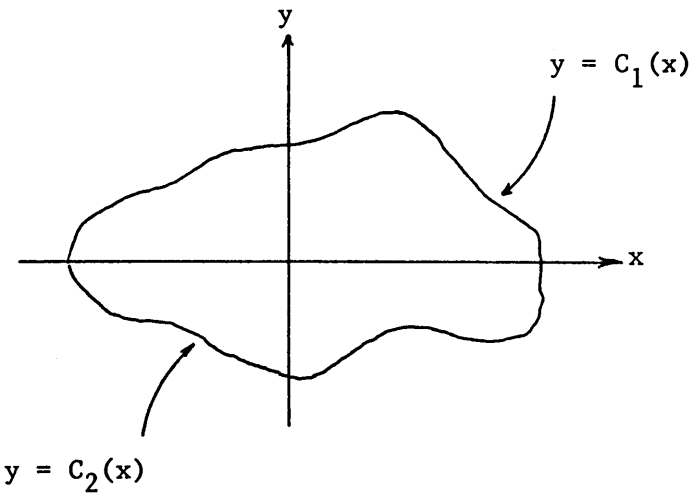

Figure 14. Two-dimensional region whose boundary may be separated into two single-valued functions of x.

functions may be obtained. The boundaries of a region as shown in Figure 15 in which $C_1(u)$ and $C_2(u)$ are single-valued functions of position u along a dividing line D are detected by using such a coordinate transformation. Variables x and y are transformed to u and v by

$$\begin{aligned} u &= x\cos\beta - y\sin\beta - a \\ v &= x\sin\beta + y\cos\beta - b \end{aligned} \tag{4-21}$$

In (u,v) coordinates the criterion that a random walk reaches the boundary is

$$\begin{aligned} &v = C_1(u) \qquad v > 0 \\ \text{or} \qquad &v = C_2(u) \qquad v < 0 \end{aligned} \tag{4-22}$$

For objects of arbitrary shape in which no such transformation results in two single-valued functions C_1 and C_2, the boundary is detected by dividing the interior region into subregions R_1, R_2, ..., R_n that have dividing lines D_i. The entrance of a random walk into each subregion is detected by the previous methods. The resultant signals are combined with an OR gate to give a single signal when the random walks leave any of the R_i regions and hence the total region R.

The outer boundary C' and other circular or elliptical boundaries may be detected by comparing the function

$$f(x,y) = \left(\frac{x+a}{b}\right)^2 + \left(\frac{y+c}{d}\right)^2 \tag{4-23}$$

with 1. Hence only two multipliers and one comparator are required.

These general methods may be extended to three-dimensional regions if the boundary surface is a single function of two variables. If

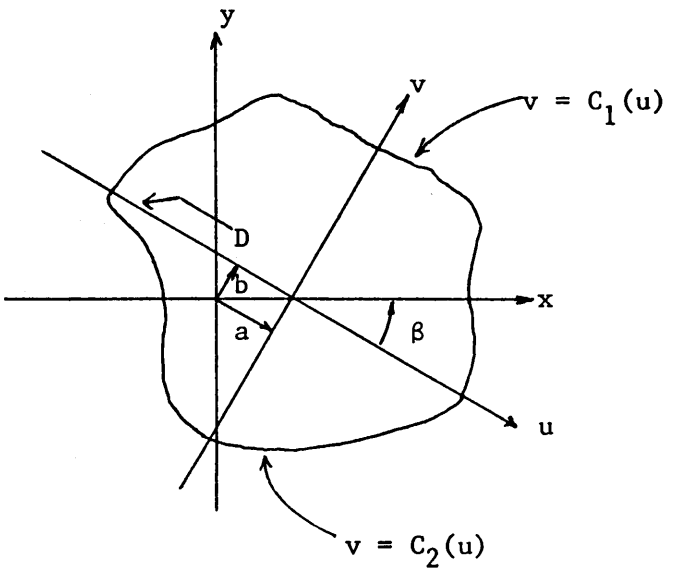

Figure 15. Coordinate transformation used for boundary detection of two-dimensional regions.

this is not the case, special purpose function generator techniques[135] are necessary. The boundaries of three-dimensional regions with some type of symmetry often can be detected by combining the methods described for two-dimensional regions. For example, spheres and ellipsoids can be detected by using three multipliers and a single comparator in the same way that two multipliers and a comparator are used for circles and ellipses.

The greatest advantage of using the analog computer to detect the boundaries is that in the analog domain, boundary detection becomes a continuous, parallel, real-time process. No additional computer time is needed, and the random walk is stopped the instant the boundary is crossed. If a digital boundary detection scheme is used, the digital computer must test each point of the random walk to see if the random walk has crossed the boundary, requiring as much, or more, computer time as the random walk itself. Finally, different scatterers may be studied by changing only the boundary detection circuitry which in practice requires merely repatching analog computing elements. No other programming changes are necessary.

4.3.4 Summary of Advantages and Disadvantages

As can be seen in the previous sections, the Unimoment - Monte Carlo method offers a different set of advantages and disadvantages than is offered by the much more widely used matrix methods. In fact, the greatest advantage of the Unimoment - Monte Carlo technique is that it overcomes the limitations of the other approaches. Specifically,

the Unimoment - Monte Carlo method has the following characteristics:

1. The spatial variables appear in continuous form; no discretization into mesh points is necessary.

2. Boundary detection is instantaneous; no extra computer time is needed.

3. The fields need be found only at points along C', not everywhere.

4. Problems of increased size and complexity require the addition of only one extra integration per dimension. Little extra computer time is needed.

5. The method is a general technique. Different scatterers may be studied by merely repatching the boundary detection circuitry.

6. The method is capable of solving both "new" and "old" problems more efficiently since only one small real matrix inversion is necessary.

The disadvantages of the Unimoment - Monte Carlo method are few. The most severe limitation is the requirement of a medium-scale hybrid computer. However, as the cost of large-scale digital computing systems increases with the simultaneous decrease in computer funding, the hybrid computer becomes more monetarily attractive. Because of this, hybrid computers are becoming more plentiful. The second limitation is one of background. In order to use a hybrid computer efficiently, one must become familiar with the "ins and outs" of hybrid computing. This is similar to the situation that occurred in the mid-sixties when matrix method techniques required the electromagneticist to become familiar with digital computers. The final limitation is a limitation due to the mathematics of the Monte Carlo

method, not the hybrid computer.

Monte Carlo solutions as described above will not converge at frequencies above the first resonant frequency of the interior region being studied.[136] This restriction is not as severe as it may seem for two reasons. First, the region being studied by the Unimoment - Monte Carlo method is the region between C' and the scatterer, not the interior or exterior of the scatterer itself, and the lowest resonant frequency of this ring-like region is much higher than the first resonant frequency of the scatterer. An example of this is scattering from a circular cylinder. It has its lowest (interior) resonance at ka = 2.405... However, if this object is surrounded by a circle C' of radius 25% larger than the first cylinder, the first resonance of this smaller region occurs at ka = 12.56. Secondly, if convergence remains a problem, the probabilistic formulation of the problem may be changed so as to converge for a different range of wavelengths.[137]

If these few difficulties can be overcome, the Unimoment - Monte Carlo method will give electromagneticists a choice of solution techniques. When these difficulties cannot be overcome, the scattering problem is usually ill-suited to the analog/hybrid computer in the first place. In this case the digital methods of Chapter III may be more efficient.

CHAPTER V

IMPLEMENTATION AND TESTING

5.1 System Overview and Description

The Unimoment - Monte Carlo method was implemented on the GE 4020/EAI 580 hybrid computer facility at Virginia Polytechnic Institute and State University. A block diagram of the system is shown in Figure 16. A description of each block of the final system has been included in the chapter because the actual digital programming and analog patching of the computer was a nontrivial problem. Many seemingly sound methods had to be discarded in favor of methods more amenable to the hardware at hand. Because of this, some comments about earlier systems and their evolution to a final system will be made in the subsections below.

No system or algorithm should ever be considered finalized, and this system is no exception. To make the statement that this particular implementation was the best possible would be to make the same error that was made when digital computer techniques were considered to be the only way of solving scattering problems. While this system can be used as a guideline in implementing the Unimoment - Monte Carlo method on other hybrid computers, the individual characteristics of the available computers should be examined to see if perhaps a more efficient system might be designed.

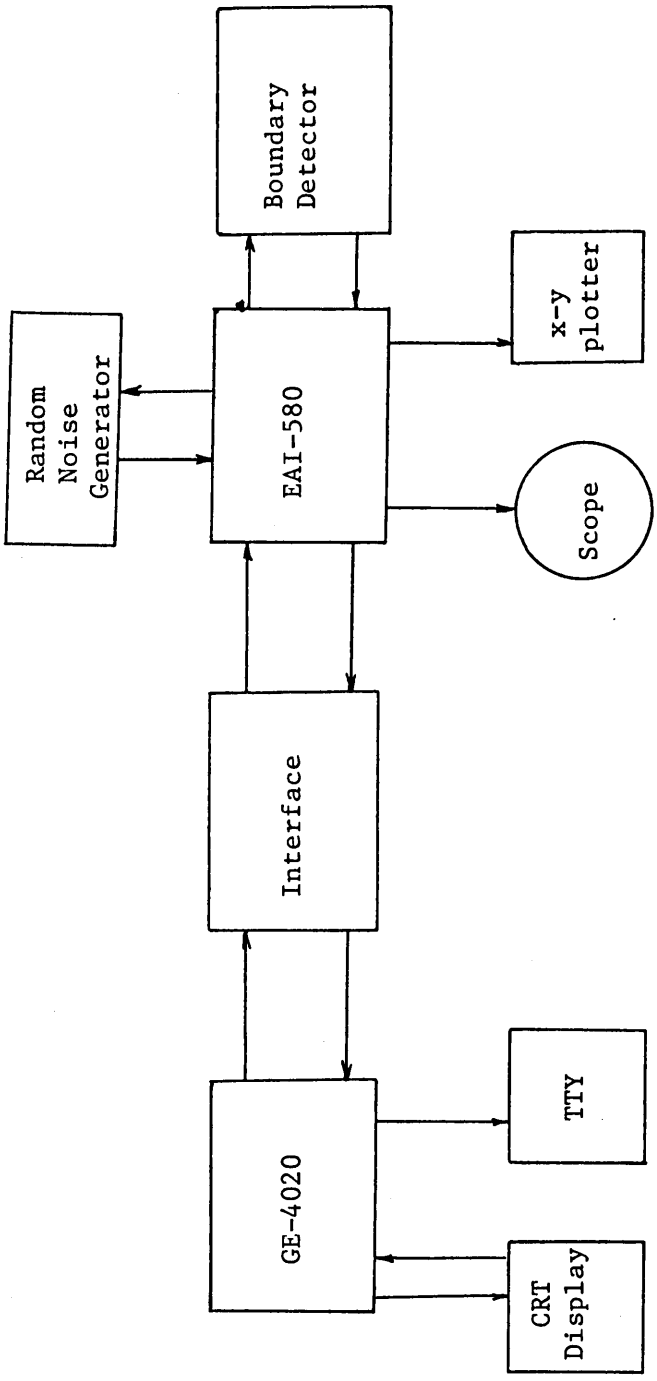

Figure 16. Unimoment - Monte Carlo method system block diagram.

5.1.1 The Random Noise Generator

For the Monte Carlo solution of partial differential equations, stable noise sources are required. In fact, a good source of random noise is the most crucial problem faced in implementing any Monte Carlo system. When used with analog/hybrid computers, noise sources should be capable of generating random signals whose amplitude distribution, d.c. unbalance, spectrum, and rms level are specified within computer accuracy limits, usually 0.1% full scale. Noise samples must not be correlated for time delays exceeding one-ten-thousandth to one-thousandth of a computer run[138]. In addition, electromagnetic scattering problems are multi-dimensional and thus require multi-dimensional random signals.

There are several possible sources of noise that fit the description above. Thyratrons in magnetic fields, noisy diodes, and photomultiplier tubes covered with radioactive paint are possible analog noise sources. However, their probabilistic characteristics change with varying environmental conditions. To stabilize these noise generators, elaborate gain control and feedback systems, sampling, and filtering have been utilized[139], but for the most part these attempts have been less than satisfactory. Also, to generate multi-dimensional noise, a separate generator must be available for each spatial dimension of the problem to be solved. The problem of maintaining stable probabilistic parameters with one generator is difficult; the problem of maintaining stable parameters with two or more separate generators is nearly impossible.

An alternative to generating noise from analog sources is to generate pseudo-random numbers on a digital computer. Several algorithms are available, but most have poor probabilistic properties. The IBM subroutine RANDU[140] is probably the most widely used generator of pseudo-random numbers. However it also has been shown to be a poor generator[141]. Other digital methods include the inner product method[142], Lehmer's method[143], and the Fibonacci Series Method[144].

There are also problems in implementing a digital pseudo-random number generator in the Unimoment - Monte Carlo method. First the digital portion of the hybrid computer must spend time calculating the random numbers. This is time taken away from the task of solving the scattering problem. Secondly the digital number must be converted into an analog variable because the random walks are simulated on the analog machine. This is done by a digital to analog converter. The net result of the above two limitations is that the random numbers cannot be generated any faster than the numbers can be generated and the D/A converter can convert the digital data to analog data. This in turn places an upper bound on the rate that random walks can be taken. The GE 4020 computer requires about 100 microseconds to generate a random number and then convert the number to an analog value. If the step size of a random walk is small enough that an average of 10000 steps are required for each walk then only one complete random walk may be taken every second on the average.

The most promising method of computing random numbers is the Feedback Shift Register technique. Periodic binary sequences may

be obtained from a digital shift register with modulo-2 adder (exclusive-or) feedback. The shift register consists of cascaded flip-flops driven at the desired rate by external clock pulses. The outputs of certain flip-flops are added modulo-2, and their sum is then fed back to the first stage of the shift register. Figure 17 illustrates three shift-register periodic sequence generators and their corresponding sequences. Each column of "1's" and "0's" corresponds to the successive states of each stage of the register. It should be noted that No. 1 and No. 2 outputs are periodic every $2^3 - 1 = 7$ bits, while No. 3 is periodic every 3 bits. In each case the periodic series is completely determined by the initial state of the flip-flops and by the feedback connections.

It is easy to show that the maximum length of any sequence produced by an n-bit shift register is $2^n - 1$, but obtaining the feedback connections necessary to obtain such a sequence is more difficult. Nonmaximum length sequences do not in general satisfy conditions required for pseudo-random sequences.[145] Consequently, to design a practical pseudo-random noise generator of n stages it is necessary to determine the feedback connections which produce a sequence of $2^n - 1$ bits in length. Tausworthe[146] showed that if the feedback configuration could be modelled as a primitive polynomial (modulo-2), then the sequence of binary numbers obtained by such a configuration would be maximal in length. A list of primitive polynomials (modulo-2) of up to order 127 is given in the literature[147]. In order to obtain a sequence of pseudo-random numbers that would

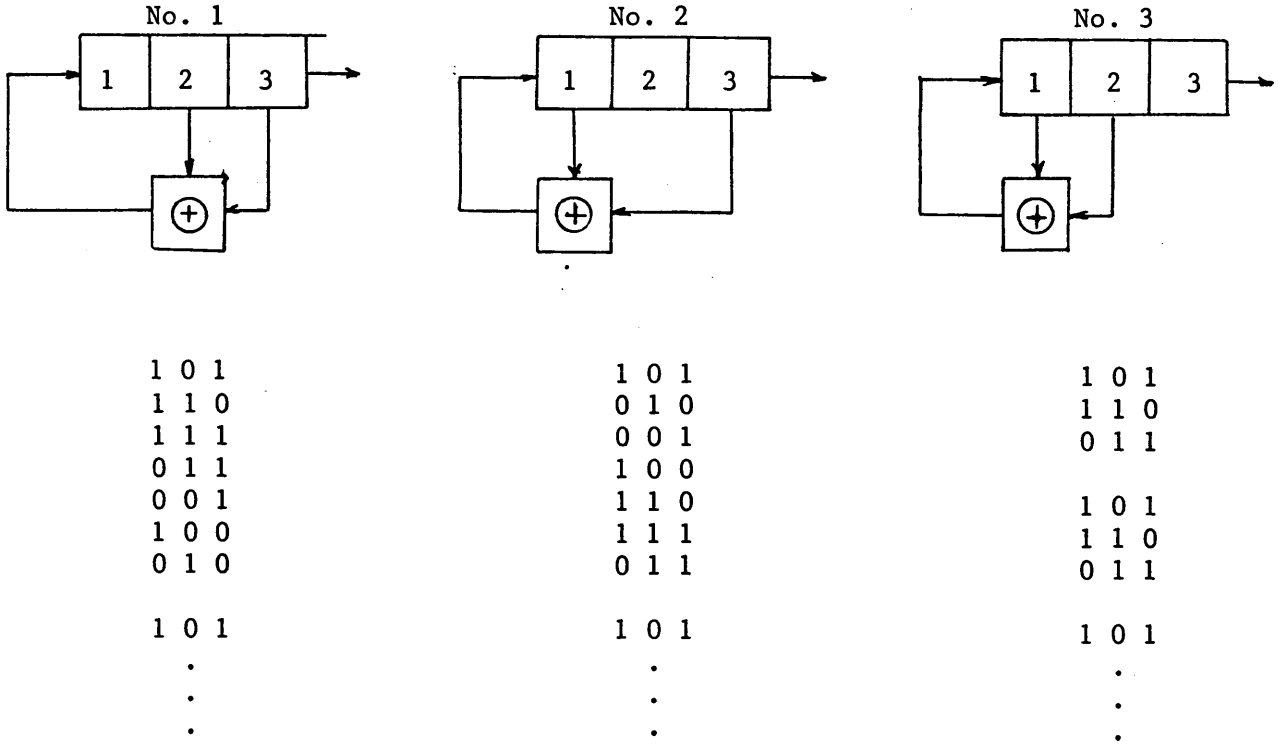

Figure 17. Three-stage periodic binary sequence generators.

not repeat during a computer run, a 47-bit shift register was chosen, giving a sequence of $2^{47} - 1 \simeq 1.4 \times 10^{14}$ bits before repeating. Even when driven at a clock rate of 5 MHz, the sequence repeats only after 325.8 days have elapsed. A block diagram of the shift register as well as interface circuitry is shown in Figure 18.

To obtain multi-dimensional binary numbers it is necessary to multiplex the output of the feedback shift register to the several individual generator outputs. Four-dimensional binary numbers may be obtained by using just two additional flip-flops (see Figure 18). Finally an interface between the digital binary numbers and the analog computer is needed. This consists of two parts: a precision clamping circuit to convert the logical "1's" and "0's" to $\pm$ 6 volts and a shaping filter to transform the binary numbers into Gaussian noise. If noise with a different distribution and spectrum is required, a Diode Function Generator may be included as shown in Figure 18.

The 47-bit feedback shift register was constructed separately from the GE 4020 digital computer so that no digital computer time would be wasted in calculating random numbers. The complete diagram of this generator is shown in Figure 19. The total cost was less than $60.00 using new components throughout.

5.1.2 The EAI-580 Analog Computer

The EAI-580 analog computer is used to carry out all random walks and to compute the value of γ_i for each walk. The bandwidth of all computing elements is 125 kHz., allowing random walks to be taken at

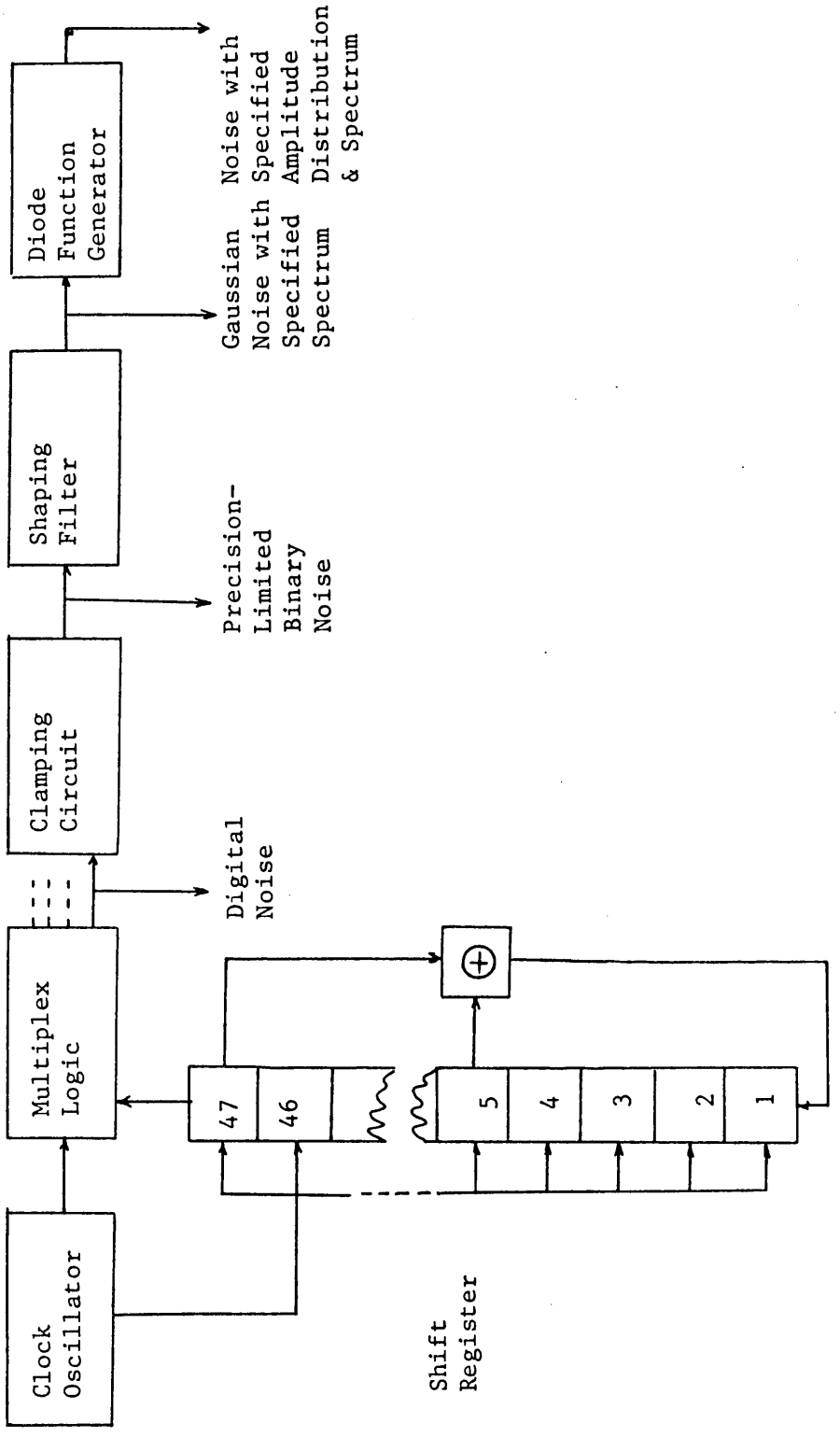

Figure 18. Block diagram of a feedback shift register noise generator.

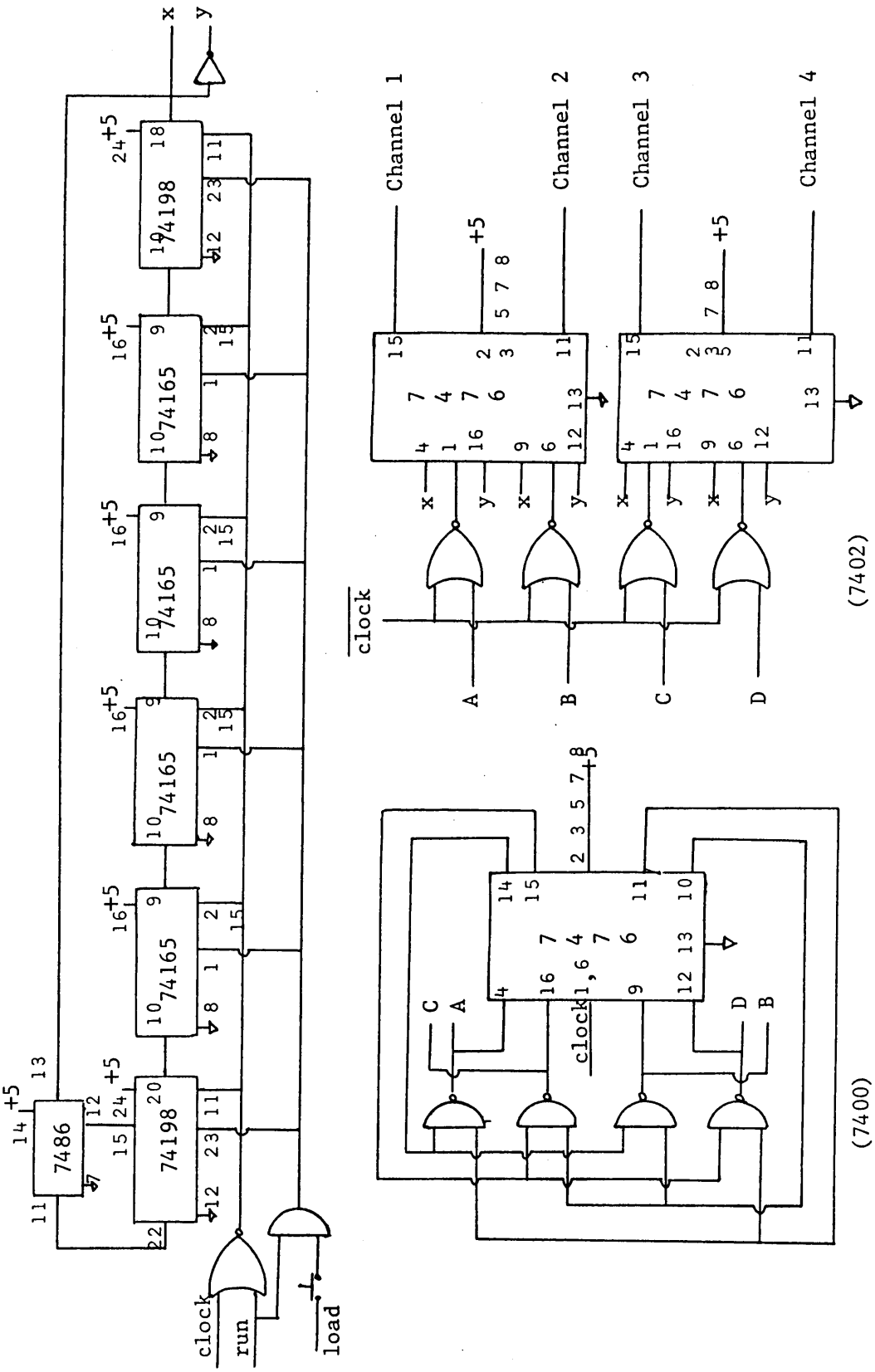

Figure 19a. Digital circuitry for the feedback shift register random noise generator.

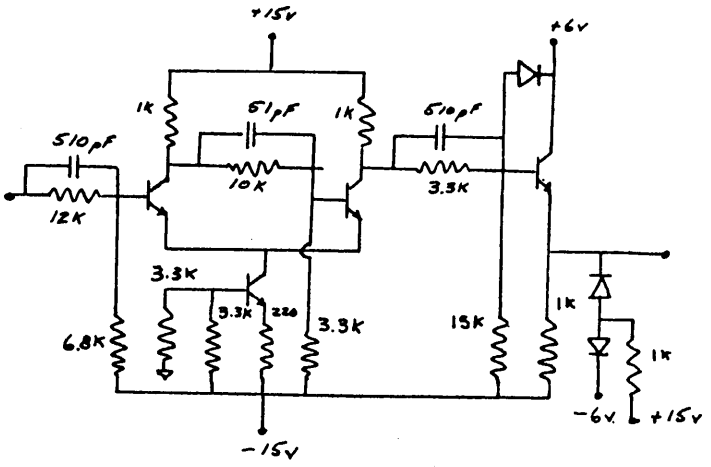

Figure 19b. Level shifting and clamping circuitry for the feedback shift register random noise generator.

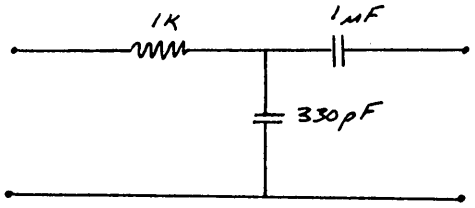

Figure 19c. Filtering circuitry for the feedback shift register random noise generator.

the fastest rate that the digital computer can process the boundary information. If it were not for the speed of the digital processing, up to 5000 walks per second may be taken. Excellent dynamic performance is illustrated by a total error of less than 0.5% full scale for any computing element used in the Monte Carlo simulation. The large number of computing components allows for the wiring of several programs on the same patch panel.

In addition to analog computing elements the EAI-580 computer contains a small number of digital registers, gates, and counters. The availability of these digital components makes it feasible to simulate multiple-boundary problems without additional outboard logic. All digital components operate at a clock rate of 1 MHz. Comparators and digital-to-analog (D/A) switches are used to interface the separate analog and digital parts of the computer. A comparator gives a digital "1" output when the sum of the analog inputs to the comparator is positive. Otherwise, the output is zero. A D/A switch closes when a digital input of "1" is applied, allowing an analog signal to flow through the switch. Otherwise the switch is open. Both the comparator and D/A switch have typical switching times of 1 microsecond.

The main limitation imposed on the overall system by the analog computer is one of accuracy. The maximum accuracy of any analog element is 0.5%. The analog signals used in the Monte Carlo simulation run through as many as four analog elements, giving a maximum possible error of 2%. The other problem encountered using the

analog computer is the finite switching time of the digital logic. If random walks are taken at a high rate, even the 1 microsecond delay of a comparator could cause a random walk to progress slightly beyond the actual boundary of the problem. Fortunately it is possible to overcome both problems to some degree by a small amount of additional digital software.

5.1.3 The GE-4020 Digital Computer

The GE-4020 is a medium-scale process control computer that is used as the other half of the Virginia Polytechnic Institute and State University hybrid computer facility. The particular model in use at V. P. I. & S. U. features 16,384 24-bit words with 1.6 microsecond memory cycle time. All standard digital arithmetic, logical, control, and input/output commands are hardware implemented with the exception of floating point arithmetic commands which are written as a separate software program.

A relatively sophisticated operating system is available to facilitate input/output operations including I/O between the GE-4020 and EAI-580. With the operating system it is easy to communicate with the digital program by entering commands through a video display terminal. Hard copy output is available through an online typewriter.

The chief limitation of the GE-4020 with respect to the total Unimoment - Monte Carlo system is one of storage space. The operating system, when used, requires 6,000 memory locations, leaving the user with only about 10,000 locations for his program. Fortunately, the

Unimoment - Monte Carlo method does not require much storage. However, the digital portion of the program must be written with great care to be sure that it will fit into 10,000 locations. Work is now in progress to add several disk packs to the system in order to increase the total storage available to the user.

Another restriction of the GE-4020 is that its programs must be written in assembly language. This is only a one-time limitation since with the Unimoment - Monte Carlo method the program, once written, may be used without change.

5.1.4 The Hybrid Interface

The Computer Engineering Laboratory at V. P. I. & S. U. has constructed a special purpose hybrid interface which couples the GE-4020 digital computer to the EAI-580 analog computer. It is through this interface that all communications between the two machines takes place. The interface contains the circuitry necessary to carry out the following operations:[148]

1. Control the analog mode from the digital computer.
2. Sense the analog mode from the digital computer.
3. Set the servo-set potentiometers on the analog computer to a digitally specified value.
4. Enable the digital computer to provide a set of analog output signals for use on the analog computer or other experimental equipment by means of a digital to analog converter and a multiplexer.
5. Enable analog signals from the analog computer or other experimental equipment to be utilized on the digital

computer by means of an analog to digital converter and a multiplexer.

6. Provide logic signals from the digital computer to the digital patch panel of the analog computer.

7. Sense logic signals on the digital patch panel of the analog computer for use by the digital computer.

8. Provide high speed operation analog values by means of digitally controlled attenuators (DCA).

9. Provide analog computer status information to the digital computer for monitoring of overloads, etc.

10. Provide a number of interrupt lines to the digital computer from the analog computer or other experimental equipment to enable computer interaction.

A block diagram of the interface and its interaction with the other elements of the hybrid system is given in Figure 20. Only data and address paths are shown. For simplicity control signal paths which control the operations within the interface are not shown.

Detailed information on the operation of the interface components is not given since every hybrid system will have a different complement of components. However, a summary of the important characteristics for each mode of communication through the interface is given in Table 1. Consideration should be given to the information contained in this table when choosing the modes of communications between the GE-4020 and the EAI-580.

The Unimoment - Monte Carlo method requires both analog and digital communication between the GE-4020 and EAI-580. Analog input to the EAI-580 is needed to specify the starting point (x_o, y_o) of the random walk. Analog output is needed from the EAI-580 to the GE-4020 to determine the coordinates (x_b, y_b) of the point where the random walk

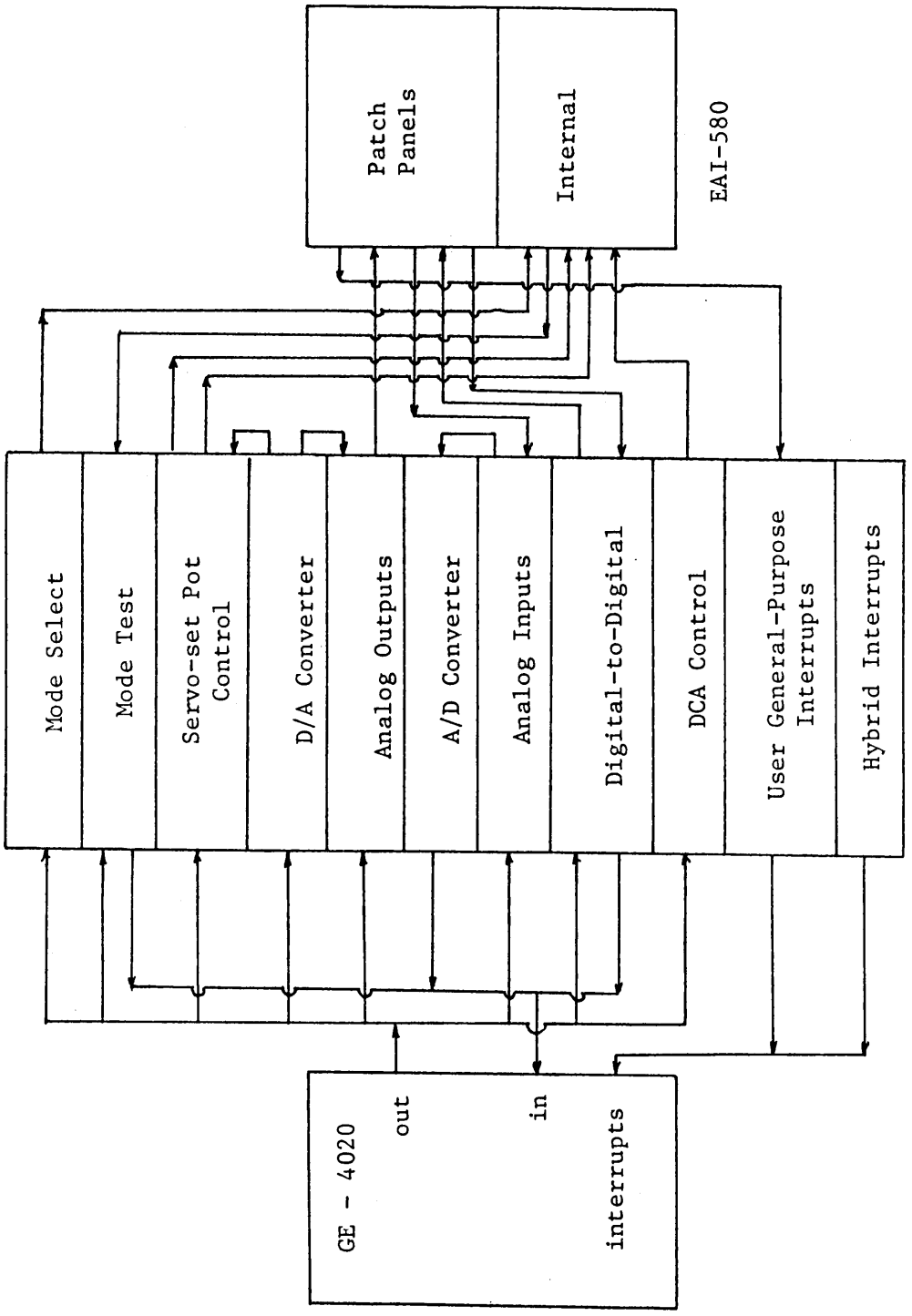

Figure 20. Simplified view of the hybrid interface.

Device	Function	From	To	Time	Accuracy	Number
Mode Select	Control	4020	580	1 msec.	----	---
Mode Sense	Control	580	4020	1 msec.	----	---
Servo - set Pots	Data	4020	580	1 sec.	0.1%	40
DCA's	Data	4020	580	20 μsec.	0.005%	5
Analog Outputs	Data	4020	580	250 μsec.	0.05%	8
Analog Inputs	Data	580	4020	500 μsec.	0.5%	32
Digital Outputs	Data	4020	580	16 μsec.	----	16
Digital Inputs	Data	580	4020	27 μsec.	----	16
User Interrupts	Control	580	4020	3.2 μsec.	----	8

Table 1. Summary of important characteristics of the hybrid interface

intersected the boundary and to determine the coefficients $\{\gamma_i\}$. Digital (or control) information is needed from the GE-4020 to the EAI-580 to start the random walks; digital information must be passed to the GE-4020 to indicate when the random walk is over and when data can be taken.

There are several ways that the starting coordinates may be specified to the EAI-580, but from Table 1 it can be seen that the DCA's provide the greatest accuracy with the least execution time. Only one choice is available to read the points (x_b, y_b) and the $\{\gamma_i\}$ into the GE-4020. This must be done using the very slow analog to digital converter. Since each A/D conversion takes 500 microseconds, a total of 1500 microseconds is required at the end of each random walk just to take in the date. It turns out that this is the severest restriction for the entire Unimoment - Monte Carlo method. Using the previously described random number generator and the EAI-580, a random walk only requires an average of 50 microseconds. Thus 95% of the time spent in solving the scattering problem is spent making A/D conversions. Fortunately, much faster A/D converters are available, and work is under way to replace the present A/D converter with one whose conversion time is about 5 microseconds.

The Digital Input and Digital Output modes of Table 1 are used to signal the start and end of a random walk by setting and resetting a "mode control flip-flop" on the EAI-580 digital patch panel. While the interrupt system would have been much faster, the additional amount

of programming needed to implement the interrupt was not considered worthwhile.

5.1.5 Boundary Detection Circuitry

Perhaps the single most important advantage of the Unimoment - Monte Carlo method over other scattering solution techniques is the continuous, parallel, real time boundary detection scheme. Either analog computing elements or separate circuitry may be used to implemnt the boundary detection mechanism. Most frequently, enough analog computing elements will be available to implement detection without using outside circuitry. The general approach to boundary detection was described in Chapter IV. Actual circuits that might be used will be given here.

The first boundary to be considered is the outer circular boundary C'. Referring to Figure 21, note that the variables x and y are written as functions of time. This is to emphasize that x and y are available to the boundary detection circuitry at all times during the random walk, Random variables x(t) and y(t) enter multipliers 22 and 25 whose outputs are $-x^2(t)$ and $-y^2(t)$ respectively. These are summed by amplifier 48 whose output is $x^2(t) + y^2(t)$. Pot 32 is set to the value a^2, where a is the radius of the circle C'. Thus the input to comparator 01 is $x^2(t) + y^2(t) - a^2$. If this composite signal is positive, then a logical "1" appears at the output of the comparator indicating that (x,y) is outside C' and that the walk should be terminated. Otherwise a "0" appears at the comparator which indicates (x,y) is still inside C'. The output of "1" resets the mode control

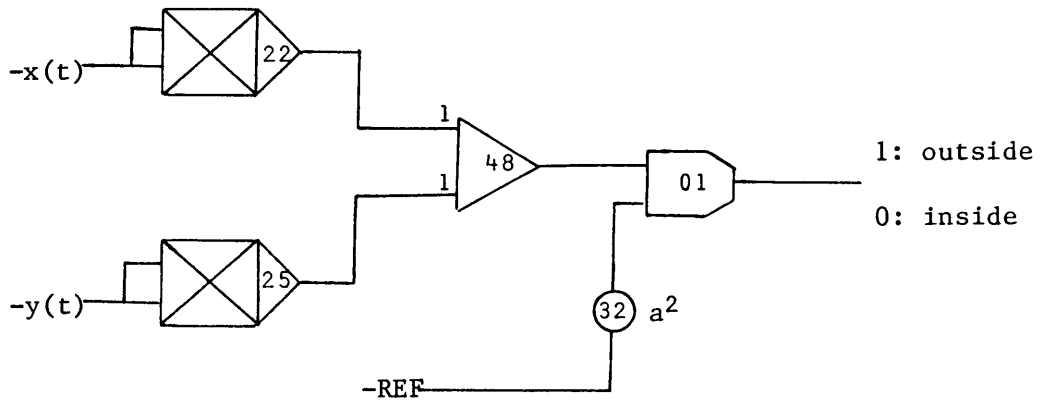

Figure 21. Detection of the outer boundary C'.

flip-flop stopping the random walk immediately, and the digital computer is signaled via the interface that data should now be taken.

If the region of interest is the area between two circles, the circuit of Figure 22 may be used instead. Notice that only one additional comparator and one AND gate are needed to extend Figure 21 to this case.

If the scatterer is an ellipse then the circuitry of Figure 23 should be used. The elements in common with Figure 21 are used to detect the outer boundary C'; all other elements detect the ellipse boundary.

If a more general scatterer is to be studied then it may usually be modelled by the circuit of Figure 24. Function generator DFG1 generates the scatterer boundary for $y > 0$; function generator DFG2 generates the scatterer boundary for $y < 0$.

Scattering from more then one object can be easily handled also. Figure 25 shows two parallel circular cylinders enclosed by the outer boundary C'. Figure 26 describes the circuitry needed to detect these boundaries.

Because analog elements are used to detect boundaries, the same restrictions of Section 5.1.2 apply here. In other words, the speed at which random walks are taken is not limited by the boundary detection devices as would be the case in a strictly digital simulation.

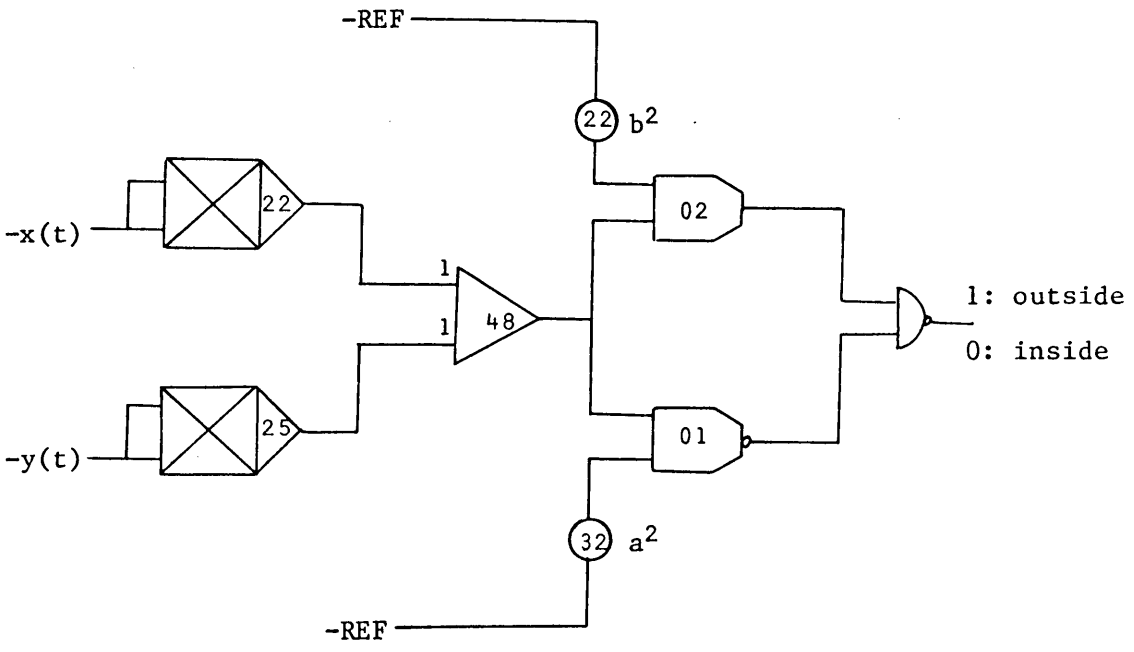

Figure 22. Detection of the boundaries of an annulus.

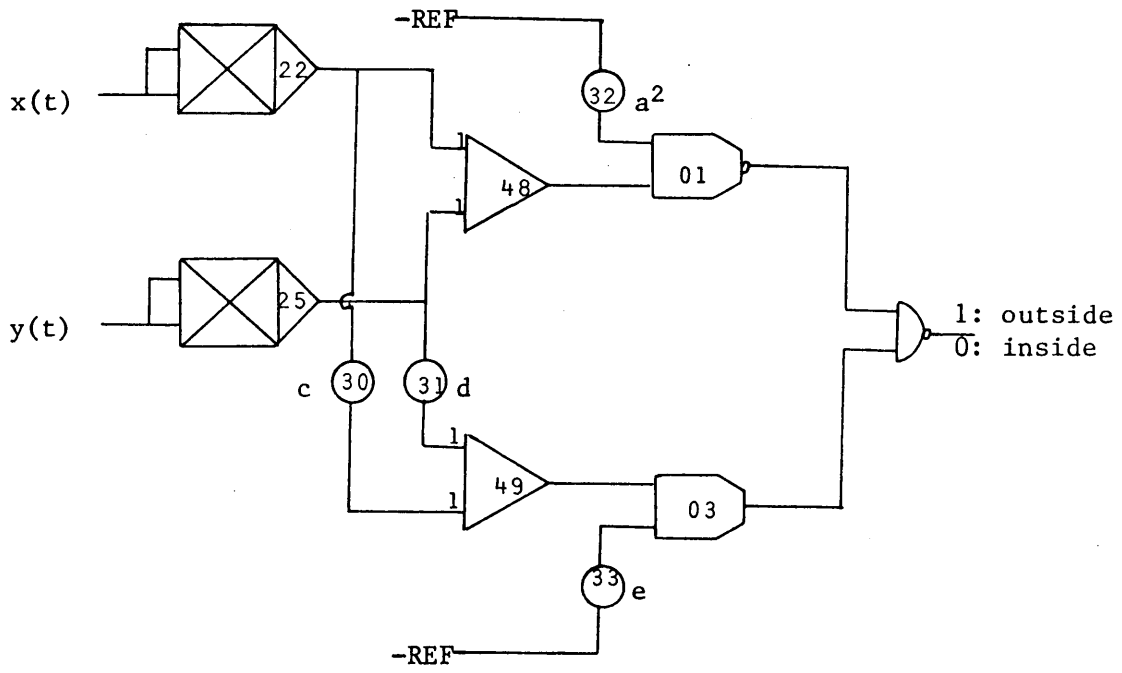

Figure 23. Boundary detection circuitry for an elliptical scatterer, $cx^2 + dy^2 = e$.

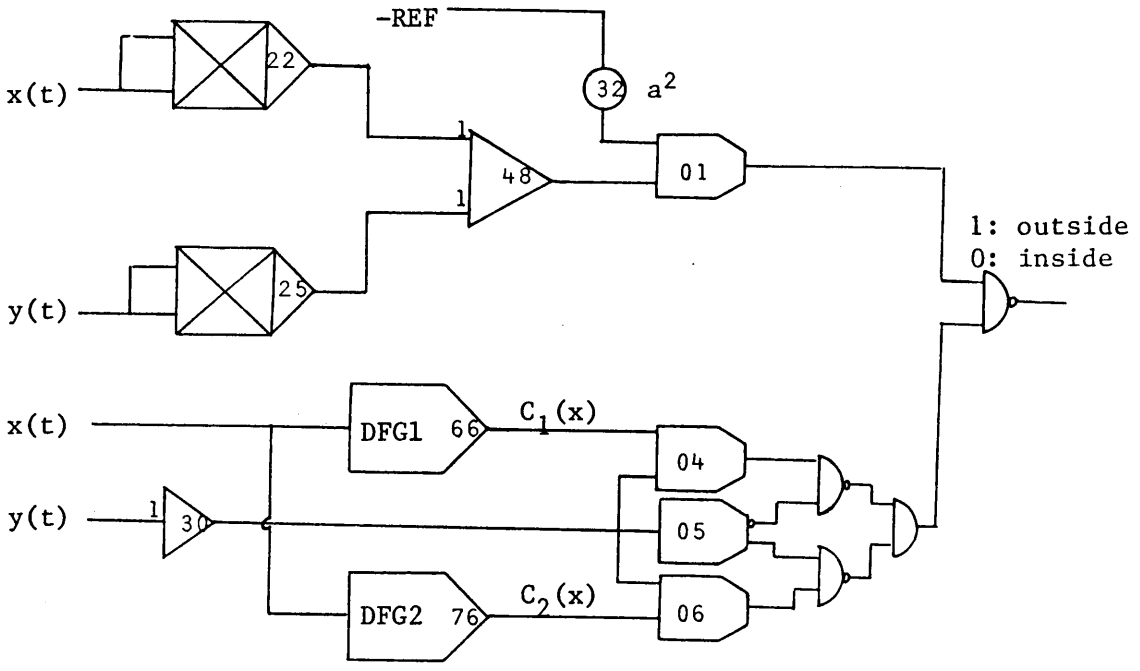

Figure 24. Boundary detection circuitry for a general scatterer.

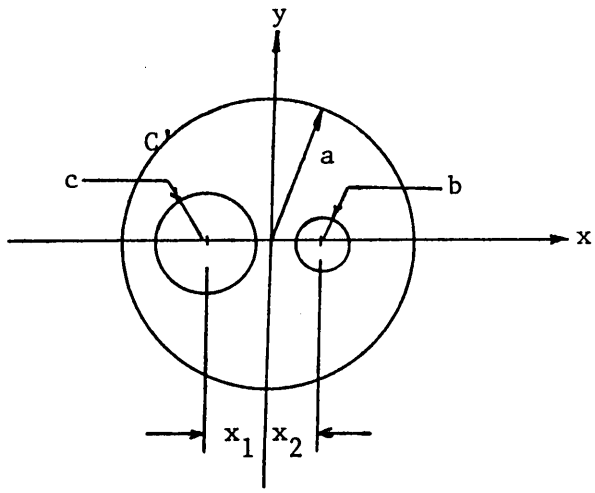

Figure 25. Two parallel cylinders enclosed by outer boundary C'.

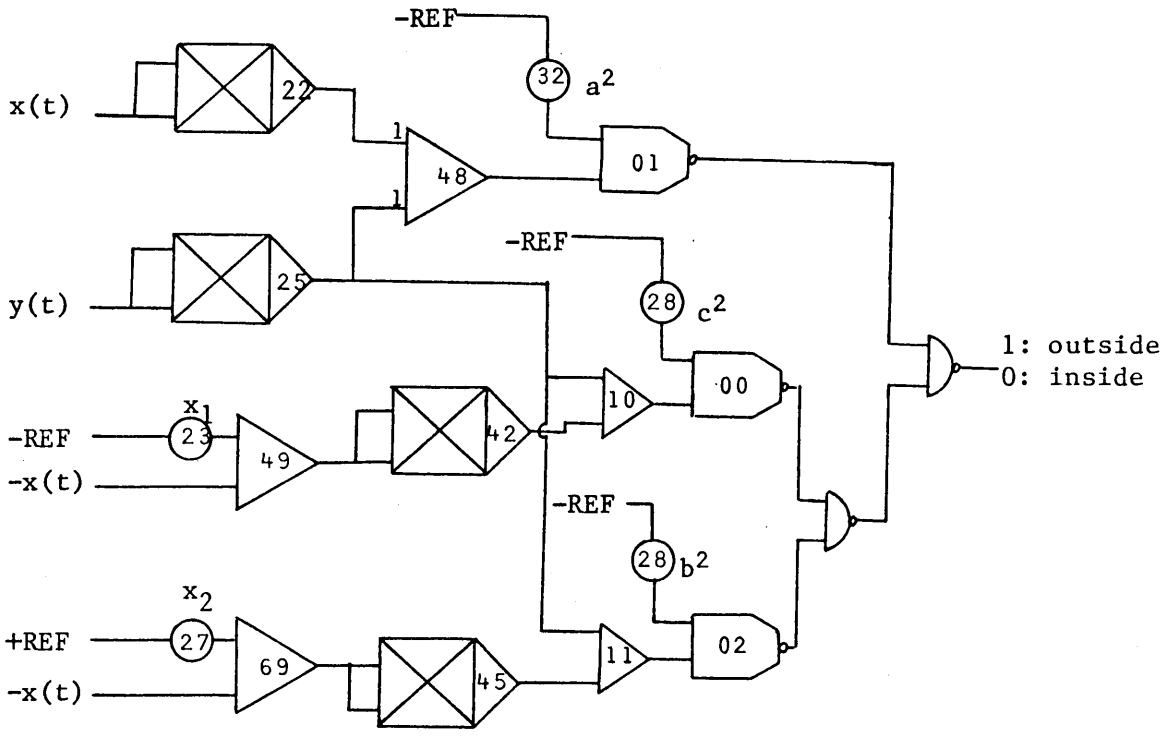

Figure 26. Boundary detection circuitry for the object in Figure 25.

5.2 Digital Computer Program Description

In any hybrid computer system a choice must be made as to which computer has control over the other computer. The Virginia Polytechnic Institute and State University hybrid facility interface dictates that choice to be the digital computer. The analog computer is a "slave" computer. Because of this the digital program has to include statements which control the operation of the analog computer as well as commands to process the data. A flow chart of the digital program is given in Figure 27. This program must be run under the GE-4020 operating system. It requires 7,000 storage locations.

The program begins execution when it is read into the GE-4020. Input data is entered at this time via the video display terminal. Values for the number of modes, NMODES, and the number of random walks per point, NWALKS, are required. Other data may be entered by using the COR command of the operating system, but this is not necessary. Default values of important variables are:

NPTS = 401:	number of sample points
ARAD = 0.5:	radius of C'
H = 5% of ARAD:	separation of boundaries C' and C"

Block B initializes all other run parameters and counters.

Block C sends a digital input to the EAI-580 to start a random walk, and the digital computer is put into a wait state until the random walk is completed. When the random walk terminates, the EAI-580 sends a digital signal back to the GE-4020 indicating that the walk is complete and that the analog computer is ready to send data.

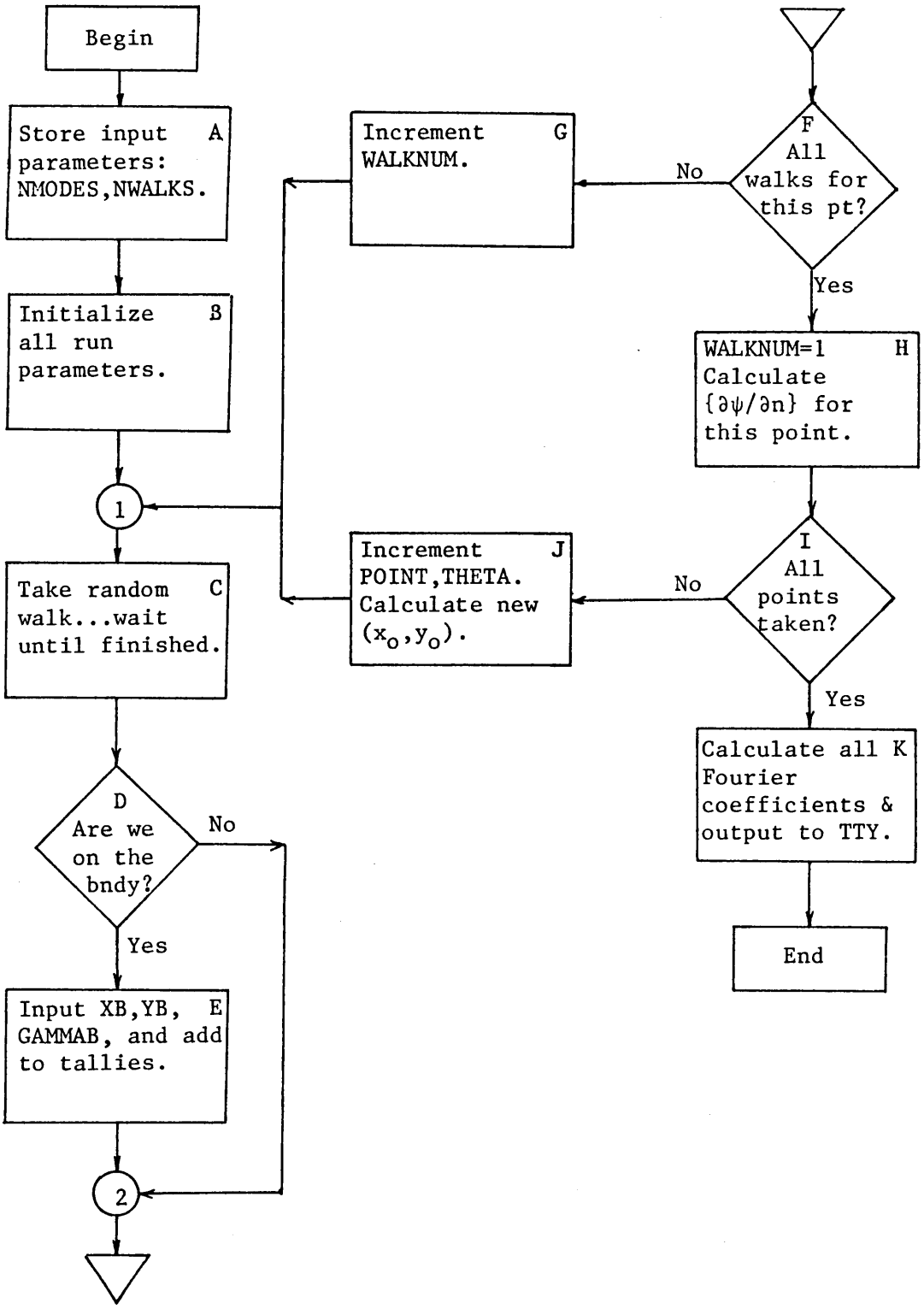

Figure 27. Flow chart of the digital program.

When this signal is received by the digital computer, the digital computer inquires if the random walk terminated on the outer boundary. If so, data is taken and added to appropriate tallies. If not, no data is taken since the walk must have terminated on the scatterer boundary. The only time this will occur is in the case of TM scattering from a perfect conductor in which case the field is zero on the surface of the scatterer. TE random walks will never terminate on the scatterer surface. (See section 5.3.3). Random walks in the presence of dielectric scatterers will continue into the dielectric rather than terminating on the boundary of the scatterer. Thus the same digital program may be used for all types of scattering.

Block E needs to be explained more fully. The values (x_b,y_b) and γ_b are used to calculate the boundary value at that point on the boundary C'. This is simple to do when the trial functions are $\{\cos(n\theta)\}$ and $\{\sin(n\theta)\}$. For n = 0, the boundary values are constant. The cosine boundary values are all one, and the sine boundary values are all zero. For n = 1

$$\begin{aligned} \cos\theta_b &= x_b/a \\ \sin\theta_b &= y_b/a \end{aligned} \tag{5-1}$$

where θ_b is the value of θ at (x_b,y_b). The boundary values for higher order modes may be calculated recursively using trigonometric identities.

$$\begin{aligned} \cos(n+1)\theta_b &= \cos(n\theta_b)\cos\theta_b - \sin(n\theta_b)\sin\theta_b \\ \sin(n+1)\theta_b &= \sin(n\theta_b)\cos\theta_b + \cos(n\theta_b)\sin\theta_b \end{aligned} \tag{5-2}$$

If enough storage space is available, all NMODES solutions may be determined simultaneously by using equations (5-1) and (5-2). If

this is the case, a substantial savings in execution time can be obtained since a single random walk may be used to add a boundary value to every tally. The alternative is at each point to run NWALKS random walks for each of the sine and cosine modes. With the GE-4020 computer, NMODES = 7, or 15 different boundary value problems may be run simultaneously. If more modes are desired, then two or more separate computer runs are necessary.

When all tallies have been updated, control passes to block F. If all NWALKS walks have not been taken at the point in question control is returned to block C and another random walk is begun. If all NWALKS walks have been taken, then the normal derivatives for all modes are calculated at the point by the approximation (4-16). When this is done a new starting point on C" is sent to the EAI-580 through the DCA's and the procedure continues.

If all points have been considered then the Fourier coefficients for $\partial\psi/\partial n$ of each mode are calculated and printed on the typewriter. At this point the hybrid program ends. The Fourier coefficients are then entered as data to a separate matrix inversion routine which solves equations (4-11) for a given incident field.

5.3 Analog Computer Program Patching

It can be seen from Section 5.2 that the digital computer program is nothing more than a control program that manipulates the data sent to it by the analog computer. One might think of the whole analog computer -- boundary detection -- random number generator system as a subroutine

called by the digital program. In Fortran it might be coded as CALL ANALOG(XO,YO,SB,YB,GAMMAB) where (XO,YO) are the coordinates of the starting point of the random walk, (XB,YB) are the coordinates where the random walk intersected the boundary, and GAMMAB is the integral discussed in Chapter IV. Consequently, the analog patching scheme is of vital importance.

Unlike the digital program, some differences exist in the analog programs for TM or TE scattering, perfect conductors or perfect dielectrics. These differences are minor, but each combination will be discussed separately with separate analog diagrams to avoid confusion.

5.3.1 TM Scattering from a Perfect Conductor

TM scattering from a perfectly conducting object is the simplest of the four combinations to program. Its differential equation is (2-17) with $k = k_o$ and $J_z = 0$. An appropriate analog computer diagram is shown in Figure 28.

Initial conditions (x_o,y_o) for each walk are entered by DCA's 40 and 41. Random noise $N_x(t)$ and $N_y(t)$ is integrated by integrators 20 and 21 when the "Start Random Walk" signal sets flip-flop 03 (FF03) and resets FF00. At this time integrator 01 begins calculating γ. When a random walk reaches a boundary, FF00 is set by the boundary detection circuits causing integrators 40, 41, and 31 to "hold" the boundary values (x_b,y_b) and γ_b while integrators 20, 21, and 01 are reset for the next run. After the data is read into the digital

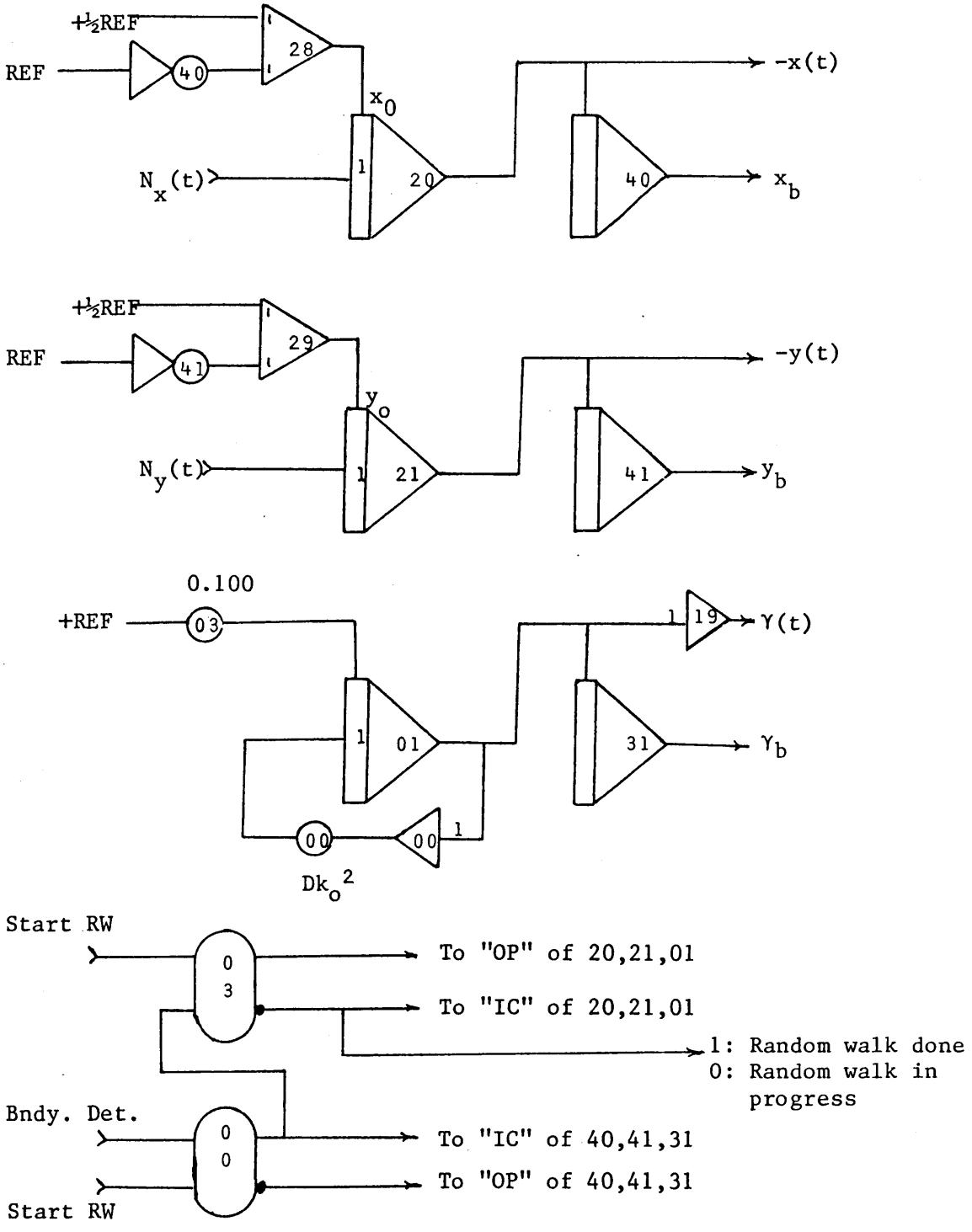

Figure 28. Analog patching for TM scattering from perfect conductors.

computer, the "Start Random Walk" signal is given again, and the process repeats. When enough random walks have been completed for a particular point the DCAs are incremented to a new starting point and another set of random walks is taken.

5.3.2 TM Scattering from a Perfect Dielectric

A slightly different analog program is needed for TM scattering from dielectric objects. The appropriate equation is (2-23) with $\mu_r = 1$ and $J_z = 0$. However, instead of the random walk terminating on the boundary of the scatterer, it continues inside the scatterer eventually emerging again. While inside the dielectric, the value of k(x,y) must be changed, and this is shown in Figures 29 and 30.

If the dielectric is uniform then this may be accomplished by seitching in additional feedback around integrator 01 with a D/A switch that is turned on whenever the random walk is inside the dielectric. If the dielectric varies with position, a diode function generator could be used as shown in Figure 30.

When dielectric scatterers are studied the only signal that terminates a random walk is the signal that occurs when the walk reaches C'. The other boundary detection circuitry is used to control the D/A switch and/or diode function generator. Consequently the Unimoment - Monte Carlo method requires more computer time for dielectrics than it does for perfectly conducting scatterers.

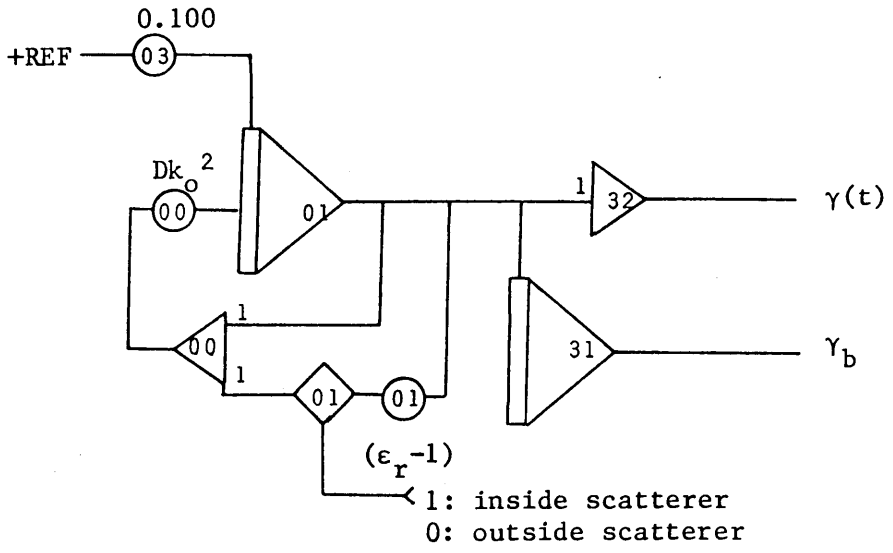

Figure 29. Patching of γ for TM scattering from a uniform dielectric object.

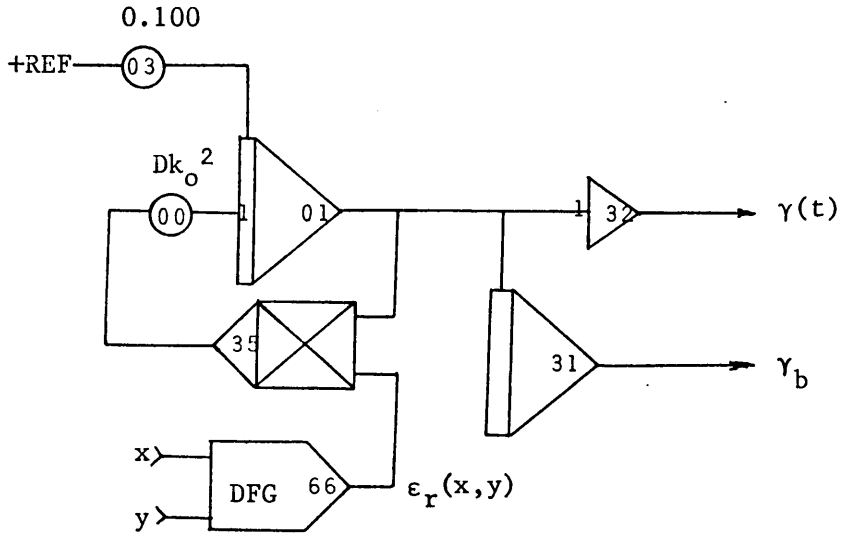

Figure 30. Patching of γ for TM scattering from a general dielectric object.

5.3.3 TE Scattering From Perfect Conductors

TE scattering is slightly more difficult to program than TM scattering since the boundary condition at a perfect conductor is $\partial\phi/\partial n = 0$ rather than $\phi = 0$. When the normal derivative on a boundary is zero, the random walk does not terminate at the boundary. Instead it "bounces off" the boundary back into the region of interest. A mathematical description of this phenomenon is given in Schrieder[149]. The random walk may bounce off the scatterer several times before finally terminating on the outer boundary C'.

The analog computer circuitry to implement this type of scattering is given in Figure 31. Notice that the majority of the patching diagram is the same as Figure 28. The additional circuitry at the initial condition inputs of integrators 20 and 21 is used to reset x(t) and y(t) to values Δr away from the scatterer whenever the scatterer is encountered. Switching is done using D/A switches.

5.3.4 TE Scattering From Perfect Dielectrics

For perfect dielectrics, the boundary condition at the surface of the scatterer is of no consequence; the random walk continues within the dielectric. However, the partial differential equation that must be solved is more complex. Performing the gradient and divergence operations in (2-24) with $\mu_r = 1$ gives:

$$\frac{\partial^2 H_z}{\partial x^2} + \frac{\partial^2 H_z}{\partial y^2} + \frac{\partial}{\partial x}\left(\frac{1}{\varepsilon_r}\right)\frac{\partial H_z}{\partial x} + \frac{\partial}{\partial y}\left(\frac{1}{\varepsilon_r}\right)\frac{\partial H_z}{\partial y} + k_o^2 \varepsilon_r H_z = 0 \qquad (5\text{-}3)$$

The first order derivatives require additional patching. Little[150]

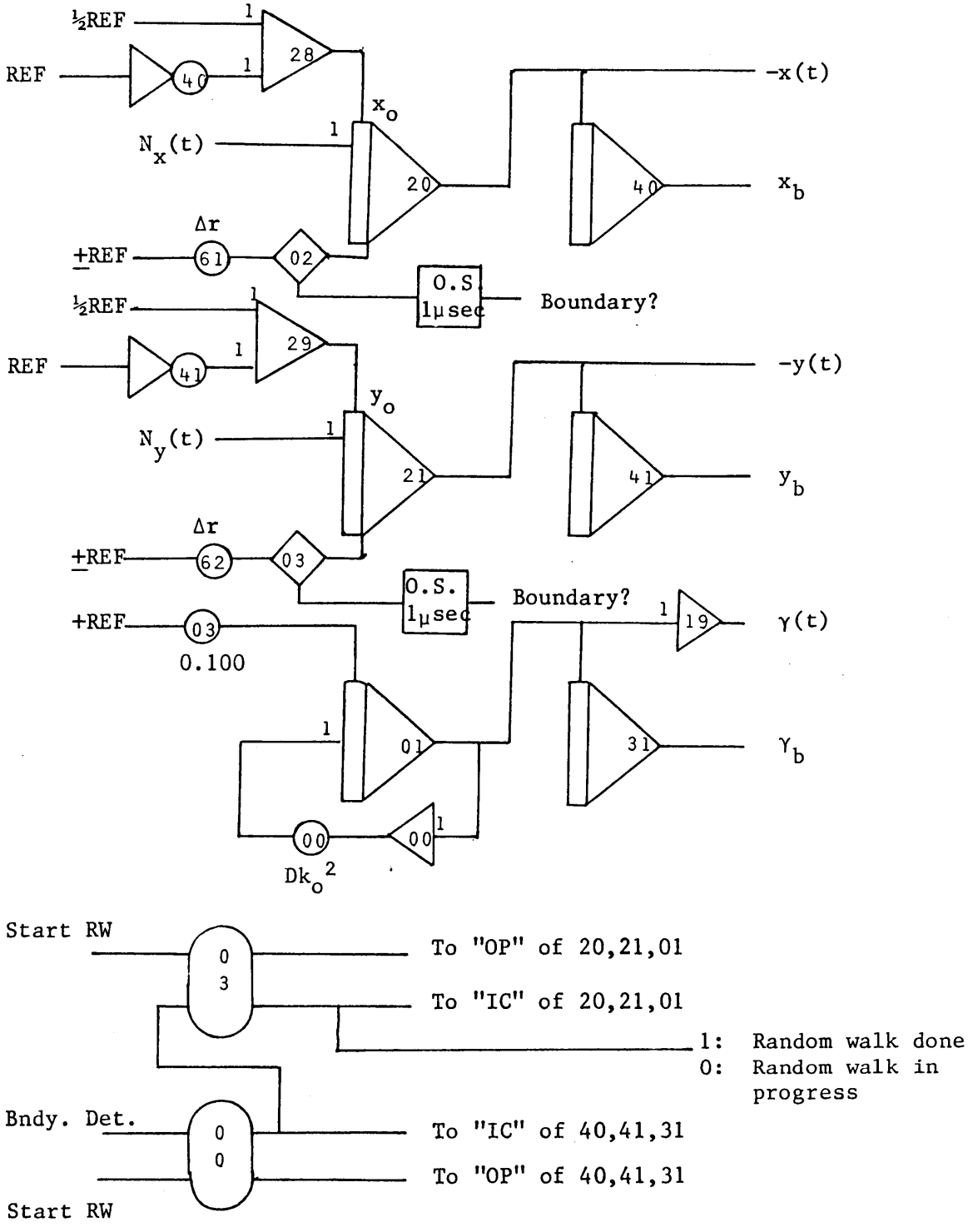

Figure 31. Analog patching for TE scattering from perfect conductors.

has shown how this might be done. Bekey and Karplus[151] have acutally implemented similar circuitry. Figure 32 shows how equation (5-3) might be patched if the derivatives of ε_r^{-1} are finite. The derivatives are approximated by the diode function generators on the analog computer.

If the dielectric scatterer is uniform, then the derivatives of ε_r^{-1} will be singular at the boundary. If the actual permittivity discontinuity can be approximated by a rapid but continuous change in $\varepsilon_r(x,y)$ at the scatterer boundary, Figure 32 may still be used. A somewhat better approximation can be obtained if D/A switches are used to switch on a large impulse of voltage when the random walk crosses the boundary. As an example, suppose $\varepsilon_r = 1$ outside the scatterer and $\varepsilon_r = 4$ inside the scatterer. Then the derivative of $1/\varepsilon_r$ would be $-3/4\ \delta(C)$. With integrator gains of 5000 and a random number generator voltage output of $\pm$ 6 volts, the boundary is traversed at the rate of 30,000 volts per second. Thus a pulse of 10 volts in height and 1/400,000 seconds in length would give the same effect as the $3/4\ \delta(C)$ impulse. This is implemented as shown in Figure 33 by using D/A switches.

5.4 System Testing

Before subjecting the entire Unimoment - Monte Carlo hybrid program to an exterior electromagnetic scattering problem, many simpler problems were first run to test the accuracy and reliability of the system. Several of these problems are described below.

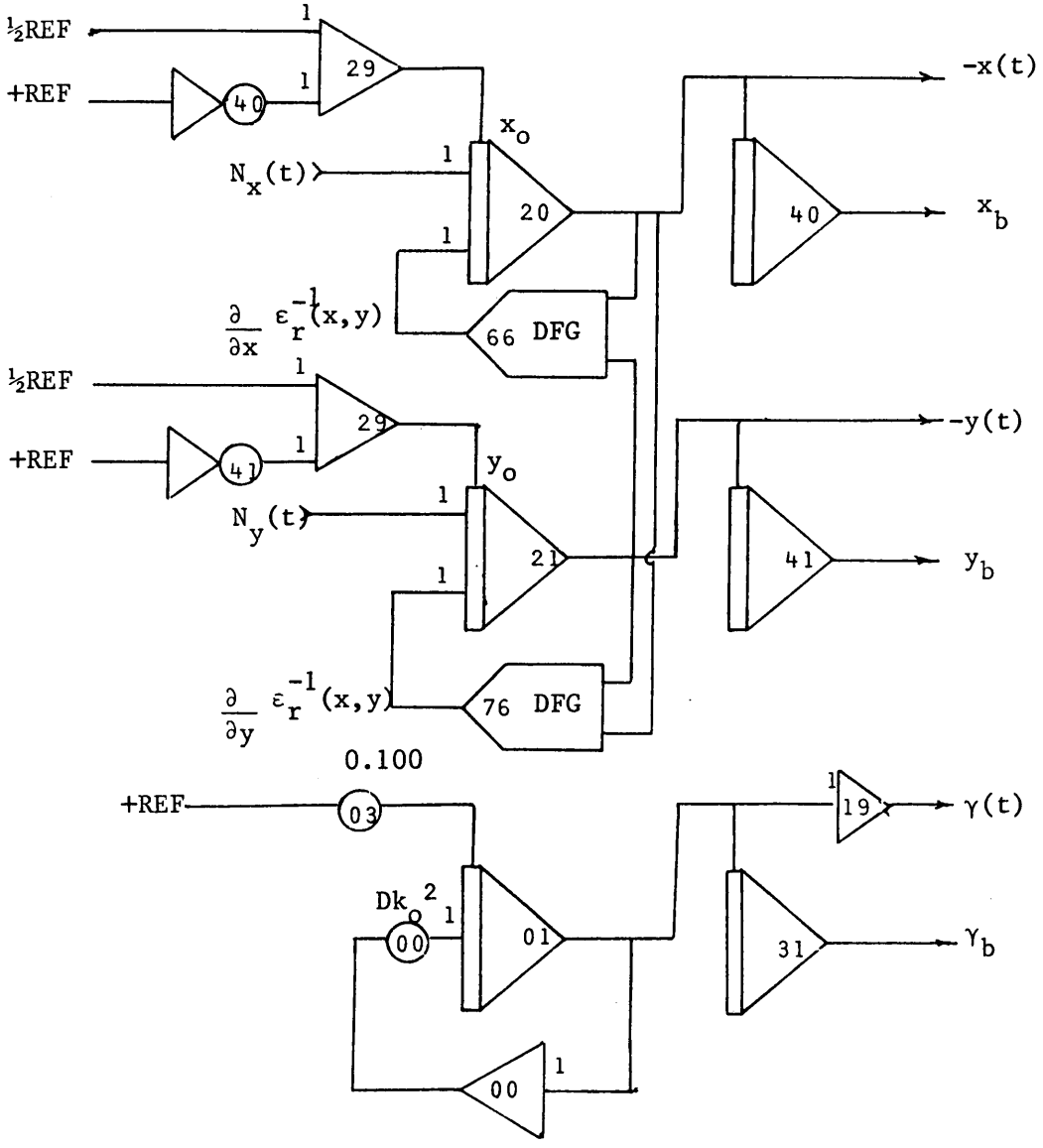

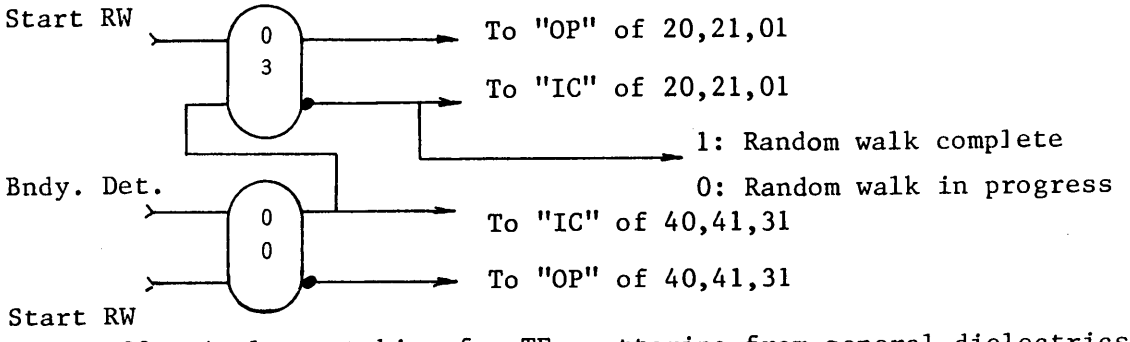

Figure 32. Analog patching for TE scattering from general dielectrics.

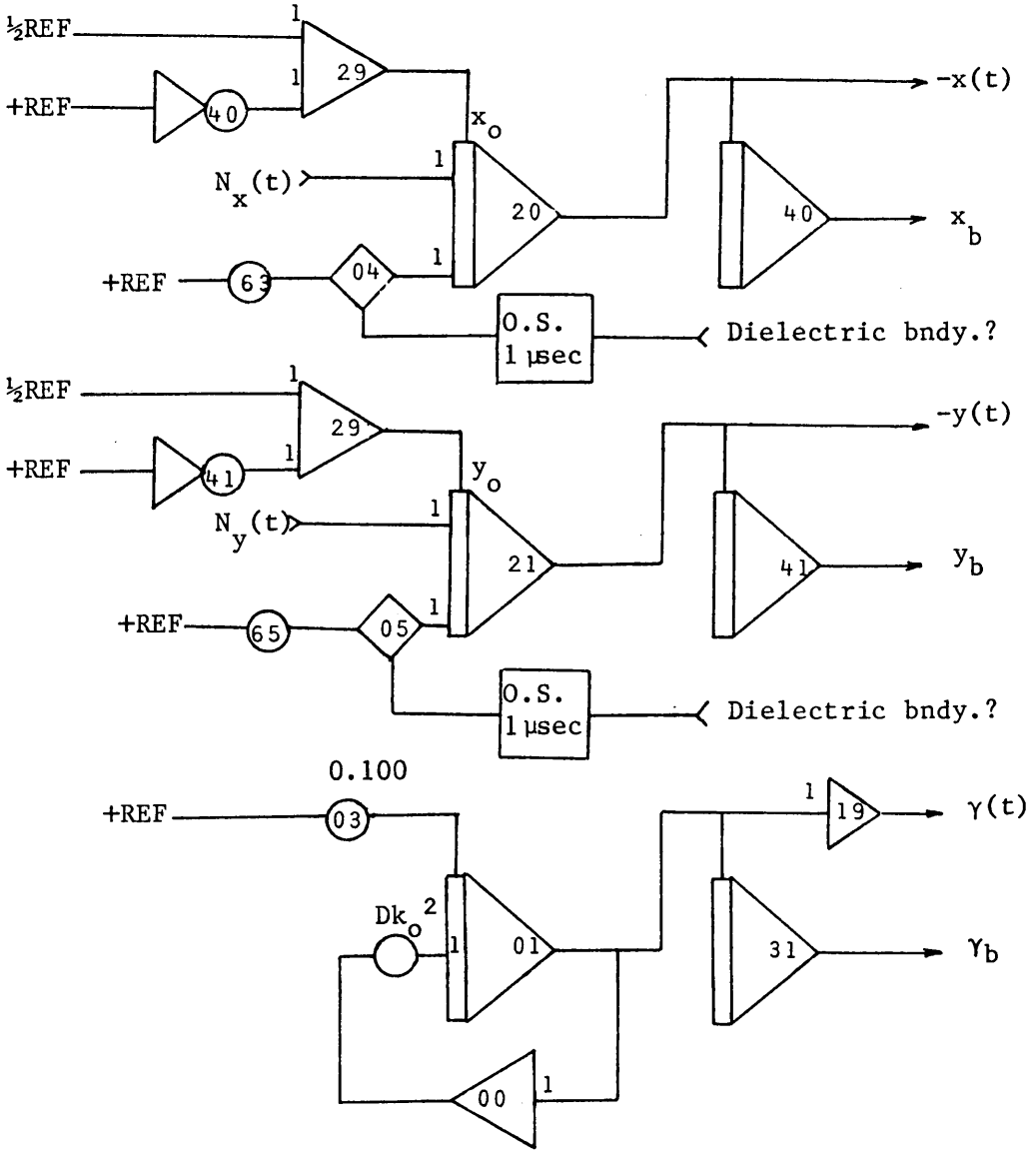

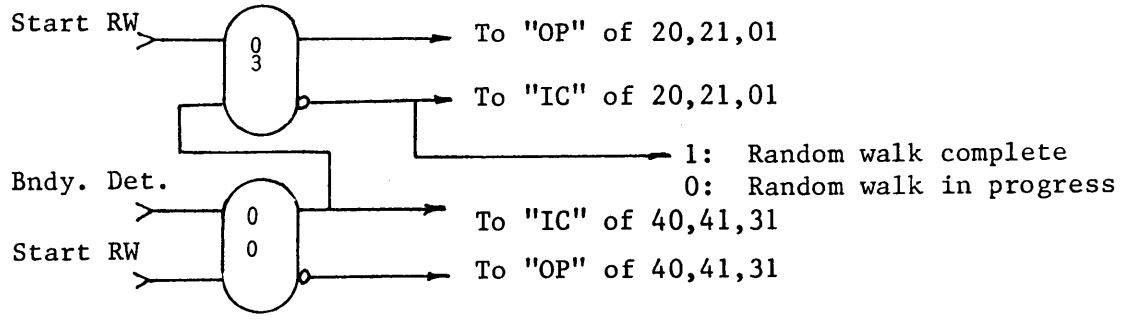

Figure 33. Analog patching for TE scattering from uniform dielectrics.

5.4.1 Random Noise Generator Testing

Even though the the theory of the feedback shift registers would lead one to believe that the random number generator implemented in the Unimoment - Monte Carlo method was performing properly, several test programs were run to firmly establish this fact. It was also necessary to determine the relationship between the power spectral density of the generator and the pot setting of the feedback loop of integrator 01 in Figure 28.

The time average of the pseudo-random noise may be measured by filtering it with a low pass filter. The filter output is then sampled and converted into an appropriate number for a digital counter. The direction of the counter is determined by the polarity of the sample. When the program stops, say, after m computer runs, the number indicated on the counter will be m times the mean value of the random noise. Alternatively, the time average may be found by using an analog integrator with a long time constant. Both of these methods were used with the feedback shift register random number generator, and it was initially found that the mean value of the output was slightly positive. To overcome this a d.c. blocking capacitor was added at the output of each channel of the random number generator, and the mean value dropped to less than 0.01 volts (0.001% full scale), which was considered quite acceptable.

The power spectral density of the random number generator could have been calculated by using standard techniques[152,153], but it was thought that analog amplifier bandwidth limitations might

invalidate the results. Instead, a value was experimentally determined by running several programs whose solution depended upon the power spectral density of the random signal passing through the entire system. Consider the solution of the two-dimensional Helmholtz equation within a circle of radius "a" with boundary value of 1. It is well known that the solution ϕ is given by

$$\phi(r) = \frac{J_o(kr)}{J_o(ka)} \tag{5-4}$$

By starting random walks at the origin, we find that the solution there is $\{J_o(ka)\}^{-1}$. By solving this interior problem many times for different pot settings of POT 00 in Figure 28, data was obtained relating the pot settings to $k = 2\pi/\lambda$. This data is plotted in Figure 34. It can be seen from the figure that $k^2 = 70.3$ (POT SETTING). Since this was the only information needed to solve exterior scattering problems, no other measurements were made.

5.4.2 Monte Carlo Solutions of One-Dimensional Problems

The solution of one-dimensional problems using Monte Carlo methods is quite similar to the solution of the two-dimensional problems of Section 5.3. However, since exact solutions of one-dimensional problems were more plentiful then exact solutions of two-dimensional problems, a more thorough test of the Monte Carlo method could be made in one dimension. Three of these test programs will be mentioned.

The first program run was used in the feasibility study for this dissertation. It was simply the solution of

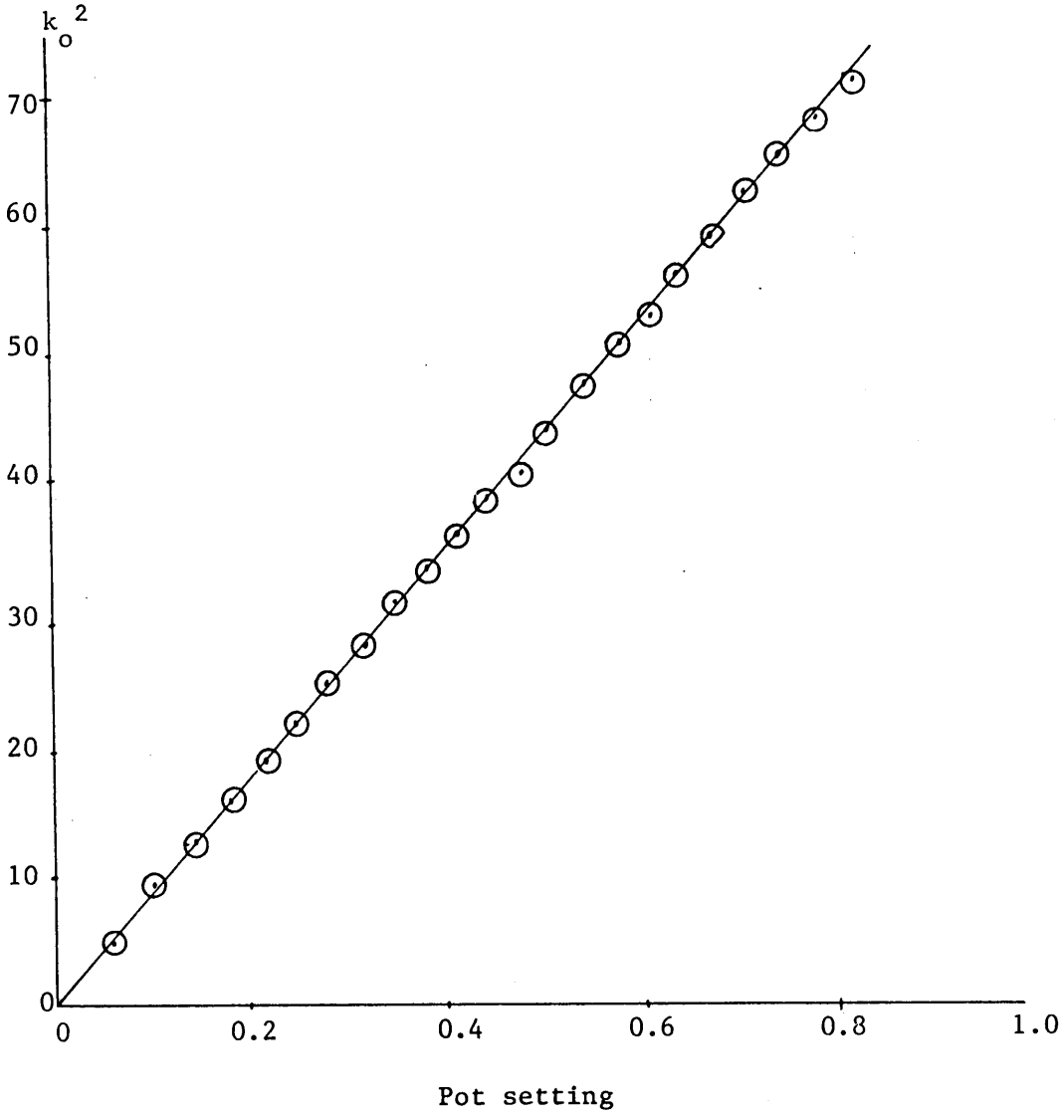

Figure 34. k_o^2 versus pot setting of POT00, Figure 28.

$$\frac{d^2\phi}{dx^2} = 0 \tag{5-5}$$

with $\phi(0) = 0$ and $\phi(1) = 1$. Its solution is $\phi(x) = x$. Since only the second derivative appears, no concern needed to be given to the power spectral density of the random number source. In fact, analog, digital, and feedback shift register random number generators were all used in the solution of this problem. The results are given in Figures 35 and 36. Notice that at no time did the error exceed 0.8% full scale for only 1000 random walks per point.

The second problem solved was

$$\frac{d^2\phi}{dx^2} + \lambda \frac{d\phi}{dx} = 0 \tag{5-6}$$

for $\phi(-1) = -1$ and $\phi(1) = 1$. The Monte Carlo solution and the analytical solutions are plotted in Figure 37 for various values of λ.

Finally the problem

$$\frac{d^2\phi}{dx^2} - (1 - x^2)\phi = 0 \tag{5-7}$$

for $\phi(-1) = 1$ and $\phi(1) = A$. Analytical and Monte Carlo solutions for $A = -1$, 0, and 1 are given in Figure 38.

5.4.3 Monte Carlo Solutions of Two-Dimensional Interior Problems

Two interior partial differential equations were solved using the Monte Carlo method. Since they do not fit under the heading of scattering problems they will be discussed in this section.

The simplest two-dimensional partial differential equation that could be simulated was Laplace's equation. Laplace's equation was

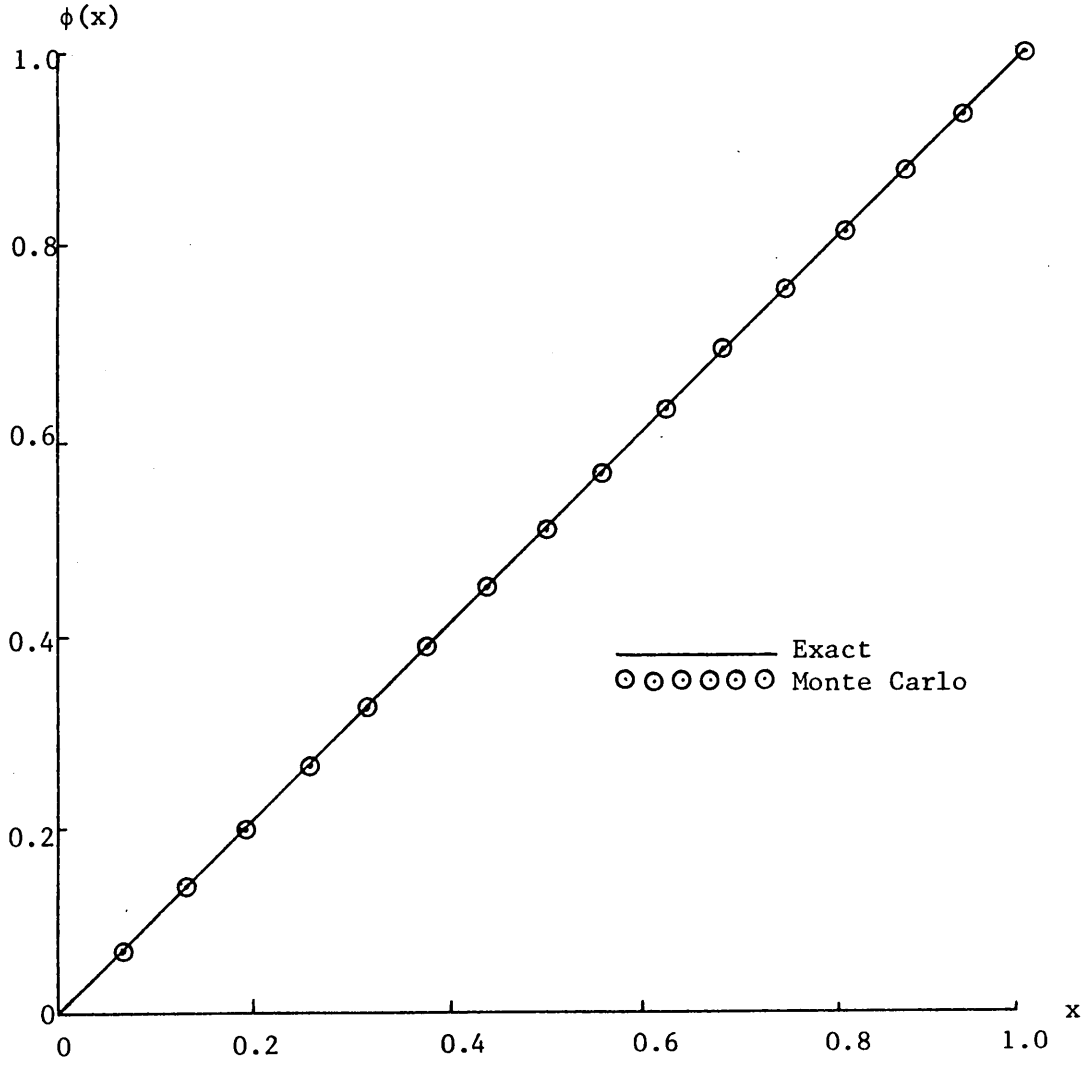

Figure 35. Analytical and Monte Carlo solutions of $\phi''(x) = 0$ with $\phi(0) = 0$ and $\phi(1) = 1$.

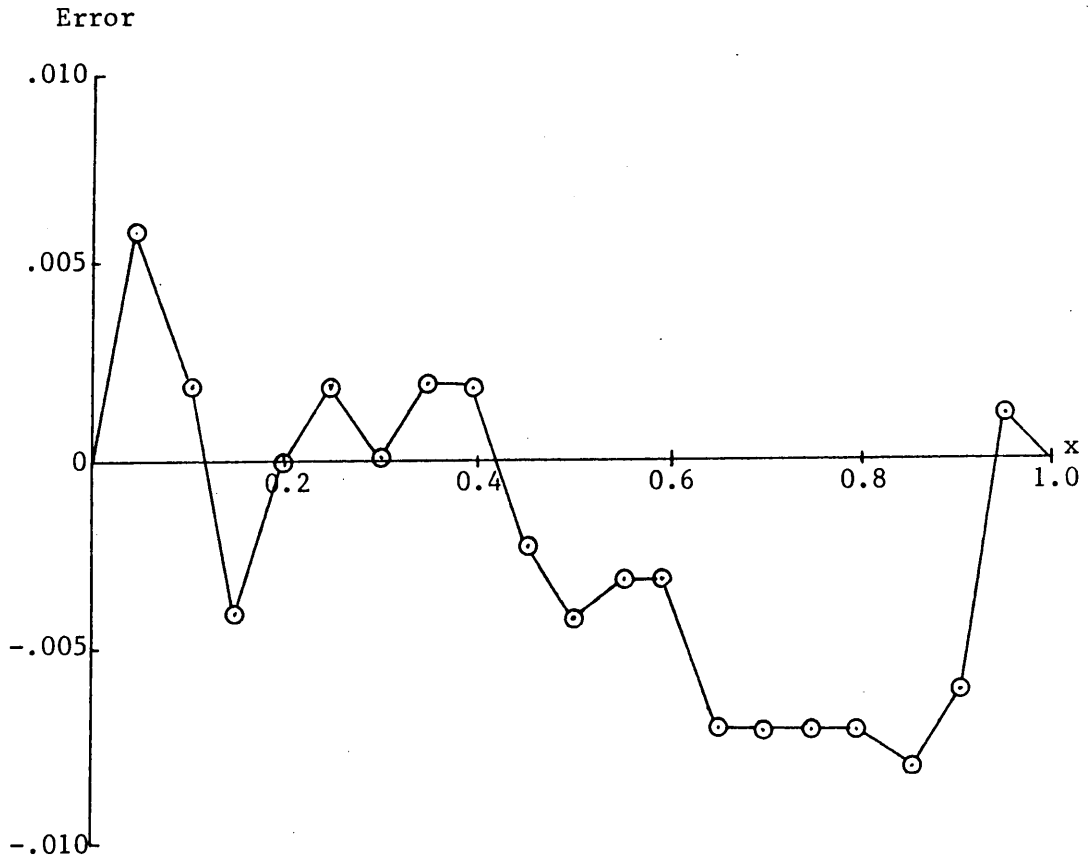

Figure 36. Absolute error between the analytic and Monte Carlo solutions of $\phi''(x) = 0$ shown in Figure 35.

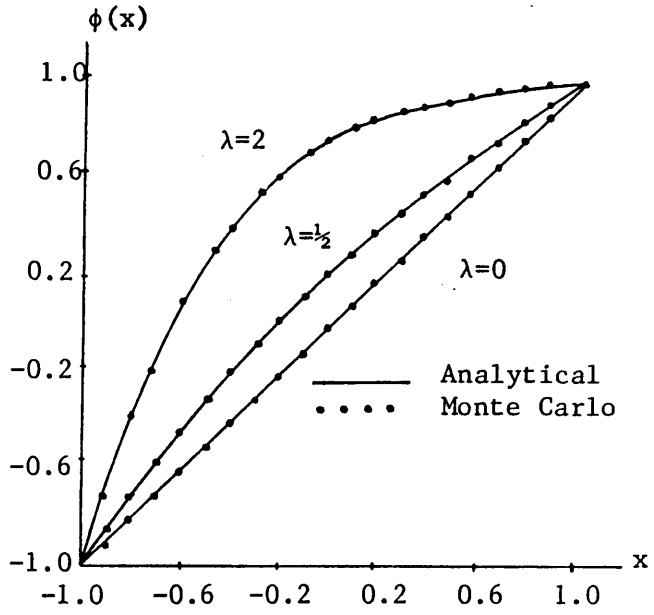

Figure 37. Analytical and Monte Carlo solutions of $\phi'' + \lambda\phi' = 0$ with $\phi(-1) = -1$ and $\phi(1) = 1$.

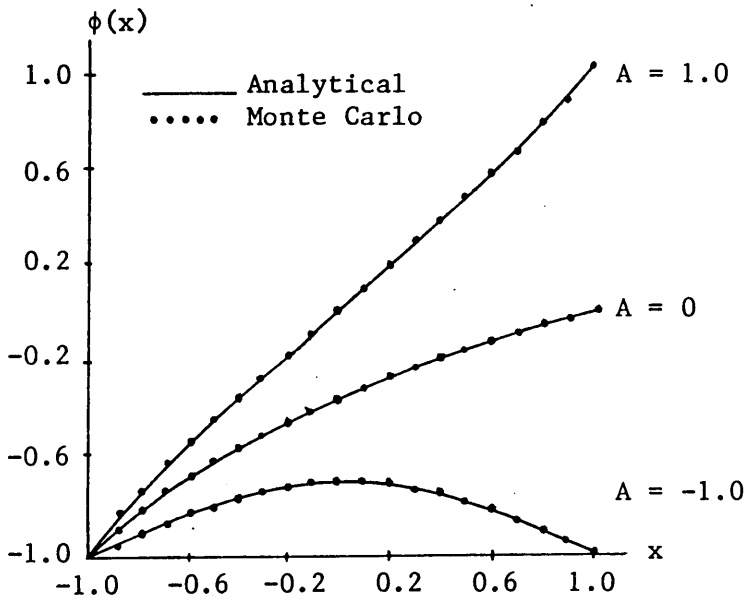

Figure 38. Analytical and Monte Carlo solutions of $\phi'' - (1 - x^2)\phi = 0$ with $\phi(-1) = -1$ and $\phi(1) = A$.

solved for the square, rectangle, and circle, with a variety of boundary conditions. In all cases, the errors produced by Monte Carlo simulation were less than 0.5% when at least 1000 random walks were taken. One example was run with 10,000 random walks and the resulting error was still 0.5%. This indicates that the analog computer component tolerances were masking out the increased accuracy of the Monte Carlo method when more then 1000 random walks were taken. A plot of error versus number of random walks for the potential at the center of a circle with sinusoidal boundary conditions is given in Figure 39.

The other interior example programmed was the Helmholtz equation within a circle of radius "a" with sinusoidal boundary conditions. This problem was chosen because the solutions are Bessel functions, which made error calculations easy. At no time did the error at any point measure more then 0.8% as long as at least 1000 random walks were taken and k was kept below resonance. (ka = 2.405) As k was increased, more error occurred, and this is plotted in Figure 40. By increasing the number of random walks, some reduction in error could be obtained, but the solution would not converge at ka = 2.405, regardless of the number of random walks. This is the same problem that was discussed at the end of Chapter IV.

5.4.4 Testing of the Fourier Analysis Algorithm

Because of the large amount of data that must be manipulated, the Fourier Analysis routine was a necessity in a practical implementa-

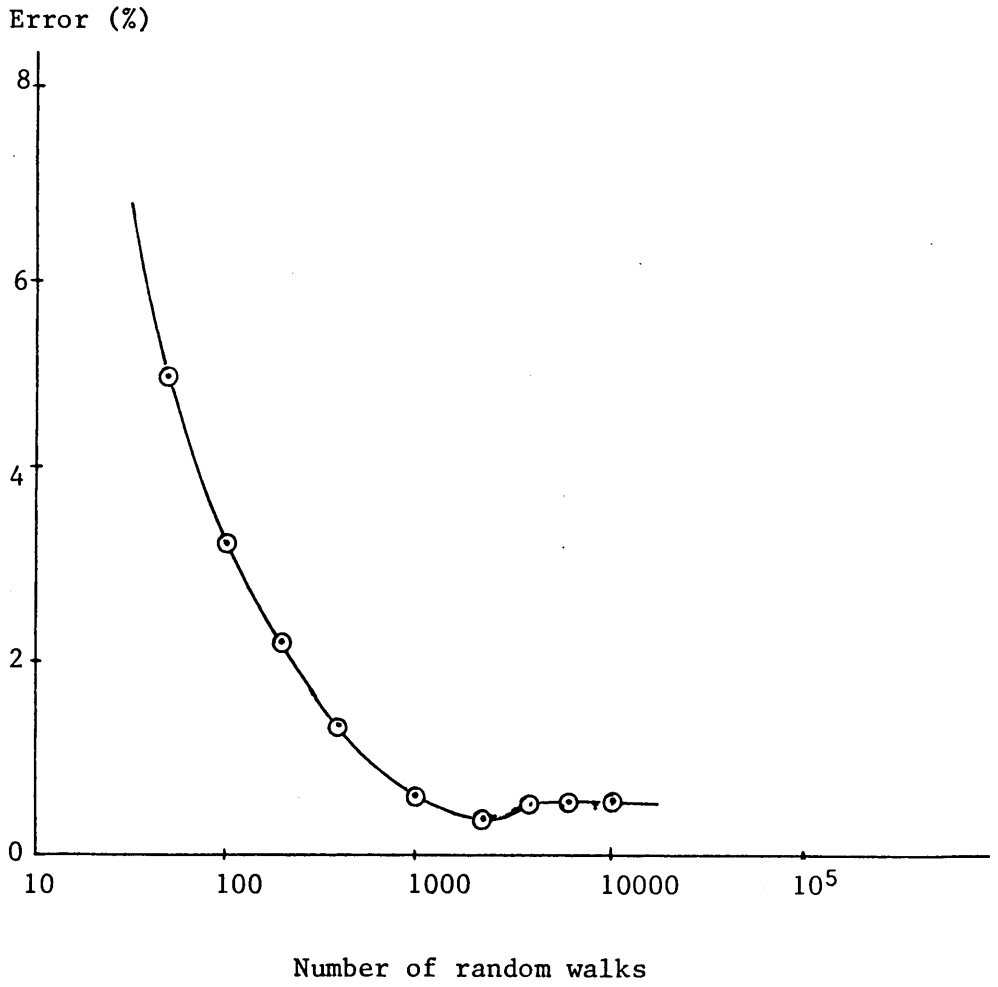

Figure 39. Error versus number of random walks in the Monte Carlo solution of $\nabla^2\phi = 0$ at the origin, $\phi(1,\theta) = \cos\theta$.

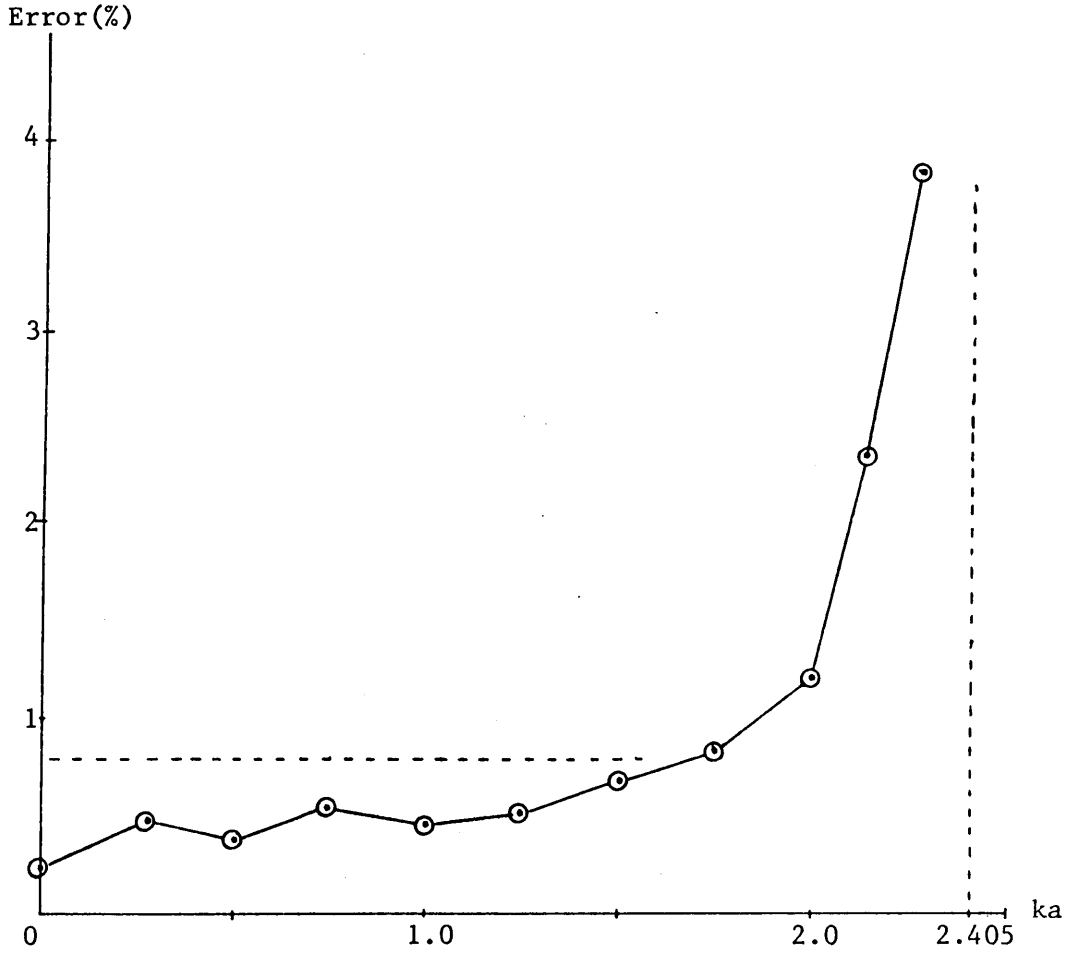

Figure 40. Error versus ka in the Monte Carlo solution of $\nabla^2\phi + k^2\phi = 0$ at the origin with $\phi(a,\theta) = \cos\theta$.

tion of the Unimoment - Monte Carlo method. The algorithm that was used has been thoroughly investigated by Goertzel.[154] However, to insure that no errors were made in programming the algorithm, it was tested with various input functions. Using a square wave function, the results of the algorithm as implemented on the GE-4020 are compared to the results of an exact expansion and to the results of the algorithm written in Fortran in Table 2. Notice that the error of the GE-4020 program is somewhat less than the error of the Fortran program. In all cases, the coefficients are within 0.1% of the exact values.

5.5 Summary

The Unimoment - Monte Carlo method has been described as it was implemented on the Virginia Polytechnic Institute and State University hybrid computer facility. An external source of multi-dimensional random noise had to be constructed, but all other computing hardware was already available. This should be true at most hybrid installations.

Two limitations of the Unimoment - Monte Carlo method were found. The speed at which random walks could be taken was limited by the conversion speed of the analog to digital converter. Only a change in hardware can remedy this constraint. Also, the accuracy of the data gathered from the random walks is limited by the electronic component accuracy of the analog computer to about 0.1%. However, this figure is usually acceptable in electromagnetics since it is equivalent to a -60dB noise level.

MODE #	COSINE COEFFICIENTS			SINE COEFFICIENTS		
	GE-4020	FORTRAN	ANALYTIC	GE-4020	FORTRAN	ANALYTIC
0	0.0	0.0	0	0.0	0.0	0
1	5×10^{-3}	0.001230	0	0.6365509	0.634144	0.63620
2	-2×10^{-6}	4×10^{-6}	0	-6×10^{-5}	-5×10^{-5}	0
3	5×10^{-3}	0.004665	0	0.2120171	0.211964	0.212206
4	-4×10^{-6}	-6×10^{-6}	0	-10^{-4}	-10^{-4}	0
5	5×10^{-3}	0.0046673	0	0.127012	0.12700	0.127324
6	-9×10^{-6}	-8×10^{-6}	0	-1.7×10^{-4}	-1.7×10^{-4}	0
7	5×10^{-3}	0.004838	0	0.0905113	0.090515	0.090946
8	-1.5×10^{-5}	-1×10^{-5}	0	-2.3×10^{-4}	-2.3×10^{-4}	0
9	5×10^{-3}	.0048951	0	0.070179	0.0701829	0.0707355
10	-2.5×10^{-5}	-2×10^{-5}	0	-2.94×10^{-4}	-2.85×10^{-4}	0
11	5×10^{-3}	.0048663	0	.0571957	.057203	0.0578745
12	-3.4×10^{-5}	-3.2×10^{-5}	0	-3.5×10^{-4}	-3.4×10^{-4}	0
13	5×10^{-3}	.004863	0	0.048168	.0481781	0.0489708
14	-4.5×10^{-5}	-4×10^{-5}	0	-4×10^{-4}	-4×10^{-4}	0

Table 2. Fourier series coefficients for a symmetric square wave

CHAPTER VI

SOLVING EXTERIOR SCATTERING PROBLEMS USING THE UNIMOMENT - MONTE CARLO METHOD

In this chapter, several two-dimensional problems will be studied using the Unimoment - Monte Carlo method. The results of these problems will be compared to previously published data and/or analytical solutions. Both TM and TE examples will be presented, and both perfect conductors and perfect dielectrics will be used as scatterers. Following this work, an investigation of system parameters will be made in order to determine which parameters are most critical to program accuracy and execution time.

6.1 Scattering From Circular Cylinders

6.1.1 TM Scattering From Perfectly Conducting Circular Cylinders

Since the solution of exterior scattering from perfectly conducting circular cylinders is well known, many examples were run for this type of problem. A series form of the scattered field is given by Harrington[155]

$$E_z^s = -E_o \sum_{n=0}^{\infty} \frac{j^{-n} J_n(ka)}{H_n^{(2)}(ka)} H_n^{(2)}(kr) e^{jn\theta} \qquad r > a \qquad (6\text{-}1)$$

where a is the radius of the cylinder, and the incident wave is of the form

$$E_z^i = E_o e^{-jkx} = E_o \sum_{n=-\infty}^{\infty} j^{-n} J_n(kr) e^{jn\theta} \qquad (6\text{-}2)$$

Several examples using the Unimoment - Monte Carlo method were run for circle radius of 0.3 with k equal to 1.1859, 1.67714, 2.0541, 2.371835, 2.6518, 3.24777, 4.19285, 4.7806, 5.9296, and 8.3857. When at least 400 random walks were taken at 401 points spaced equally around C', the error of these solutions when compared to the exact solution (6-1) was never greater than 0.5%. In fact, when only 100 random walks were taken, the error never exceeded 2%. Plots of solutions for several values of k are compared to the series solution (6-1) in Figure 41. Documentation of the trial function pairs and the actual coefficients of equation (6-1) are given in Table 3.

It is also interesting to note that the error increases with values of k. A plot of the maximum error in the far field patterns for several values of k is shown in Figure 42. It was thought that increasing the number of random walks would decrease this error for larger values of k. Additional program runs were made with 800, 1600, 2400, and 3200 random walks per point. Figure 43 shows only some decrease in error, but apparently the main contributor to the error is the approximation of the normal derivative, equation (4-16). The distance h of (4-16) was 5% of the radius of C' for the above examples. Decreasing this distance to 1% of C' gave much better results for the lower order modes. This is due to the nature of the approximation (4-16). The higher order mode trial functions exhibited a much steeper normal derivative compared to the first few modes. (See Table 3). This is because when the slopes are small, equation (4-16) requires the subtraction of two numbers which are almost equal.

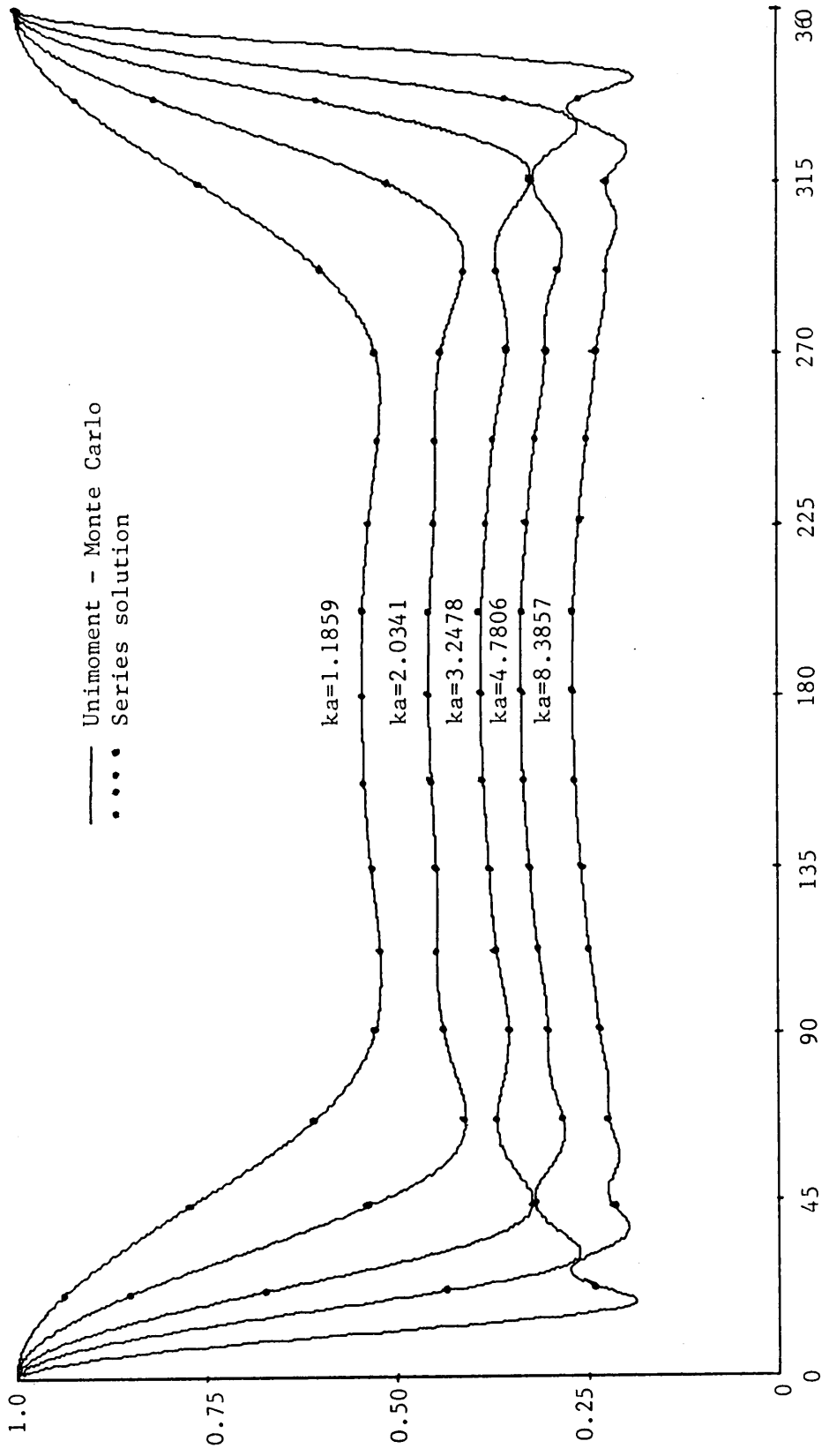

Figure 41. Normalized far-field patterns for TM scattering from perfectly conducting circular objects.

Table 3. Trial functions and their normal derivatives for TM scattering from a perfectly conducting cylinder of radius 0.3.

k = 1.1859

Trial function	Normal derivative along C'
1	$3.822 + .02484\cos\theta - .0201\cos 3\theta + .0326\sin\theta + .016\sin 4\theta$
$\cos\theta$	$.0370 + 4.174\cos\theta - .0031\cos 3\theta + .0140\sin 2\theta$
$\cos 2\theta$	$-.045 + .1071\cos\theta + 5.112\cos 2\theta + .0083\cos 3\theta$
$\cos 3\theta$	$-.0130 + .076\cos 2\theta + 6.517\cos 3\theta - .0446\sin 2\theta$
$\cos 4\theta$	$.0044 + .0606\cos 3\theta + 8.207\cos 4\theta - .0619\sin 3\theta$
$\sin\theta$	$.023 - .0128\cos 2\theta + 4.170\sin\theta - .02554\sin 3\theta$
$\sin 2\theta$	$.0071 - .01974\cos 4\theta + .0312\sin\theta + 5.123\sin 2\theta - .016\sin 3\theta$
$\sin 3\theta$	$-.0167 + .0401\cos 2\theta - .003158\cos 3\theta - .00701\sin\theta + 6.531\sin 3\theta - .0032\sin 4\theta$
$\sin 4\theta$	$-.0094 + .0629\cos 2\theta + .0052\sin 3\theta + 8.214\sin 4\theta$

n	a_n(calculated)	a_n(exact)
0	-.6642+j.4723	-.66412+j.47229
1	-.0157+j.1769	-.15644+j.17619
2	0+j.0030	0+j.00301
3	0	0+j.00001
4	0	0+j0

Table 3. (continued)

$k = 2.0541$

Trial function	Normal derivative along C'
1	$3.642 + .0873\cos2\theta + .0114\cos4\theta + .0072\sin\theta + .126\sin3\theta$
$\cos\theta$	$.0457 + 4.010\cos\theta + .0110\cos2\theta + .00712\sin3\theta$ $-.02685\sin4\theta$
$\cos2\theta$	$.00692 + .033\cos\theta + 4.942\cos2\theta + .03179\cos4\theta$ $-.01596\sin\theta + .04910\sin3\theta$
$\cos3\theta$	$.008532 + .0095\cos\theta + .04145\cos2\theta + 6.341\cos3\theta$ $-.00855\sin\theta - .02925\sin2\theta$
$\cos4\theta$	$.02022 + .01171\cos\theta + .0624\cos3\theta + 8.045\cos4\theta$ $+.05688\sin\theta - .01051\sin2\theta - .04931\sin3\theta$
$\sin\theta$	$.01555 + .00376\cos\theta - .04077\cos3\theta + 3.962\sin\theta$ $+.1651\sin2\theta + .02914\sin3\theta$
$\sin2\theta$	$.02929 + .01838\cos\theta - .00289\cos4\theta + .031704\sin\theta$ $+4.910\sin2\theta + .0650\sin4\theta$
$\sin3\theta$	$-.01031 + .03353\cos2\theta + .04714\cos3\theta - .0249\cos4\theta$ $-.03994\sin\theta + .05107\sin2\theta + 6.294\sin3\theta + .0081\sin4\theta$
$\sin4\theta$	$-.04940 + .03256\cos2\theta + .04593\cos3\theta + .01121\sin\theta$ $+.0602\sin3\theta + 8.011\sin4\theta$

n	a_n(calculated)	a_n(exact)
0	-.9090+j.2876	-.90829+j.28860
1	-.1081+j.4523	-.10756+j.45117
2	-.0003+j.0251	-.00031+j.02478
3	0+j.0004	0+j.00042
4	0	0+j.00001

Table 3. (continued)

$k = 3.2478$

Trial function	Normal derivative along C'
1	$3.214 + .05349\cos\theta - .0091\cos3\theta + .02575\cos4\theta + .01678\sin\theta - .04467\sin2\theta + .01025\sin4\theta$
$\cos\theta$	$.01682 + 3.581\cos\theta + .06576\cos2\theta - .0110\cos4\theta - .04196\sin\theta + .03683\sin2\theta + .02163\sin3\theta + .00703\sin4\theta$
$\cos2\theta$	$.0222 + .02626\cos\theta + 4.599\cos2\theta + .03692\cos4\theta - .030245\sin\theta + .01242\sin3\theta - .01052\sin4\theta$
$\cos3\theta$	$.00254 + .07083\cos\theta + .0320\cos2\theta + 6.091\cos3\theta + .07083\cos4\theta + .01705\sin2\theta - .00561\sin3\theta + .0014\sin4\theta$
$\cos4\theta$	$-.07141 + .01361\cos2\theta + .06066\cos3\theta + 7.694\cos4\theta - .01625\sin\theta + .05019\sin3\theta$
$\sin\theta$	$.01431 - .01254\cos\theta + .05412\cos4\theta + 3.617\sin\theta + .01910\sin3\theta$
$\sin2\theta$	$-.02386 + .01836\cos\theta + .03375\cos3\theta + .027679\sin\theta + 4.559\sin2\theta + .03024\sin4\theta$
$\sin3\theta$	$-.010484 + .04216\cos2\theta + .052877\sin2\theta + 5.898\sin3\theta + .04049\sin4\theta$
$\sin4\theta$	$-.00993 - .09036\cos\theta + .06014\cos3\theta + .01253\sin\theta + .05757\sin3\theta + 7.581\sin4\theta$

n	a_n (calculated)	a_n (exact)
0	-.9922-j.0876	-.99241-j.08681
1	-.4489+j.8344	-.44756+j.83355
2	-.00821+j.1279	-.00810+j.12702
3	0+ j.0059	0+j.00581
4	0+j.0001	0+j.00012

Table 3. (continued)

$k = 4.7806$

Trial function	Normal derivative along C'
1	$2.280 + .036685\cos\theta - .021896\cos 3\theta + .09741\sin\theta + .02704\sin 3\theta$
$\cos\theta$	$.02593 + 2.664\cos\theta - .011505\cos 4\theta + .04575\sin 2\theta + .07534\sin 4\theta$
$\cos 2\theta$	$-.03004 + .03570\cos\theta + 3.742\cos 2\theta - .025262\sin\theta + .07537\sin 2\theta$
$\cos 3\theta$	$.02037 + .05107\cos 2\theta + 5.338\cos 3\theta - .04516\sin 2\theta$
$\cos 4\theta$	$.10003 - .08325\cos 2\theta + 7.083\cos 4\theta - .05668\sin 3\theta + .01359\sin 4\theta$
$\sin\theta$	$.02851 - .014526\cos 4\theta + 2.6841\sin\theta + .01795\sin 2\theta - .010438\sin 4\theta$
$\sin 2\theta$	$.00289 + .03210\cos\theta + .03882\sin\theta + 3.699\sin 2\theta + .05969\sin 3\theta$
$\sin 3\theta$	$.07424\cos\theta + .04569\cos 2\theta + .08306\cos 3\theta + .05576\sin 2\theta + 5.421\sin 3\theta$
$\sin 4\theta$	$.08166 + .06506\cos 3\theta + .02117\sin\theta + .068289\sin 3\theta + 7.014\sin 4\theta$

n	a_n(calculated)	a_n(exact)
0	-.7054-j.4558	-.70588-j.45564
1	-1.181+j.9834	-1.1814+j.98341
2	-.0918+j.4185	-.09073+j.41621
3	-.0011+j.0474	-.00109+j.04679
4	0+j.0024	0+j.00229

Table 3. (concluded)

$k = 8.3857$

Trial functions	Normal derivative along C'
1	$-2.032 + .08975\cos 2\theta - .04371\cos 3\theta + .0313\sin 3\theta - .02567\sin 4\theta$
$\cos\theta$	$.07318 - 1.458\cos\theta - .02830\cos 2\theta - .01578\cos 3\theta - .02298\sin 3\theta$
$\cos 2\theta$	$.04699 + .014965\cos\theta + .05314\cos 2\theta - .01169\cos 3\theta - .02045\sin\theta - .02189\sin 2\theta$
$\cos 3\theta$	$-.05491 - .05999\cos 2\theta + 2.341\cos 3\theta - .044967\sin 2\theta$
$\cos 4\theta$	$.08059 + .07883\cos 3\theta + 4.612\cos 4\theta - .020684\sin 2\theta - .069921\sin 3\theta$
$\sin\theta$	$.05519 + .020343\cos 2\theta - .01357\cos 4\theta - 1.512\sin\theta - .032196\sin 4\theta$
$\sin 2\theta$	$.04295 + .028494\cos\theta + .01850\cos 3\theta + .03503\sin\theta + .0625\sin 2\theta - .030621\sin 3\theta - .01303\sin 4\theta$
$\sin 3\theta$	$.01185 - .05130\cos\theta + .02559\cos 4\theta + .042718\sin 2\theta + 2.234\sin 3\theta - .02875\sin 4\theta$
$\sin 4\theta$	$.09757 + .08751\cos 2\theta - .08288\sin\theta + .07261\sin 3\theta + 4.623\sin 4\theta$

n	a_n(calculated)	a_n(exact)
0	-.0129+j.1128	-.012673+j.118580
1	-1.823-j.5681	-1.82485-j.565353
2	-1.179+j.9837	-1.17845+j.983950
3	-.1587+j.5405	-.158661+j.540507
4	-.0056+j.1065	-.005699+j.106605

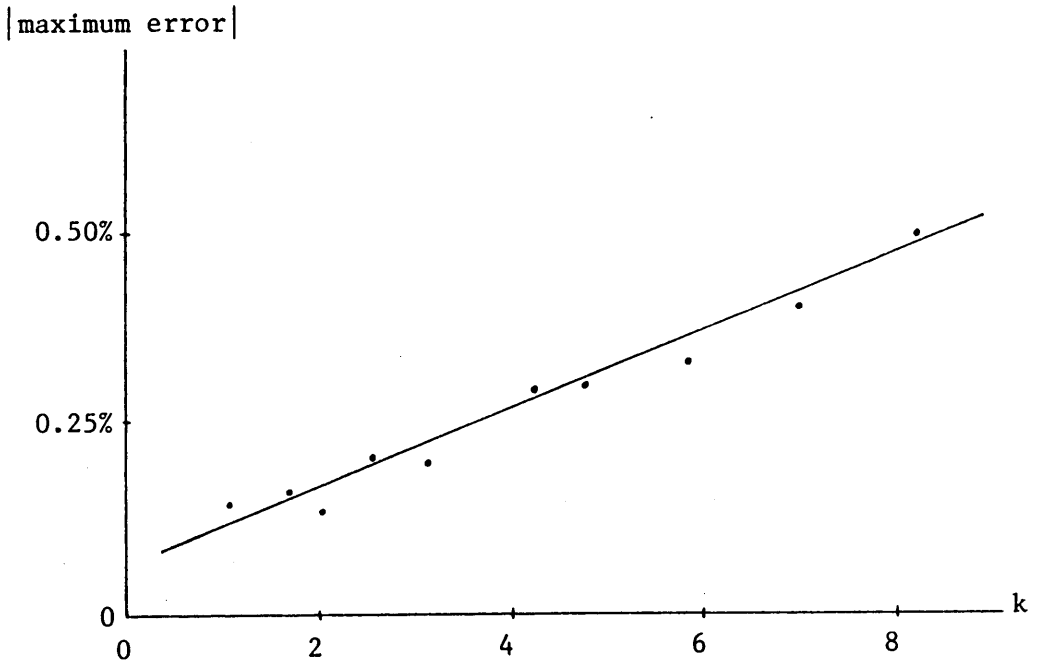

Figure 42. Maximum far-field pattern error versus k for several sizes of perfectly conducting cylinder of radius 0.3.

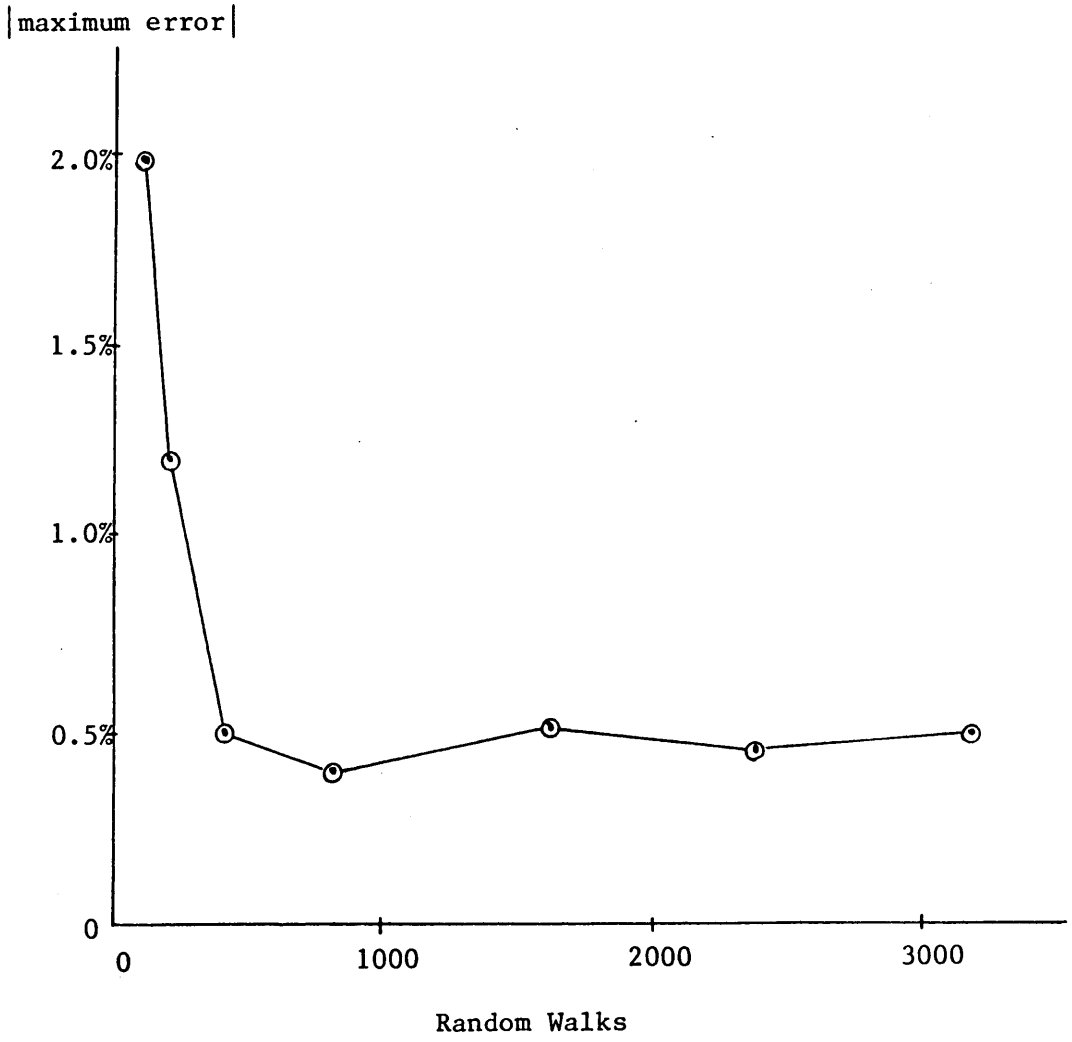

Figure 43. Maximum far-field pattern error versus number of random walks per point for a perfectly conducting circular cylinder of radius ka = 2.516.

Since fixed point arithmetic was used throughout the digital program, a loss of significance occured. To avoid this problem, a quadratic or cubic approximation might have been used instead of the linear approximation (4-16). Examples of higher order approximations are given in Abramowitz and Stegun[156].

The solution time of each problem remained the same since the physical dimensions were constant. Only when the number of random walks was increased did the solution time increase. The average soltuion time for 400 random walks was 20 minutes, 19 minutes of which were spent in analog to digital conversion of the data.

6.1.2 TM Scattering From Dielectric Circular Cylinders

Several examples of scattering from circular dielectric cylinders with $\varepsilon_r = 4$ were run. These solutions were compared to Harrington's series solution[157]

$$E_z^s = E_o \sum_{n=-\infty}^{\infty} (j)^{-n} a_n H_n^{(2)}(kr) e^{jn\theta}$$

where the incident field is given by (6-2), $k_o = \omega^2 \mu_o \varepsilon_o$, $k_1^2 = \omega^2 \mu_o \varepsilon_o \varepsilon_r$ and

$$a_n = \frac{k_o J_n(k_1 a) J_n'(k_o a) - k_1 J_n'(k_1 a) J_n(k_o a)}{k_1 J_n'(k_1 a) H_n^{(2)}(k_o a) - k_o J_n(k_1 a) H_n^{(2)\prime}(k_o a)} \qquad (6\text{-}4)$$

The data for the trial functions for two values of wave number k_o are given in Table 4. The far-field patterns are plotted in Figure 44. Notice that the error is somewhat greater than the error for the

Table 4. Trial functions and their normal derivatives for TM scattering from a dielectric ($\varepsilon_r = 4$) circular cylinder of radius 0.3.

k = 2.500

Trial function	Normal derivative along C'
1	-39.82 + .2157cosθ + .1686cos2θ - .2083cos4θ -.12966sin2θ + .02093sin4θ
cosθ	-0.3210 + .6239cosθ + .07635cos2θ + .06185cos4θ - .02109sinθ + .04412sin3θ
cos2θ	0.1361 + .03936cosθ + 3.344cos2θ + .24902cos3θ - .05837cos4θ - .07015sinθ - .08151sin2θ - .06187sin4θ
cos3θ	-.05047 - .01339cosθ + 5.571cos3θ + .02874cos4θ - .014346sinθ - .03294sin2θ - .28445sin4θ
cos4θ	-.17251 + .01471cosθ + .1554cos3θ + 7.6217cos4θ - .01668sinθ - .06338sin3θ
sinθ	-.04627 + .0248cosθ + .02822cos3θ + .67721sin2θ + .04997sin4θ
sin2θ	0.02525 + .02865cosθ + .033590cos2θ + .03824cos3θ - .01395cos4θ - .10418sinθ + 3.322sin2θ - .02359sin3θ + .04172sin4θ
sin3θ	0.10594 - .034945cosθ + .08538cos2θ + .01061cos4θ - .043084sinθ + 5.812sin3θ - .08963sin4θ
sin4θ	-.02610 + .024417cosθ + .038674cos2θ + .070852cos3θ - .02726sinθ + .07582sin3θ + 7.601sin4θ

Table 4. (continued)

k = 6.667

Trial function	Normal derivative along C'
1	-54.86 - .1032cos2θ - .08468cos3θ + .0808cos4θ + .24105sinθ + .13790sin2θ + .13433sin3θ + .00942sin4θ
cosθ	0.04472 + .41230cosθ - .05654cos2θ - .06213cos3θ + .013946sin2θ + .08587sin4θ
cos2θ	0.057705 + 12.143cos2θ - .04824cos3θ - .17483sinθ + .01110sin2θ + .09439sin3θ + .07266sin4θ
cos3θ	0.07464 + .06878cosθ + 1.823cos3θ - .10687cos4θ - .03903sinθ - .00582sin3θ
cos4θ	0.03595 + .01749cosθ + .09013cos2θ + .029641cos3θ + 5.437cos4θ - .06036sin2θ - .031933sin4θ
sinθ	0.027630 + .06268cosθ - .07785cos2θ - .01026cos4θ + .41340sinθ - .03027sin2θ - .08422sin4θ
sin2θ	0.06182 + .18841cosθ - .08511cos3θ - .09640cos4θ + .08477sinθ + 12.347sin2θ - .12557sin4θ
sin3θ	0.01397 + .08660cosθ + .027554cos2θ - .05108cos3θ + .046081sinθ + 1.861sin3θ - .11148sin4θ
sin4θ	0.04603 + .09610cosθ + .03523cos3θ + .06661sinθ + .079379sin2θ + .02873sin3θ + 5.332sin4θ

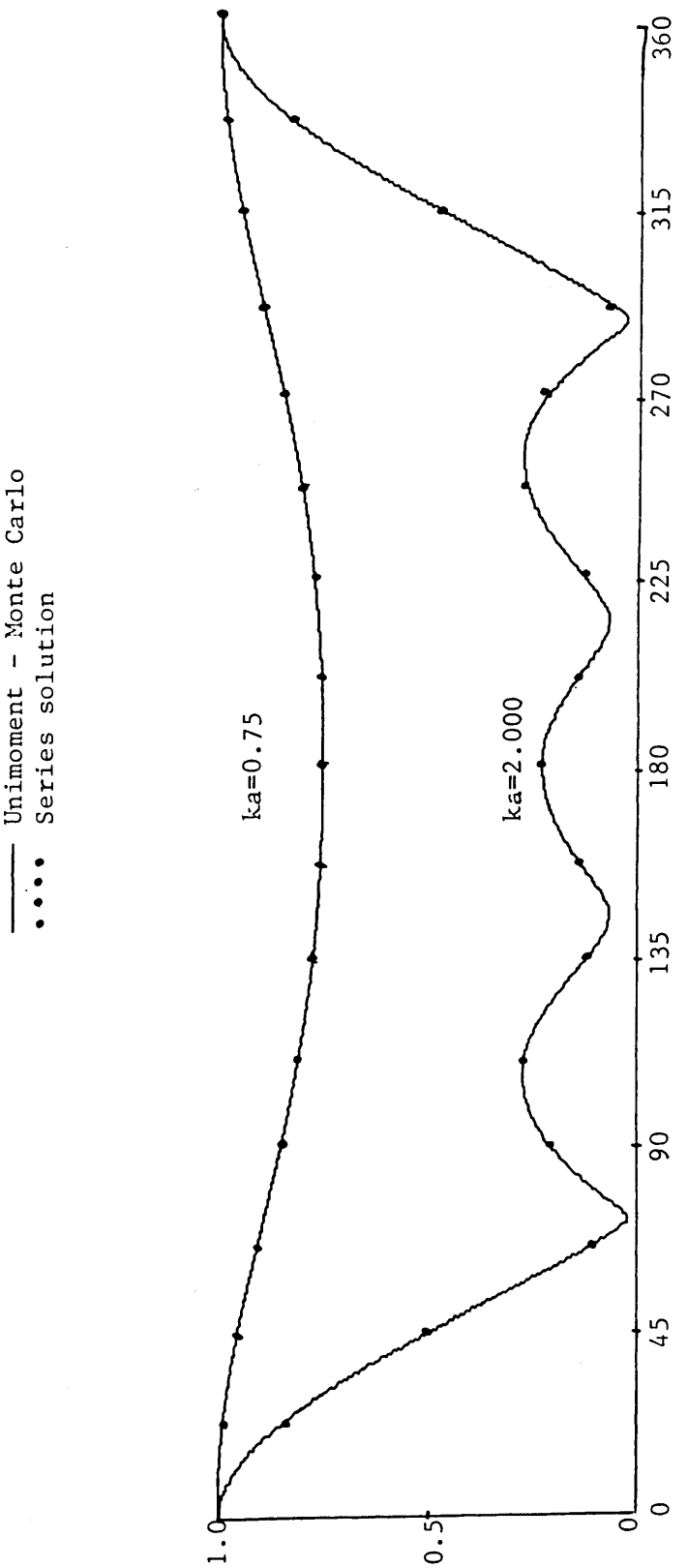

Figure 44. Normalized far-field pattern error for TM scattering from circular dielectric (ε_r=4) cylinders.

perfectly conducting case. Since each random walk must traverse more area, the average elapsed time for each random walk is greater than that for the perfect conducting circle. It is believed that analog amplifier offset and drift account for this increase in error because any offset in integrators 20 and 21 of Figure 29 will be integrated over a longer time period.

6.1.3 TE Scattering From Perfectly Conducting Cylinders

Two different examples were run for this case, and the results were compared to the series solution[158]

$$H_z^s = -H_o \sum_{n=-\infty}^{\infty} j^{-n} \frac{J_n'(ka)}{H_n^{(2)\prime}(ka)} H_n^{(2)}(kr) e^{jn\theta} \qquad (6\text{-}5)$$

with incident field

$$H_z^i = H_o e^{-jkx} = H_o \sum_{n=-\infty}^{\infty} j^{-n} J_n(kr) e^{jn\theta} \qquad (6\text{-}6)$$

The data for the trial functions is given in Table 5, and the far-field patterns are plotted in Figure 45. The maximum error that occured was 0.8%, and the average execution time was 22 minutes per program. Again, 19 of these minutes were spent performing analog to digital conversions.

It should be noted that TE scattering from perfect conductors is the most difficult circular cylinder problem to patch on the analog computer, since it is the normal derivative of the H-field that is zero at the scatterer boundary rather than the H-field itself.

Table 5. Trial functions and their normal derivatives for TE scattering from a perfectly conducting circular cylinder of radius 0.3.

k = 2.500

Trial function	Normal derivative along C'
1	-1.071 + .01917cosθ + .08256cos2θ - .01645cos3θ + .01461sinθ + .06005sin3θ
cosθ	0.01423 + .01873cosθ + .01004cos2θ + .00871cos3θ - .00177sinθ - .00802sin3θ
cos2θ	0.03378 + .02097cosθ + 2.401cos2θ + .06390cos3θ + .02636cos4θ - .02353sinθ + .0741sin3θ + .02661sin4θ
cos3θ	0.00867 + .11196cosθ + .03912cos2θ + 5.078cos3θ + .01513sinθ - .03098sin2θ + .05346sin4θ
cos4θ	0.10832 + .05151cosθ + .05248cos2θ + 7.398cos4θ + .10177sinθ - .01434sin2θ - .04114sin3θ + .06417sin4θ
sinθ	0.011306 - .01879cosθ - .00563cos2θ - .04681cos4θ + .01549sinθ + .01277sin2θ - .00231sin3θ
sin2θ	-.01685 + .15396cosθ - .03292cos3θ + .02191cos4θ + .08321sinθ + 2.342sin2θ + .02230sin3θ + .06118sin4θ
sin3θ	-.07365 + .01565cosθ + .03207cos2θ + .03871cos4θ - .05966sinθ + .03371sin2θ + 5.007sin3θ + .00241sin4θ
sin4θ	.01739 - .08312cosθ + .05072cos2θ + .19380cos3θ + .05813cos4θ - .01062sinθ + .03976sin2θ + .05134sin3θ + 7.497sin4θ

Table 5. (continued)

$k = 6.667$

Trial function	Normal derivative along C'
1	$-15.249 + .20223\cos\theta + .06893\cos 2\theta + .00496\cos 3\theta + .08471\sin\theta - .011578\sin 2\theta$
$\cos\theta$	$0.30041 - 10.381\cos\theta + .06216\cos 2\theta + .04214\cos 3\theta - .04934\cos 4\theta - .06176\sin\theta + .02505\sin 2\theta - .09127\sin 3\theta + .04226\sin 4\theta$
$\cos 2\theta$	$0.03604 + .26190\cos\theta - 3.521\cos 2\theta - .06121\cos 3\theta + .00769\cos 4\theta - .2035\sin\theta - .03796\sin 2\theta$
$\cos 3\theta$	$0.04341 + .08758\cos\theta + 1.513\cos 3\theta + .02139\cos 4\theta + .02692\sin 2\theta + .07019\sin 3\theta$
$\cos 4\theta$	$0.06822 + .04492\cos\theta + .01660\cos 2\theta + 5.063\cos 4\theta + .11166\sin\theta + .08474\sin 2\theta - .031704\sin 3\theta + .13211\sin 4\theta$
$\sin\theta$	$.07910 - .07180\cos\theta - .01843\cos 2\theta - .06304\cos 4\theta - 11.021\sin\theta + .09027\sin 2\theta - .05859\sin 4\theta$
$\sin 2\theta$	$-.01362 + .05011\cos\theta - .00552\cos 4\theta + .02215\sin\theta - 3.498\sin 2\theta + .06201\sin 4\theta$
$\sin 3\theta$	$-0.09745 + .02552\cos 2\theta + .09790\cos 4\theta - .00671\sin\theta + .03699\sin 2\theta + 1.488\sin 3\theta + .05410\sin 4\theta$
$\sin 4\theta$	$-.07337 - .12930\cos\theta + .01001\cos 2\theta + .04735\cos 3\theta + .04605\cos 4\theta + .05111\sin\theta + .07897\sin 2\theta + .08535\sin 2\theta + 5.117\sin 4\theta$

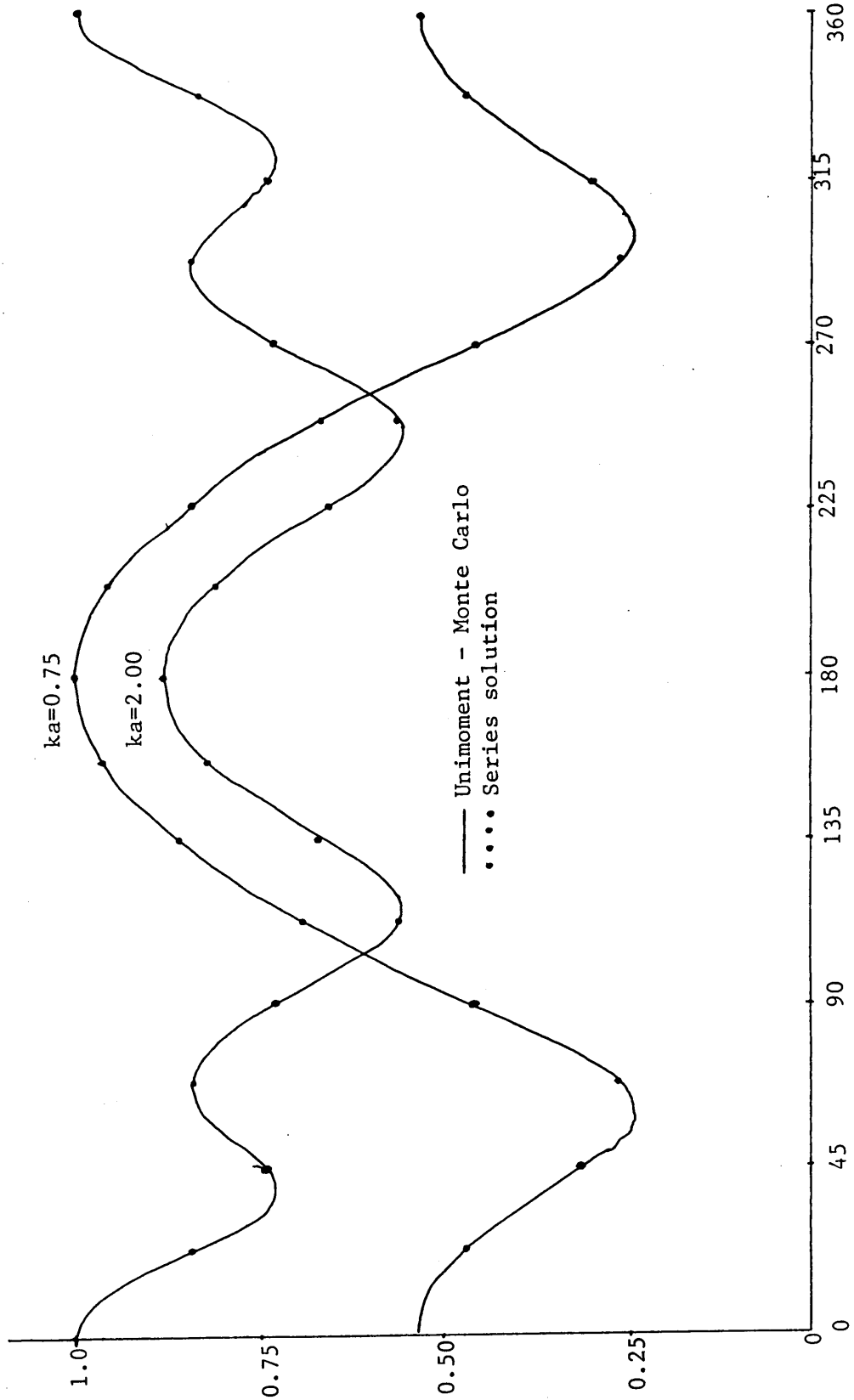

Figure 45. Normalized far-field patterns for TE scattering from perfectly conducting circular cylinders.

6.1.4 TE Scattering From a Dielectric Circular Cylinder

One example of this type was run, and the results were compared to the series solution

$$H_z^s = H_o \sum_{n=-\infty}^{\infty} (j)^{-n} a_n H_n^{(2)}(kr) e^{jn} \tag{6-7}$$

with the incident field biven by (6-6) and

$$a_n = \frac{-J_n(ka)}{H_n^{(2)}(ka)} \left(\frac{J_n'(k_d a)/k_d a J_n(k_d a) - J_n'(ka)/kaJ_n(ka)}{J_n'(k_d a)/k_d a J_n(k_d a) - H_n^{(2)\prime}(ka)/kaH_n^{(2)}(ka)} \right) \tag{6-8}$$

Harrington[159] does not state this formula but does outline the method used to derive it.

The trial function data are presented in Table 6, and the far-field pattern is plotted in Figure 46. Accuracy was always better then 0.75%, and the execution time was 21 minutes.

6.2 Scattering From Elliptic Cylinders

The elliptic cylinder is the most general scatterer of finite cross section for which the exterior scattering problem can be solved by separation of variables. The exact solution, however, requires a coordinate transformation, and the transformed problem solution is usually expressed as a series of Mathieu functions. The equations for TM and TE scattering may be found in Bowman[160] or in Stratton[161].

Several examples for which data had been tabulated were run using the Unimoment - Monte Carlo method. The first example was TM

Table 6. Trial functions and their normal derivatives for TE scattering from a dielectric ($\varepsilon_r = 4$) circular cylinder of radius 0.3.

k = 6.6667

Trial function	Normal derivative along C'
1	-18.761 + .07824cosθ + .00312cos2θ + .01431sinθ + .00041sin2θ
cosθ	.04111 - .0475cosθ + .02133cos2θ + .02060cos3θ + .01950sinθ - .01019sin3θ
cos2θ	-.04226 - .07385cosθ - 7.273cos2θ + .10870cos3θ + .02911cos4θ - .10092sinθ + .09539sin2θ + .03610sin4θ
cos3θ	.039035 + .02086cosθ + .14935cos2θ + 5.368cos3θ + .09109cos4θ + .07177sinθ + .09643sin2θ + .03323sin4θ
cos4θ	+.01718 - .02731cosθ + .03109cos3θ + 7.875cos4θ + .02905sinθ + .03347sin3θ + .01197sin4θ
sinθ	-.04126 - .03552cosθ - .09762cos2θ - .03454cos4θ - .93475sinθ + .10122sin2θ - .01974sin4θ
sin2θ	-.05670 + .08172cosθ - .04473cos2θ - .03671cos4θ - .05279sinθ - 7.273sin2θ + .16500sin3θ - .06048sin4θ
sin3θ	.04771 + .02188cosθ + .01863cos2θ - .07406cos3θ - .01254cos4θ + .01329sinθ + .07119sin2θ + 1.581sin3θ + .02038sin4θ
sin4θ	-.07577 - .02066cosθ + .04226cos2θ + .03314cos3θ - .04113cos4θ + .00695sinθ + .03588sin2θ + .05884sin3θ + 7.891sin4θ

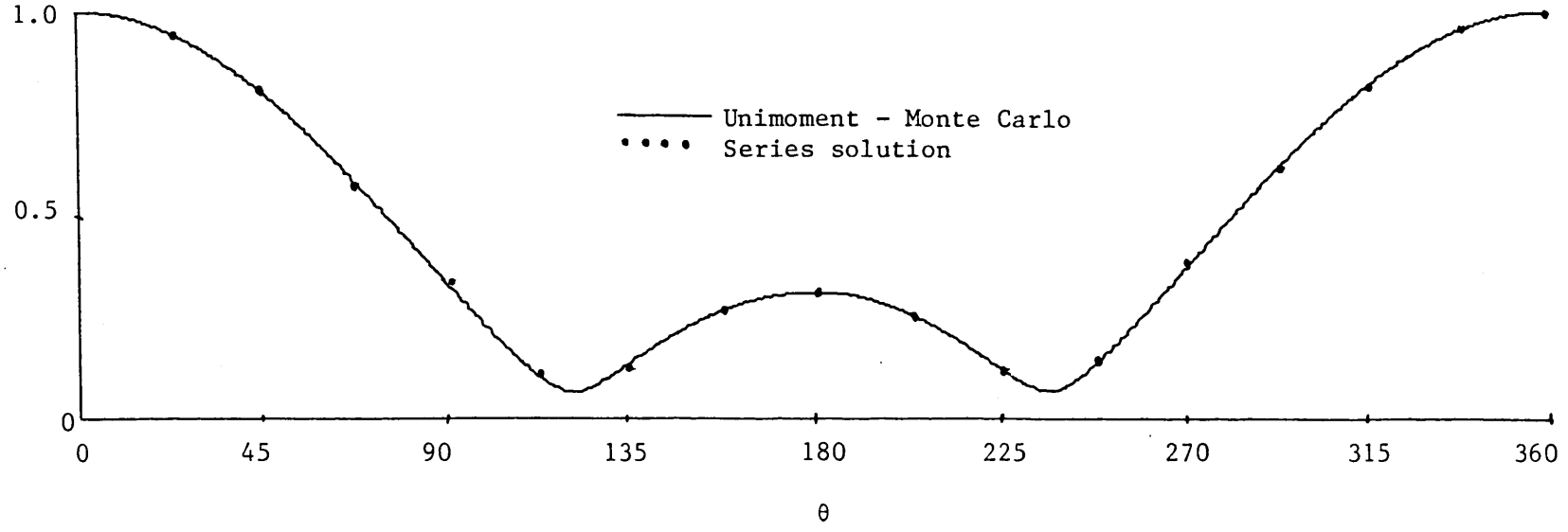

Figure 46. Normalized far-field pattern for TE scattering from a circular dielectric (ε_r=4) cylinder, ka = 2.0.

scattering from a perfectly conducting ellipse of dimensions 2λ by $\frac{1}{2}\lambda$. Results for the incident field of equation (6-2) are plotted in Figure 47 along with Andreasen's solution[162] and Harrington's Method of Moments solution[163]. Program execution time was slightly longer for this example than for the circular cylinder example since the average length of a random walk was greater. TE scattering from the same object was also studied, and the resultant far-field pattern of the scattered field is plotted in Figure 48 along with the results of Andreason and Harrington.

Mei [164] solved for the TM far-field patterns of a dielectric ellipse with $\varepsilon_r = 2$, a semi-major axis of 0.5675252λ, and a semi-minor axis of 0.26226316λ using his unimoment method with finite elements. A Unimoment- Monte Carlo program was run in order to compare results. Both field patterns are plotted in Figure 49. There is no noticeable difference in far-field patterns. Mei gave no information concerning execution time, but the Unimoment - Monte Carlo method required 24 minutes, of which 19 minutes were spent in performing analog to digital conversions.

6.3 Scattering From Other Two-dimensional Objects

6.3.1 TM Scattering From a Dielectric Annulus

Richmond has solved the problems of TM[165] and TE[166] scattering from a dielectric annulus of inner radius 0.25λ, outer radius of 0.30λ, and $\varepsilon_r = 4$. A Unimoment - Monte Carlo program was run to solve the same problem, and the power patterns of both TM and TE scattering are plotted

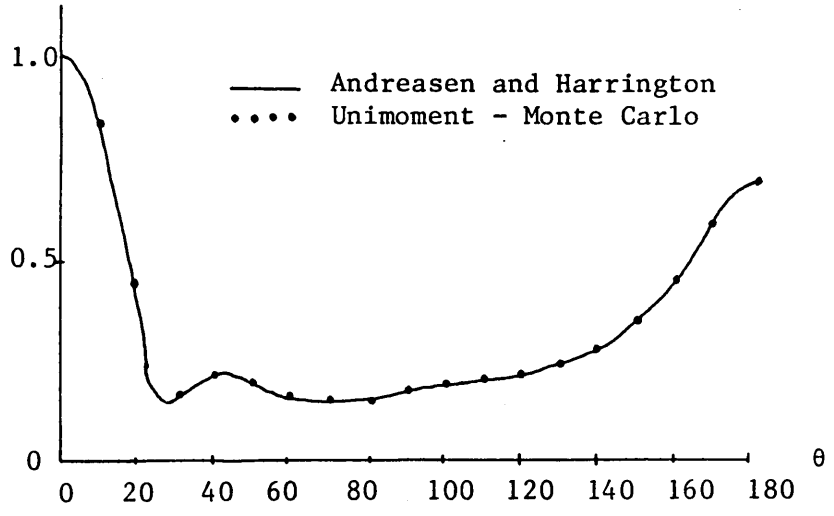

Figure 47. Normalized far-field pattern for TM scattering from a dielectric ($\varepsilon_r = 4$) ellipse, $2\lambda \times \frac{1}{2}\lambda$.

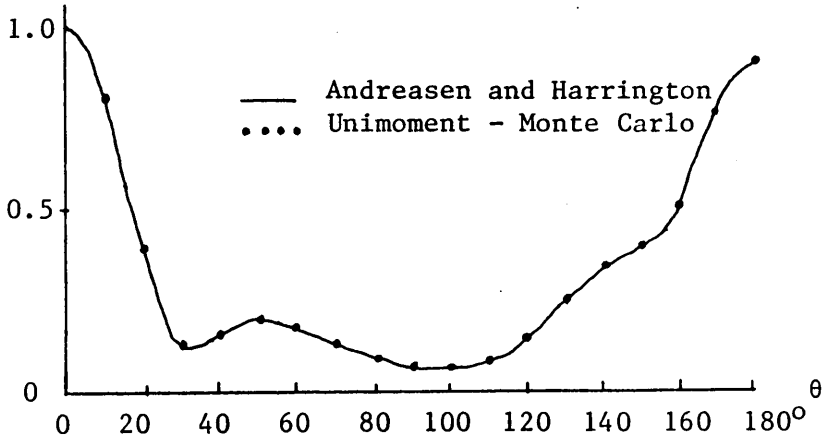

Figure 48. Normalized far-field pattern for TE scattering from a dielectric ($\varepsilon_r = 4$) ellipse, $2\lambda \times \frac{1}{2}\lambda$.

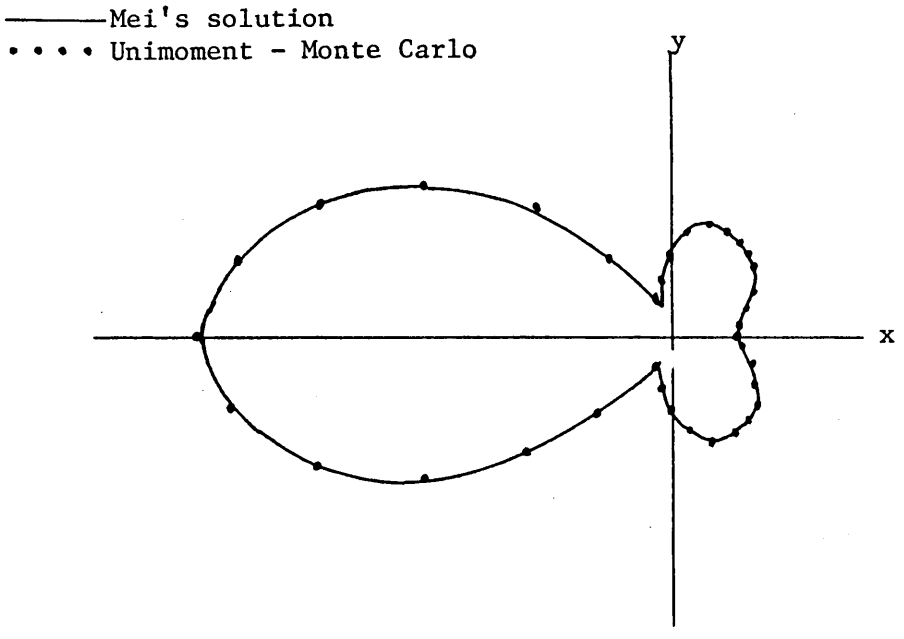

(a)

Incidence at 180 degrees.

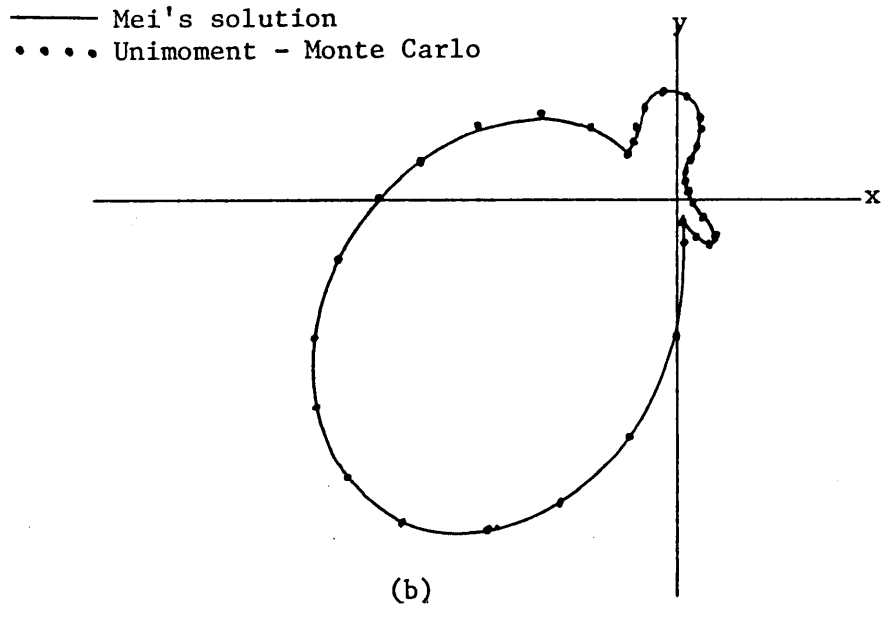

(b)

Incidence at -135 degrees.

Figure 49. TM scattering from a dielectric ellipse.

in Figures 50 and 51. Computation time for both cases was 22 minutes, and all errors were less than 1%.

6.3.2 TM Scattering From an Irregularly Shaped Object

Scatterers of the general type shown in Figure 52 have never been considered because of the difficulty in the previously mentioned boundary detection/mesh point location problem. The Unimoment - Monte Carlo method detects boundaries quite differently from other popular methods, and as a result the solution of TM scattering from this object requires no more computer time than scattering from the more regular circle or ellipse. Since this is the first time that this object has appeared in the literature, more extensive documentation of the results will be made than for the ellipse of annulus.

Four hundred random walks were taken at each of the 401 points on C' at k_o = 1.6769 and 2.6514. The object extended a distance of 0.3 in the positive and negative x directions. The separation between C' and C" was 0.025. The trial function pair data is tabulated in Table 7, and the resulting coefficients $\{A_n^e\}$ and $\{A_n^o\}$ are given in Table 8 for the plane wave incidence of equation (6-2). The far-field patterns for each value of k_o are given in Figures 53 and 54. Execution time for both programs was 21 minutes.

6.4 Investigation of Critical Parameters

A list of some of the parameters that may be varied at the discretion of the user is given on the next page. They are:

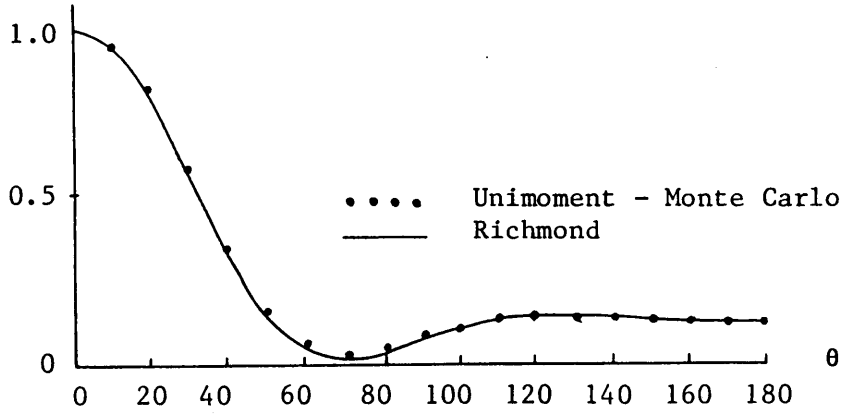

Figure 50. Normalized scattered power pattern for a dielectric annulus, $0.25\lambda < r < 0.3\lambda$, $\varepsilon_r = 4$, TM case.

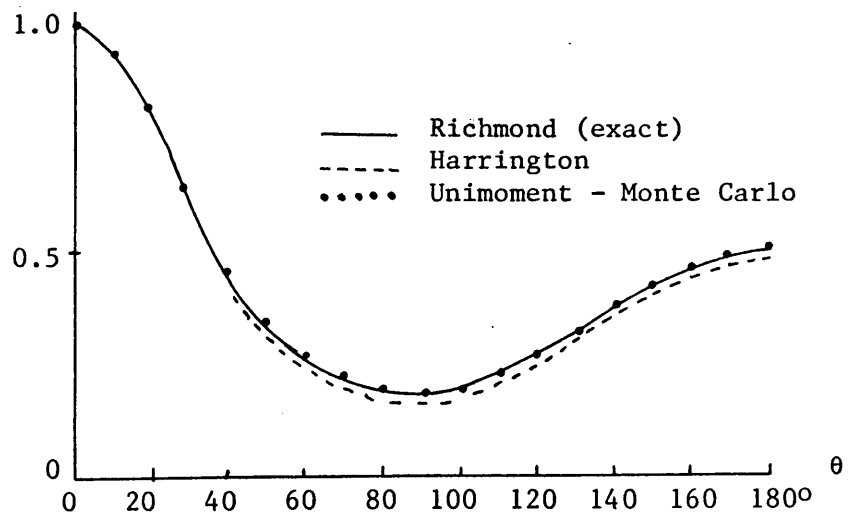

Figure 51. Normalized scattered power pattern for a dielectric annulus, $0.25\lambda < r < 0.3\lambda$, $\varepsilon_r = 4$, TE case.

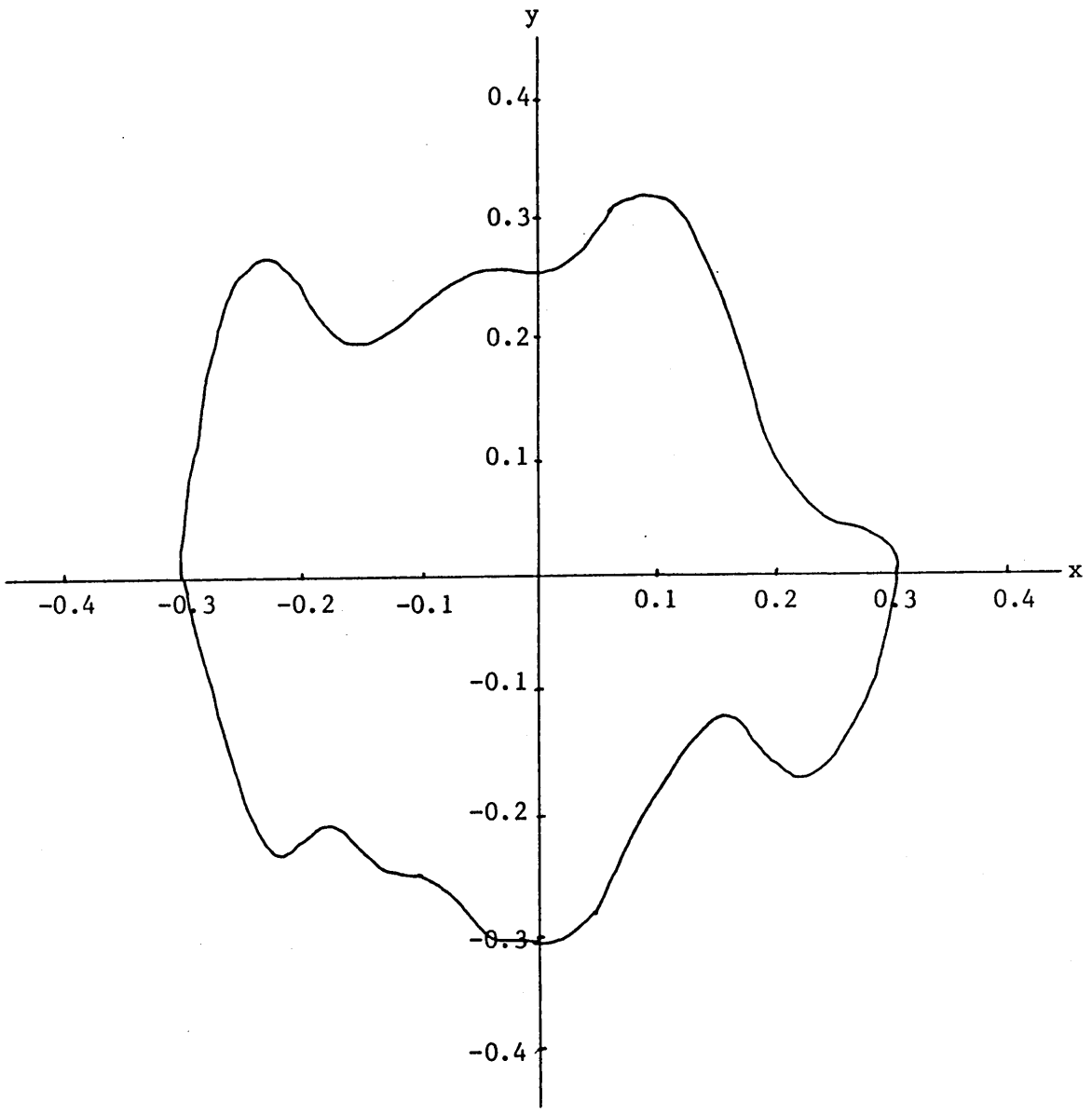

Figure 52. An irregularly shaped scatterer.

Table 7. Trial functions and their normal derivatives for TM scattering from the irregular object of Figure 52.

k = 1.6769

Trial function	Normal derivative along C'
1	$3.8936 - .43518\cos\theta + .10678\cos 2\theta + .03628\cos 3\theta - .08859\cos 4\theta - .03369\sin\theta + .02062\sin 2\theta - .00277\sin 3\theta + .21124\sin 4\theta$
$\cos\theta$	$-.16173 + 4.28097\cos\theta - .12844\cos 2\theta + .00924\cos 3\theta + .09057\cos 4\theta + .01870\sin\theta - .07650\sin 2\theta + .14184\sin 3\theta + .08950\sin 4\theta$
$\cos 2\theta$	$0.09500 + .10031\cos\theta + 5.0458\cos 2\theta - .00369\cos 3\theta + .03582\cos 4\theta - .21659\sin\theta + .13946\sin 2\theta + .03680\sin 3\theta - .05758\sin 4\theta$
$\cos 3\theta$	$0.12813 + .11920\cos\theta + .35922\cos 2\theta + 6.240\cos 3\theta - .14416\cos 4\theta + .04769\sin\theta - .21420\sin 2\theta - .07778\sin 3\theta - .10690\sin 4\theta$
$\cos 4\theta$	$.01538 + .27389\cos\theta + .12585\cos 2\theta + .37542\cos 3\theta + 7.65057\cos 4\theta + .13079\sin\theta - .20727\sin 2\theta - .50726\sin 3\theta + .01977\sin 4\theta$
$\sin\theta$	$.03751 + .03320\cos\theta + .13986\cos 3\theta + .05001\cos 4\theta + 4.14312\sin\theta - .26541\sin 2\theta + .09411\sin 3\theta - .12551\sin 4\theta$
$\sin 2\theta$	$.05124 + .06774\cos\theta + .16342\cos 2\theta + .13366\cos 3\theta - .04968\cos 4\theta - .12481\sin\theta + 5.0985\sin 2\theta - .28009\sin 3\theta + .08108\sin 4\theta$
$\sin 3\theta$	$-.09029 + .22384\cos\theta + .37094\cos 2\theta - .05111\cos 3\theta + .00115\cos 4\theta + .12213\sin\theta + .04339\sin 2\theta + 6.27526\sin 3\theta - .03213\sin 4\theta$
$\sin 4\theta$	$.10477 - .02581\cos\theta + .05816\cos 2\theta + .39773\cos 3\theta + .03836\cos 4\theta - .01386\sin\theta + .14447\sin 2\theta + .46606\sin 3\theta + 7.4747\sin 4\theta$

Table 7. (continued)

$k = 2.6544$

Trial function	Normal derivative along C'
1	$3.6380 - .53225\cos\theta + .01043\cos2\theta + .11294\cos3\theta - .02288\cos4\theta - .10574\sin\theta - .03759\sin2\theta - .03735\sin3\theta + .26596\sin4\theta$
$\cos\theta$	$-.24477 + 3.09434\cos\theta - .17538\cos2\theta + .01980\cos3\theta + .27554\cos4\theta - .02798\sin\theta - .16912\sin2\theta + .13153\sin3\theta + .04403\sin4\theta$
$\cos2\theta$	$-.00708 - .04867\cos\theta + 4.86764\cos2\theta + .06478\cos3\theta + .13732\cos4\theta - .28689\sin\theta + .08950\sin2\theta - .11129\sin3\theta - .09838\sin4\theta$
$\cos3\theta$	$.07376 - .08264\cos\theta + .37359\cos2\theta + 6.14398\cos3\theta - .05236\cos4\theta + .01818\sin\theta - .32879\sin2\theta - .23907\sin3\theta - .15319\sin4\theta$
$\cos4\theta$	$-.06480 + .29626\cos\theta - .02947\cos2\theta + .41366\cos3\theta + 7.58615\cos4\theta + .10839\sin\theta - .33065\sin2\theta - .49893\sin3\theta - .12649\sin4\theta$
$\sin\theta$	$.03091 + .02154\cos\theta + .03921\cos2\theta + .16796\cos3\theta + .08203\cos4\theta + .10839\sin\theta - .33065\sin2\theta + .04519\sin3\theta - .12756\sin4\theta$
$\sin2\theta$	$.04060 + .02191\cos\theta + .21902\cos2\theta + .14874\cos3\theta - .04754\cos4\theta - .18807\sin\theta + 4.90975\sin2\theta - .42327\sin3\theta + .03729\sin4\theta$
$\sin3\theta$	$-.17051 + .22424\cos\theta + .29455\cos2\theta - .00674\cos3\theta + .11523\cos4\theta + .00250\sin\theta - .17144\sin2\theta + 6.05462\sin3\theta - .18594\sin4\theta$
$\sin4\theta$	$.057220- .19906\cos\theta - .01879\cos2\theta + .48257\cos3\theta + .17968\cos4\theta - .20989\sin\theta - .13394\sin2\theta + .26632\sin3\theta + 7.22357\sin4\theta$

Table 8. Coefficients of equations (4-11) for TM scattering from the object of Figure 52.

k = 1.6769

n	A_n^e	A_n^o
0	-.971260 - j.059232	----------
1	.769552 + j.362867	-.011459 + j.017792
2	.003447 - j.002305	.005801 - j.091397
3	-.002054 + j.003648	.005508 + j.001513
4	.000760 + j.000948	-.000643 - j.000443

k = 2.6514

n	A_n^e	A_n^o
0	-.973083 + j.000338	----------
1	.687125 + j.278954	-.010989 + j.017870
2	-.003224 - j.004418	.002017 - j.066837
3	-.003795 + j.002745	.005481 + j.003049
4	.000874 + j.000931	-.001002 - j.000071

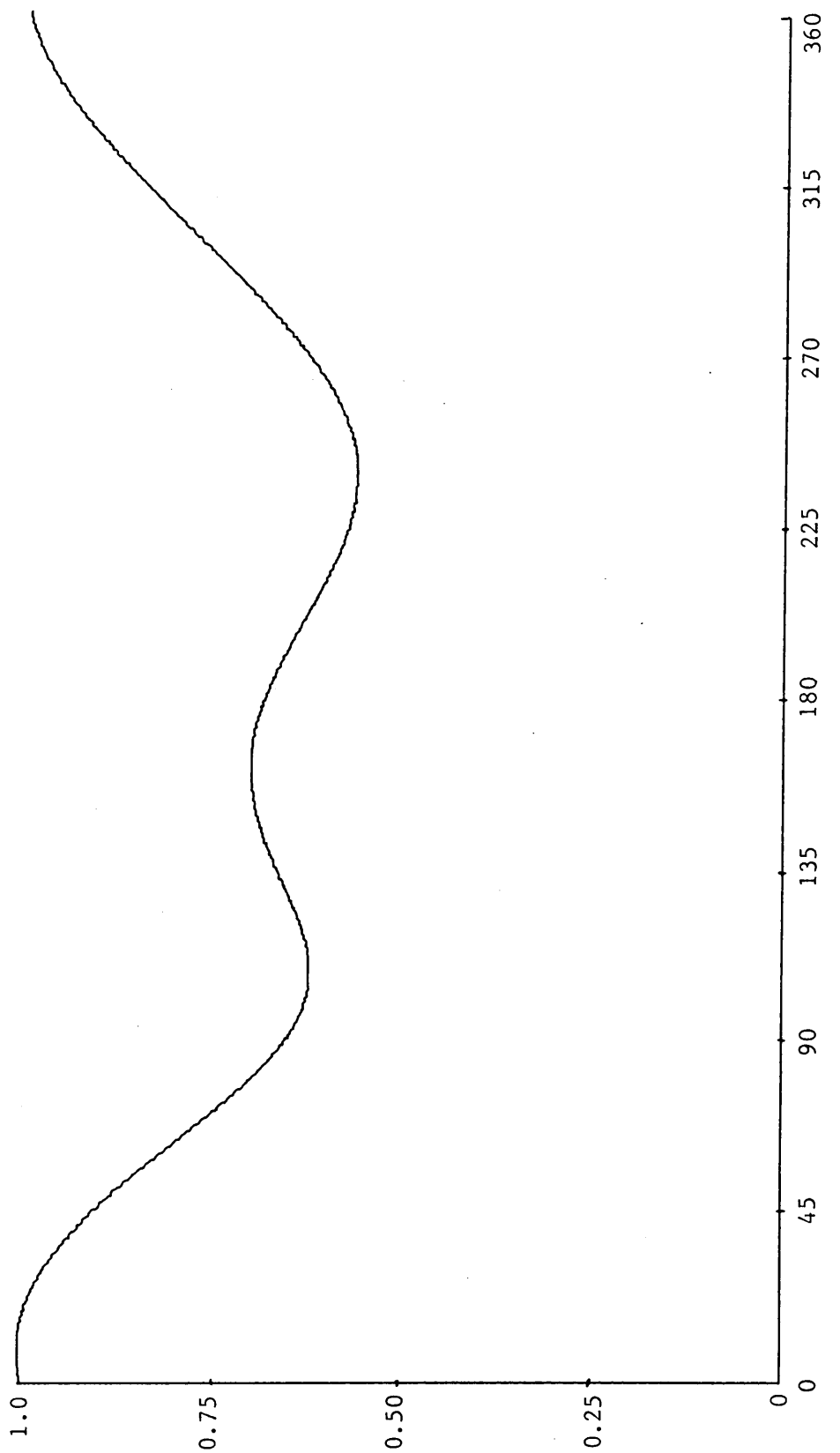

Figure 53. TM scattering from the irregularly shaped perfectly conducting object of Figure 52 with k = 2.812.

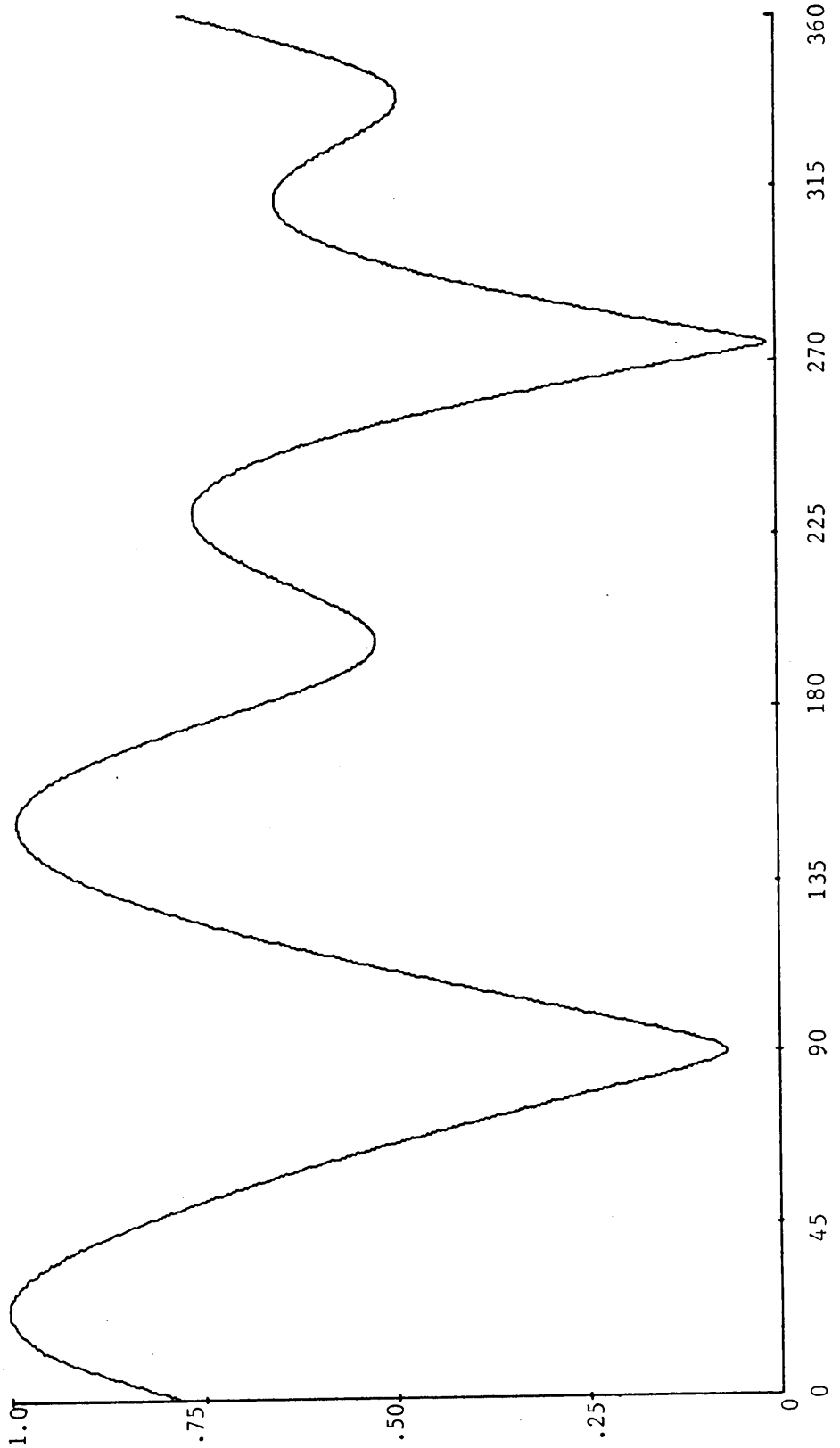

Figure 54. TM scattering from the irregularly shaped perfectly conducting object of Figure 52 with k = 7.030.

1. Outer boundary radius -- "a" (0.5)
2. Separation between C' and C" -- h (5% of a)
3. Number of Random Walks (400 to 1000)
4. Number of sample points along C' (401)
5. Analog integrator gains (5000)
6. Random number generator clock frequency (500 kHz per channel)
7. Number of modes (Up to 10 per pass)
8. Random number generator output voltage level (± 6 volts)

The numbers in parentheses indicate values used in previous section. All of these parameters affect the accuracy of the final result; some affect the total time required to execute the program. A few parameters affect both accuracy and execution time. This section will examine these parameters and discuss trade-offs that may be made between the precision of the answer and the time required to obtain that answer.

6.4.1 Parameters Affecting Accuracy

All of the above parameters affect the accuracy of the results to some extent. One of the more critical parameters is the separation between C' and C". This distance affects the derivative approximation (4-16) which in turn adds error to the far-field pattern calculations. This was discussed earlier in Section 6.1.1.

More obvious errors can be detected when either the number of random walks per point or the number of sample points falls below some critical value. It was discovered experimentally that 100 random

walks were the least that could be taken that would still give meaningful results. As the number of random walks was increased the accuracy improved until about 1000 random walks were taken. At this point other errors and inaccuracies masked out the improvement in accuracy caused by any further increase in the number of random walks.

The number of sample points affect the higher modes only. As discussed in Section 3.4.3, 50 samples per cycle, or per mode, would yield a discretization error of 0.1%. Ten samples per cycle would cause an amplitude error of 1.1% and a phase error of 18%; thirty samples per cycle would give an amplitude error of 0.7% and a phase error of 6.5%. Further information is given in the literature[167].

Analog integrator gain, random number generator clock frequency, and random number generator output voltage act together to increase or decrease the average step size. Increasing the integrator gain, decreasing the random number generator clock frequency, or increasing the random number generator output voltage will increase the average random walk step size causing more error in the solution.

6.4.2 Parameters Affecting Execution Time

Disregarding hardware speed limitations, particularly analog to digital conversion times, the execution time required for a given accuracy is most sensitive to the random number generator clock frequency. The faster random walk steps can be taken, the faster the problem can be solved. There is an upper bound on the maximum clock

frequency, however. This is the bandwidth of the analog components. It can be shown that for a feedback shift register pseudo-random number generator, the bandwidth of the output noise is approximately 0.32 times the clock frequency[168]. With an analog bandwidth of 125 kHz, the maximum clock frequency is 390 kHz. Higher clock frequencies can be used, but the bandwidth of the power spectral density will be limited by the analog computer.

The outer boundary radius obviously has an effect on execution time, for the closer this boundary can be made to the scatterer, the less time each random walk will need to terminate.

Number of random walks, number of sample points, and number of modes all affect execution time since increasing any or all of the three requires more random walks to be taken.

CHAPTER VII

SUMMARY AND CONCLUSIONS

In this dissertation a study of several numerical methods that might be used to solve exterior scattering problems was made. It was shown that while these methods were able to solve certain classes of problems, no single technique could qualify as a general solution method. It was found that the drawbacks of these popular scattering techniques were not mathematical restrictions but computational restrictions. The principle limitation was using the digital computer to solve problems for which it was not designed. Further investigation into computing hardware led to the discovery that the same algorithms that were ill-suited to the digital computer were well-suited to the analog computer. But an analog computer alone did not possess the power to solve large-scale scattering problems.

A study of hybrid computer techniques was then begun, and it was found that the Monte Carlo method, when properly programmed, could solve interior boundary value problems at speeds competitive with digital computer techniques. This was insufficient in itself, however, since electromagnetic scattering problems are exterior boundary value problems.

To take advantage of both the good qualities of digital computer programs and the speed of the hybrid Monte Carlo method, a new scattering technique, the Unimoment - Monte Carlo method, was developed. The original scattering problem was decoupled into a simple exterior

the analog program permits experimentation by allowing one to adjust coefficients directly on the computer, thereby gaining physical insight into the scattering problem. This last advantage is quite important when inverse problems, such as antenna synthesis, are studied.

The Unimoment - Monte Carlo method has its share of disadvantages also, but these are of a different type than the ones normally associated with strictly digital methods. The greatest restriction of the method is a hardware restriction. First and foremost is the availability of a suitable hybrid computer facility. There is no way that this method can be efficiently programmed on a digital computer. Closely related to this is the number of analog elements available. For complicated structures having multiple boundaries, external boundary detection hardware may be needed. Electronic limitations of the analog elements, such as bandwidth and precision, are important also since they in turn will limit the speed and precision of the overall system. Another restriction on execution time is the conversion time of the analog to digital and/or digital to analog converters that are used to interface the separate analog and digital portions of the hybrid computer. It was this restriction that was the most severe on the V. P. I. & S. U. system. The last hardware problem is the availability of multi-dimensional random noise sources. Analog noise generators are too unstable to be used in scattering problems, so digitally generated random numbers that are filtered into Gaussian noise are required. The final drawback of the Unimoment - Monte Carlo method is a problem of education. Hybrid computer methods are new to the engineer, and

problem and an interior problem by enclosing the scatterer within a circle (in two dimensions) or a sphere (in three dimensions). The resulting interior problem was solved for several different boundary values along this artificial boundary using Monte Carlo techniques. The linear combination of these solutions that gave the best continuity across the outer boundary was found by inverting a small matrix, and this combination was then used to generate the fields everywhere. It was essential that the Unimoment - Monte Carlo technique be programmed on a hybrid computer to take advantage of analog boundary detection and random noise generation.

This new method offers several advantages over other approaches to the exterior scattering problem. First, by utilizing both analog and digital hardware, the speed of solution and memeory requirements of the computer are greatly reduced. Less hardware is needed in implementing this approach than is required by digital computer programs. The hardware that is required is usually inexpensive enough that it may be purchased outright. Therefore, it is not necessary to pay for computer time on a "per program" basis. Another advantage is the versatility of the method. Most computer techniques require that a program be rewritten when different scatterers are to be studied. Many different types of objects, including multiple scatterers, may be studied without rewriting any portion of the Unimoment - Monte Carlo digital program. The only alteration needed in the analog program is a change in the patching of the boundary detection circuit, which can be accomplished in about ten minutes for all but the most complicated scatterers. Finally,

training in hybrid computer techniques is necessary to successfully implement the method.

After extensive testing of the individual system components, several examples of plane wave exterior scattering were run using the Unimoment - Monte Carlo method, and the results were compared to exact solutions (whenever available) and numerical solutions generated by other scattering solution techniques. These examples included perfect conductors and perfect dielectrics incident with both TM and TE fields. Among the scatterer shapes studied were the circular cylinder, the elliptical cylinder, and an annulus. Results using the Unimoment - Monte Carlo method compared favorably with available data, and all far-field patterns were within one percent of the calculated patterns. In addition to the above canonical problems, an irregularly shaped object was used as a scatterer to show the power of the method. No data is available for this object; however, the far-field patterns generated by TM plane wave scattering are plotted for two different frequencies.

It was found that TM scattering from perfect conductors was the scattering problem best suited for the particular Monte Carlo technique implemented. However, TE scattering and scattering from dielectrics could be handled with only a slight increase in computer time. Scattering from lossy objects was not attempted since it would have required the use of complex permittivity. It is felt that the Unimoment - Monte Carlo technique could be extended to this class of problmes by solving simultaneous scattering problems for the real and

imaginary parts of the fields. Because of the parallel nature of the analog computer, no increase in computer time is expected.

This dissertation has proved the feasibility of using hybrid computers in electromagnetics, but much work is still left for others. Problems associated with transmission lines and waveguides, propagation, and antennas can be handled more efficiently on hybrid computers than on digital computers, whether the Unimoment - Monte Carlo method or another hybrid computer technique is used. Little or no hybrid work has been attempted in these areas.

For the Unimoment - Monte Carlo method itself, there are several areas where further work might lead to an enhancement of the technique. One such area is the investigation of other possible probabilistic formulations that might be used in a Monte Carlo simulation. It should be possible to play a different "game" that would extend the usefulness of the Unimoment - Monte Carlo method to frequencies above resonance. Another mathematical task would be to reformulate the dielectric boundary condition into a Robbin boundary value problem. This would limit the excursions of the random walks and thus reduce the average time of a random walk since not all walks would continue into the dielectric. Infinite scatterers have not yet been considered using the Unimoment - Monte Carlo method. Some effort in this area would open up a whole new class of problems that could be solved. A final mathematical suggestion is to extend the method to three dimensions. This would involve solving simultaneous partial differential equations since a three-dimensional scatterer will depolarize the incident field. This

work is quite important since most practical problems are three-dimensional.

In addition to mathematical work, some hardware development could lead to significant improvements in the method. It should be possible to generate the boundary values on the analog computer rather than generating them on the digital computer. If this could be implemented, fewer analog to digital conversions would be necessary, and execution time would be decreased. It is also possible to take more than one random walk at a time by using several sets of integrators to integrate and store the random noise. More random noise sources would be needed, but this is easy to obtain by adding additional multiplexer channels to the existing feedback shift register circuit. Construction of special boundary detection hardware that is oriented away from a detailed knowledge of analog computers would make it possible for the average engineer to use the hybrid program more easily. Such a device might use a mini-computer to set up diode function generators, specify attenuator coefficients, and connect the appropriate circuitry as the boundary was traced by moving a light-pen over the screen of a computer graphics display terminal. Finally, some thought might be given to the possibility of using the Unimoment - Monte Carlo method as a teaching tool in electromagnetics. If additional digital software were coupled with the boundary detector just mentioned, it would be possible for a student to specify the object to be studied by entering data via a graphics terminal and then receive a plot of the scattered field patterns, surface current density, etc. on the same device.

Even though the Unimoment - Monte Carlo method as described here is implemented in only two dimensions, some specific applications do exist. These include the study of certain microstrip antennas[169] and sea surface scattering in shallow water[170]. By moving the C' boundary inside the object, interior scattering may be studied as well. One application of this would be the investigation of waveguide modes in guides of irregular cross section.

The Unimoment - Monte Carlo method promises to revolutionize traditional approaches to electromagnetics scattering problems. It is hoped that other investigators will continue this work and add to it.

LITERATURE CITED

1. R. W. P. King, The Scattering and Diffraction of Waves, Harvard University Press, Cambridge, Mass., 1959, p.3.

2. M. G. Andreasen, "Scattering from Parallel Metallic Cylinders with Arbitrary Cross Section," IEEE Trans. on Ant. and Prop., vol. AP-12, pp.746-754, Nov. 1964.

3. R. L. Tanner and M. G. Andreasen, "Numerical Solution of Electromagnetics Problems," IEEE Spectrum, pp. 53-61, Sept. 1967.

4. R. F. Harrington, Field Computation by Moment Methods, MacMillan Co., New York, 1968.

5. R. Mittra, Computer Techniques for Electromagnetics, Pergamon Press, New York, 1973, p.2.

6. Op. cit. (Reference 4)

7. K. K. Mei, "Unimoment Method of Solving Antenna and Scattering Problems," IEEE Trans. on Ant. and Prop., vol. AP-22, pp. 760-766, Nov. 1974.

8. A. Wexler,"Computation of Electromagnetic Fields, " IEEE Trans. on Microwave Theory and Techniques, vol. MTT-17, pp.416-439, Aug. 1969.

9. R. F. Harrington, Time-Harmonic Electromagnetic Fields, McGraw-Hill, Inc., New York, 1961, p.2.

10. J. J. Bowman (ed.), Electromagnetic and Acoustical Scattering by Simple Shapes, John Wiley and Sons, New York, 1969, p.5.

11. Op. cit. (Reference 9) p.34.

12. Ibid.

13. Ibid.

14. J. A. Stratton, Electromagnetic Theory, McGraw-Hill, Inc., New York, 1941, p.485.

15. C. R. Chester, Techniques in Partial Differential Equations, McGraw-Hill, Inc., New York, 1971, p.389.

16. Op. cit. (Reference 9) pp. 32-34.

17. Op. cit. (Reference 9) pp. 113-114.

18. Op. cit. (Reference 9) pp. 106-107.

19. Op. cit. (Reference 9) pp. 100-103.

20. Op. cit. (Reference 9) p.113.

21. Op. cit. (Reference 9) pp. 114-116.

22. Op. cit. (Reference 9) p. 24.

23. Op. cit. (Reference 9) pp. 266-269.

24. Op. cit. (Reference 5)

25. Op. cit. (Reference 9) p. 269.

26. R. E. Stovall and K. K. Mei,"Numerical Solutions of Inhomogeneous Loaded Biconical Antennas," URSI Symposium on Electromagnetic Theory, 1974, pp. 166-167.

27. M. A. Morgan and K. K. Mei, "Computation of Scattering by Inhomogeneous Dielectric Bodies of Revolution," URSI Symposium on Electromagnetic Wave Theory, 1974, pp. 163-164.

28. Op. cit. (Reference 5) pp. 182-184.

29. Op. cit. (Reference 4) p.42.

30. Op. cit. (Reference 4) p.51.

31. Op. cit. (Reference 4) p.51-52.

32. Op. cit. (Reference 4) p.59.

33. Op. cit. (Reference 5) p.167.

34. Op. cit. (Reference 5) p.168.

35. Op. cit. (Reference 5) p.169.

36. G. A. Bekey and W. J. Karplus, Hybrid Computation, John Wiley and Sons, New York, 1968, p. 5.

37. Ibid.

38. Op. cit. (Reference 36) p. 13.

39. E. L. Coffey, "Synthesis of Antenna Radiation Patterns Using Rectangular Sources," (M. S. Thesis, Virginia Polytechnic Institute and State University, 1973).

40. Op. cit. (Reference 5) pp. 184-185.

41. Op. cit. (Reference 5) p. 305.

42. Op. cit. (Reference 5) p. 306.

43. Op cit. (Reference 5) pp. 306-338.

44. L. P. Eisenhart, Ann. Math., vol. 35, p. 284, 1934.

45. Op. cit. (Reference 10) p. 37.

46. P. R. Garabedian, "An Integral Equation Governing Electromagnetic Waves," Quart. Appl. Math., vol. 12, pp. 428-433, 1955.

47. S. Hong and R. F. Goodrich, "Applications of Conformal Mapping to Scattering and Diffraction Problems," in Electromagnetic Wave Theory, ed. J. Brown., Pergamon Press, London, 1967, pp. 907-914.

48. H. H. Meike and W. Baier, "The Characteristics of Waveguides with General Cross Section," Nachrichtentech. Z. Commun. J., vol. 7, pp. 1-8, June 1968.

49. H. H. Meike, K. P. Lange and J. F. Ruger, "TE and TM Waves in Waveguides of Very General Cross Section," Proc. IEEE, vol. 51, pp. 1436-1443, Nov. 1963.

50. P. A. Laura, E. Romanelli and M. H. Maurizi, "On the Analysis of Waveguides of Doubly-Connected Cross Section by the Method of Conformal Mapping," J. Sound Vib., vol. 20, pp. 27-38, 1972.

51. P. A. Laura, "A Simple Method For Determination of Cutoff Frequencies of Waveguides With Arbitrary Cross Sections," Proc. IEEE (Lett.), vol. 54, pp. 1495-1497, Oct. 1966.

52. E. Abaka and W. Baier, "TE and TM Modes in Transmission Lines with Circular Outer Conductor and Eccentric Circular Inner Conductor," Electron. Lett., vol. 5, pp. 251-255, May 1966.

53. Op. cit. (Reference 10) pp. 20 - 37.

54. V. H. Weston, "Recent Highlights in Diffraction Theory," in Electromagnetic Wave Theory, ed. J. Brown, Pergamon Press, London, 1967, pp. 835-844.

55. Op. cit. (Reference 5) p. 15.

56. Op. cit. (Reference 4)

57. W. Ritz, "Uber Eine Neue Methode zur Lösung Gewisser Variationsprobleme der Mathematischen Physik," J. Reine Angew. Math.- vol. 135, pp. 1-61, 1908.

58. Op. cit. (Reference 5) p. 270.

59. Op. cit. (Reference 5) pp. 199, 270.

60. D. S. Jones, "A Critique of the Variational Method in Scattering Problems," IRE Trans., vol. AP-4, no. 3, pp. 297-301, 1956.

61. J. W. Dettman, Mathematical Methods in Physics and Engineering, McGraw-Hill, Inc., New York, 1969, Chapter 3.

62. Op. cit. (Reference 4) p. 7.

63. Op. cit. (Reference 4) p. 58.

64. R. J. Garbacz, "Modal Expansions for Resonant Scattering Phenomena," Proc. IEEE, vol. 53, pp. 856-864, 1965.

65. R. J. Garbacz, "A Generalized Expansion for Radiated and Scattered Fields," (Ph. D. Dissertation, The Ohio State University, 1968).

66. R. F. Harrington and J. R. Mautz, "Computation of Characteristic Modes for Conducting Bodies," IEEE Trans. on Ant. and Prop., vol. AP-19, pp. 622-628, Sept. 1971.

67. L. Marin, "Natural-Mode Representation of Transient Scattered Fields," IEEE Trans. on Ant. and Prop., vol. AP-21, pp. 809-828, Nov. 1973.

68. Ibid.

69. Op. cit. (Reference 66)

70. Op. cit. (Reference 5) pp. 80-83.

71. Op. cit. (Reference 67)

72. Op. cit. (Reference 7).

73. Op. cit. (Reference 9).

74. Ibid.

75. M. Abramowitz and I. Stegun, Handbook of Mathematical Functions, Dover Publications, Inc., New York, 1965, Chapter 9.

76. Op. cit. (Reference 7).

77. S. Chang and K. K. Mei, "Application of the Unimoment Method to Electromagnetic Scattering of Dielectric Cylinders," IEEE Trans. on Ant. and Prop., vol. AP-24, pp. 35-42, Jan. 1976.

78. G. Strang and G. J. Fix, An Analysis of the Finite Element Method, Prentice-Hall, Inc., Englewood Hills, N.J., 1973, pp. 16-18.

79. Op. cit. (Reference 7) p. 76.

80. K. K. Mei, R. Stovall and D. Tremain, "On Difference Coupling Methods of Solving Radiation Problems," URSI Fall Meeting Digest, Sept. 1971.

81. P. Silvester and M. S. Hsieh, "Finite-Element Solution of Two-Dimensional Exterior Field Problems," Proc. Inst. Elec. Engr, vol. 118, pp. 1743-1747, Dec. 1971.

82. B. H. McDonald and A. Wexler, "Finite-Element Solution of Unbounded Field Problems," IEEE Trans. on Microwave Theory and Techniques, vol. MTT-20, pp. 841-847, Dec. 1971.

83. Op. cit. (Reference 7) p. 761.

84. Op. cit. (Reference 7) pp. 764-765.

85. Op. cit. (Reference 7) p. 763.

86. Op. cit. (Reference 78) p. 86.

87. Op. cit. (Reference 78) p. 86.

88. Op. cit. (Reference 78) Chapter 2.

89. Op. cit. (Reference 4) Chapter 7.

90. Op. cit. (Reference 80).

91. Op. cit. (Reference 81).

92. Op. cit. (Reference 82).

93. I. A. Shreider, The Monte Carlo Method, Pergamon Press, Oxford, 1966, pp. 35-47.

94. W. D. Little, "Hybrid Computer Solutions of Partial Differential Equations by Monte Carlo Methods," Proc. Fall Joint Comp. Conf. 1966, pp. 181-190.

95. Op. cit. (Reference 36) p. 239.

96. Op. cit. (Reference 93) p. 12.

97. K. Chuang, L. F. Kazda, and T. Windeknecht, "A Stochastic Method of Solving Partial Differential Equations Using an Electronic Analog Computer," Project Michigan Report 2900-91-T, Willow Run Laboratories, University of Michigan, June 1960.

98. H. Handler, "Monte Carlo Solution of Partial Differential Equations Using a Hybrid Computer," IEEE Trans. on Electronic Computers, vol. EC-16, no. 5, pp. 603-610, Oct. 1967.

99. Op. cit. (Reference 94) p. 190.

100. W. H. Jermann, M. D. Calhoun and R. C. Thomas, "Hybrid Monte Carlo Techniques with a Minimal Interface," Simulation, p. 232, Dec. 1971.

101. J. D. Kraus and K. R. Carver, Electromagnetics, Second Edition, McGraw-Hill, Inc., New York, 1973, p. 277.

102. S. Fifer, Analogue Computation, vol. 3, McGraw-Hill, Inc., New York, 1961, p. 761.

103. Op. cit. (Reference 36) p. 216.

104. A. Engel, E. H. Hochman and L. H. Michaels, Final Report on "Hybrid Computer Applications to Mathematical Models of Physical Systems," prepared for Air Force Cambridge Research Laboratories by Electronics Associates, Inc., Feb. 1969, pp. 3-1ff.

105. Op. cit. (Reference 36) p. 228.

106. S. K. T. Hsu and R. M. Howe, "Preliminary Investigation of a Hybrid Method for Solving Partial Differential Equations," 1968 Spring Joint Computer Conference, AFIPS Proc., vol. 33, pp. 601-609.

107. R. Vichnevetsky, "State of the Art in Hybrid Methods for Partial Differential Equations," presented at the AICA-IFIP International Conference on Hybrid Computation, Munich, Germany, August 31, 1970.

108. R. Vichnevetsky, "Hybrid Methods for Partial Differential Equations," Simulation, vol. 16, no. 4, pp. 168-180, Apr. 1971.

109. P. Nelson and D. W. Altom, "Hybrid Solution of Partial Differential Equations by the Application of Invarient Imbedding to the Serial Method," Simulation, vol. 17, no.4, pp. 145-153, April 1971.

110. T. C. Anderson, "Practical Considerations in the Application of Hsu and Howe's Method for Solving Partial Differential Equations," Simulation, vol. 17, no.3, pp. 125-129, Sept. 1971.

111. Op. cit. (Reference 8) p. 437.

112. Op. cit. (Reference 8) p. 438.

113. Op. cit. (Reference 2).

114. Op. cit. (Reference 3).

115. Op. cit. (Reference 8) p. 429.

116. B. H. McDonald, M. Friedman and A. Wexler, "Variational Solutions of Integral Equations," IEEE Trans. on Microwave Theory and Techniques, vol. MTT-22, pp. 237-248, Mar. 1974.

117. Op. cit. (Reference 4).

118. Op. cit. (Reference 5) p. 13.

119. J. A. Cochran, Analysis of Linear Integral Equations, McGraw-Hill, Inc., New York, 1972, p. 15.

120. Ibid., p. 17.

121. T. Carleman, "Über die Abelsche Integralgleichung mit Konstantes Integrationgrenzen," Math. Z., vol. 15, pp. 111-120, 1922.

122. G. E. Latta, "The Solution of a Class of Integral Equations," J. Rat. Mech. Anal., vol. 5, pp. 821-834, 1956.

123. Op. cit. (Reference 119) pp. 302-304.

124. Op. cit. (Reference 5) p. 168.

125. Op. cit. (Reference 119) pp. 24-26.

126. Op. cit. (Reference 5) p. 192.

127. Op. cit. (Reference 5) p. 193.

128. Op. cit. (Reference 5) pp. 212-261.

129. Op. cit. (Reference 67).

130. Op. cit. (Reference 5) p. 113.

131. Op. cit. (Reference 7) p. 763.

132. Op. cit. (Reference 36) p. 131.

133. Op. cit. (Reference 100) p. 227.

134. G. Goertzel, "Fourier Analysis," in Mathematical Methods for Digital Computers by A. Ralston, John Wiley and Sons, New York, 1960, pp. 258-262.

135. R. H. Wilkinson, "A Method of Generating Functions of Several Variables Using Analog Diode Logic," IEEE Trans. on Elec. Comp., vol. EC-12, pp. 112-129, April 1963.

136. W. Wasow, "Random Walks and the Eigenvalues of Elliptic Difference Equations," J. Res. Nat. Bur. S., vol. 46, no. 1, pp. 65-73, Jan. 1951.

137. Op. cit. (Reference 93) Chapter I.

138. R. L. T. Hampton, "A Hybrid Analog/Digital Pseudo-Random Noise Generator," Simulation, Mar. 1965, p. 179.

139. J. B. Manelis, "Generating Random Noise with Radioactive Sources," Electronics, Sept. 8, 1961.

140. IBM Application Program, System 360 Scientific Subroutine Package (360A-CM-03X) Version II Programmer's Manual, H20-0205-2, p. 54.

141. B. J. Ley, Computer Aided Analysis and Design for Electrical Engineers, Holt, Rinehart, and Winston, Inc., New York, 1970, Section 10-3.

142. Ibid., p. 524.

143. Ibid., p. 528.

144. Ibid., p. 529.

145. Op. cit. (Reference 138) p. 181.

146. T. G. Lewis, Distribution Sampling for Computer Simulation, D. C. Heath and Co., Lexington, Mass., 1975, p. 6.

147. E. J. Watson, "Primitive Polynomials (Mod-2)," Mathematics of Computing, vol. 16, pp. 368-369.

148. R. M. Amundson, Hybrid Interface User's Guide, Computer Engineering Laboratory vol. CEL-P-Hybrid-1, Dept. of Electrical Engineering, Virginia Polytechnic Institute and State University, Blacksburg, Virginia, 1975.

149. Op. cit. (Reference 93) Section I-6.

150. Op. cit. (Reference 94).

151. Op. cit. (Reference 36) pp. 240-241.

152. Op. cit. (Reference 138) p. 180.

153. H. Taub and D. L. Schilling, Principles of Communications Systems, McGraw-Hill, Inc., New York, 1971, pp. 15-16.

154. Op. cit. (Reference 134).

155. Op. cit. (Reference 9) p. 233.

156. Op. cit. (Reference 75) Chapter 25.

157. Op. cit. (Reference 9) p. 261, problem 5-34.

158. Op. cit. (Reference 9) pp. 234-235.

159. Op. cit. (Reference 9) p. 261, problem 5-35.

160. Op. cit. (Reference 10) pp. 131,146.

161. Op. cit. (Reference 14) pp. 376-380.

162. Op. cit. (Reference 2).

163. Op. cit. (Reference 4) p. 46.

164. Op. cit. (Reference 77) p. 41.

165. J. H. Richmond, "Scattering by a Dielectric Cylinder of Arbitrary Cross Section Shape," IEEE Trans. on Ant. and Prop., vol. AP-13, pp. 334-341, May 1965.

166. J. H. Richmond, "TE Wave Scattering by a Dielectric Cylinder of Arbitrary Cross Section Shape," IEEE Trans. on Ant. and Prop., vol. AP-14, pp. 460-461, July 1966.

167. Op. cit. (Reference 36) pp. 129-135.

168. Op. cit. (Reference 138) p. 182.

169. K. R. Carver, private communication.

170. K. R. Carver, "Sea Surface Multipath at UHF - Theory and Experiment," prepared for the National Environmental Satellite Service, NOAA Contract 5-35437, December 1975.

The vita has been removed from the scanned document

AN ANALOG/HYBRID COMPUTER SOLUTION

OF

ELECTROMAGNETIC SCATTERING PROBLEMS

by

Edgar L. Coffey, III

(ABSTRACT)

A study of several techniques that may be used to solve exterior electromagnetic scattering problems was made. Analytical methods, moment methods, subsectional methods, probabilistic methods, integral equation methods, and analog/hybrid computer methods were considered in the study to determine the best method to use in a general approach to scattering problems. It was shown that while all these methods were able to solve certain classes of problems, no single technique qualified as a general solution method.

A new scattering technique, the Unimoment - Monte Carlo method, was developed from the strengths and weaknesses of the more traditional methods. It is a probabilistic technique used to solve a deterministic problem. The original scattering problem is decoupled into a simple exterior problem and an interior problem by enclosing the scatterer with either a circle or a sphere. The resulting interior problem is then solved for several different boundary values using Monte Carlo techniques, and the linear combination of these solutions which gives

the best continuity across the boundary is chosen as the solution to the scattering problem along this boundary. The electromagnetic fields at any other point may then be calculated from a series expansion.

This new method was implemented on a hybrid computer to take advantage of the continuous, parallel nature of the analog portion of the computer when taking Monte Carlo random walks and when detecting boundaries that terminate these walks. A description of the Unimoment - Monte Carlo computer system along with various factors influencing performance of the method is included.

Several scattering problems were solved using this method, and all results were within one percent of the exact solutions. This inaccuracy was found to be caused by the analog computer elements, not the method itself. The scatterers studied included circular cylinders, elliptical cylinders, and an annulus, and both perfect conductors and perfect dielectrics were considered. Also, scattering from an irregular object was studied to show the versatility of the method.